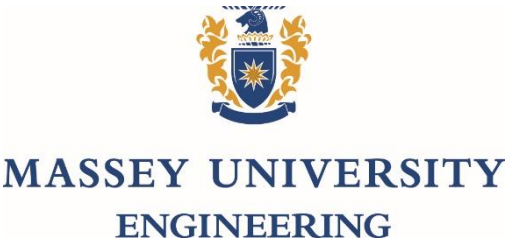

Automated 3D Weaving Continuous Natural Fibre and Optimising Harakeke Fibre Characterisation

A thesis presented in partial fulfilment of the requirements for the degree of
Master of Engineering
in
Mechatronics
at Massey University, Albany,
New Zealand

By

Junyi Lin

2019

Abstract

This research investigated the design and implementation of a continuous natural fibre filament winding robot for modern artistic and structural architectural design. The idea of a new architectural construction technique based on Arduino integration was inspired by the underwater nesting structure of water spiders. It consists of the motion component, a 3-axis sliding table with limit switches, the construction of the machine, the programming and testing of the resulting microcomputer software through to a robot manufacturing process. This was based on Arduino's new integrated development environment. In addition, the intelligent programming mode forms the preconceived pattern through winding, producing a model with unique architectural quality, and at the same time, making a structure with superior material efficiency.

In terms of hardware design, the first conceptual model focused on using an open-source integrated development environment (IDE) that could be easily configured. Arduino hardware was the primary microcontroller of choice for simplicity and ease of hardware integration and software development. Stepper motor drivers are used to control the three stepper motors to accurately move the fibre feeding mechanism on the sliding table into position. The path of the sliding table is controlled by the controller, and the machine can make forward, backward, wire feed and other movements according to the programmed commands. The developed system automatically weaves and feeds natural fibre into the desired structure. The resulting lightweight natural fibre material forms a model with unique architectural quality.

The results show that the model is of great value and significance, and it can be used to make the required structure with the desired natural fibre.

Additionally, to establish the feasibility of future work focusing on harakeke fibre development in design and construction, the tensile strength of native New Zealand flax fibre (harakeke fibre) was evaluated with a view for use in these load bearing and architectural design applications. Single filament fibres were selected in batches and tensile tested. The longitudinal strength of specimens was established, and the mechanical properties of the fibres were summarised. Comparison of these attributes with existing data was used to determine if the harakeke fibre can be applied usefully in the construction industry.

This research is based on the novel concept of architectural design in the construction industry using 3D weaving with natural fibres, in particular harakeke fibres. To achieve this, several related topics are under investigation, such as the need to design an improved feeding system (including hardware and software control), impregnation of fibre and resin (epoxy and polyester) to make preimpregnated (prepreg) fibre/resin filament, adaptive controlled programme and hardware for the required architecture and structure, and properties testing and characterisation. This project is one of the first attempts to develop an automated robot arm system combined with new material, in this case harakeke fibre, and has made a valuable contribution to this field of research.

Keywords: 3D-weaving and feeding machine, continuous fibre, architecture, tensile test, harakeke fibre

Acknowledgements

First and foremost, I would like to acknowledge my supervisor, Dr Xiaowen Yuan from the School of Engineering and Technology at Massey University, Albany for providing guiding opinions and recommendations on the research direction of my thesis. In the process of drafting the present thesis, she gave me timely advice on the doubts and difficulties I met. At the same time, she also put forward many beneficial suggestions for improvement and made a great effort. It has been a greatly enriching experience for me to work under her authoritative supervision. I would also like to express my heartfelt thanks to the teachers for their help too! By the time this thesis was finished, I had sincere respect for my supervisor, for without her guidance and diligent supervision, this project would not have been possible.

I would like to acknowledge the Massey engineering workshop staff, who contributed to many discussions that helped me shape this project. Thank you very much for your interest and help with my work.

I also wish to thank the students at Massey University who finished the graduation thesis group together. Without your support and devoted assistance, I could not solve the difficulties and doubts and finally complete this paper smoothly.

I am grateful for the monographs of the scholars cited in this paper. Without the inspiration and help from the research results of these scholars, I would not have been able to accomplish the final writing of this paper.

Special thanks go to my parents. I am grateful to my parents for bringing me into this wonderful world. They are the backbone of my education and when I deal with the uncertainty of my life choices, it's a relief when they help me out. Their selfless love and care for me are the driving force for me to keep going forward.

Table of contents

List of Figures

List of Tables

1 Chapter 1: Introduction

1.1 3D Weaving Construction

Robot technology is a rapidly advancing and new technology which integrates computer, cybernetics, mechanism science, information and sensing technology, artificial intelligence, bionics and other disciplines. Its essence is the synthesis of four major technologies: perception, decision-making, action and interaction. The volume of robot deployments is an important symbol of a country's industrial level of automation.

Industrial robots are a type of automatic production equipment with human-like operation, automatic control, repeatable programming and capable of completing various operations in three-dimensional space.

At present, the robot application field is predominantly concentrated in the automobile industry, which accounts for 43% of the total number of existing robots. Appliance manufacturing next, accounting for about 16.4%, while the chemical industry accounted for 11.7%. In addition, industrial robots are also commonly used in food, pharmaceutical equipment, aerospace and metal processing [1]. With the development of industrial robots, their fields of application have started to expand from manufacturing to non-manufacturing industries. At the same time, they are also penetrating the original manufacturing industry, deepening and expanding to the difficult processing fields such as large, different, thin, soft, narrow and thick. New application areas are wooden furniture, agriculture, forestry, animal husbandry and fishing, construction, bridges, medicine and health, office and home, education scientific research and some limited fields and other non-manufacturing industries [2].

In general, the robot system can be divided into the following four parts according to function:

1) Mechanical body and actuator: Including internal supporting structures such as body, transmission mechanism, operating mechanism, frame and mechanical connection.

2) Power plant: Including power supply, motor and other executive components and their driving circuits.

3) Detection sensor devices: Including the sensor and its corresponding signal detection circuit.

4) Control and information processing devices: Robot controls system composed of hardware and software.

Among the existing modern technology systems, robotic technology is more likely to undertake innovation in the construction industry. Robots are a highly developed product of innovative electromechanical technology and information technology. In the past 30 years, with the gradual application of robot technology, especially in the automobile industry as an example. Robotics stem from an instinctive need to gain relief from arduous working conditions, and the construction industry has almost all these downsides - intense work. Because of the difficult and dangerous conditions in which construction operates, the concept of a construction robot was born. In this way, the working environment and work efficiency of the construction industry can be improved, and complete autonomy of construction can be realized in the future through the process of replacing or assisting construction workers with robots [1-3].

This research is an introduction to the application of robots in architecture. It is mainly described in two parts: Firstly, the function, structure and common operation mode of the robot in the field of architecture are presented. Then, mainly describing its application in the field of architecture,

including international research, and three other application fields: Robot and digital construction, robot and new material combination and the robot and new technology combination. When it now comes to technical terms such as artificial intelligence and big data, people usually do not associate them with the seemingly traditional construction industry. One of the reasons is to realize the function of these technologies. Digitalization of the application layer is needed, which is the weak link in the construction industry at present. In addition, the traditional construction process not only has to deal with the use and installation of many different materials and various mechanical operations, but also needs to make changes in the construction site according to the actual situation, so the complexity and uncertainty of the construction process is also the reason why high-tech is difficult to fundamentally shake the traditional process. But like the exponential growth being held in various industries, the digitalization and even artificial intelligence of the construction industry has emerged and shown unexpected progress in some areas. Innovative technology has penetrated every link of the construction process [2, 3].

The design topic is "Design and implementation of a 3D weaving machine feeding continuous natural fibre ", which takes an Arduino microcontroller as the control core and mainly studies the wire feeding and weaving function of the machine. First, the weaving pre-processed program has to be programmed, then this Arduino IDE program is transmitted to the Arduino microcontroller. When the sliding table of each axis is within the set limits, and in the automatic mode, the microcontroller will issue instructions to let the sliding table move according to the pre-designed sequence, and then continue until the entire construction model is formed. The applications fora 3D sliding table are many and varied, and it is equipped with a feeding mechanism, which sets a different path of movement and produces different program code, which can produce various construction model enclosures or exterior walls. With this basic function, more functions can be added to it and give it more realistic value. An Arduino single-chip microcomputer was selected as the control core and limit switches were used to limit the slide table working range. A 3D weaving and feeding, construction robot is a comprehensive system integrating automatic movement, weaving, planning and decision-making, automatic wire feeding and other functions. It combines the computer, information, communication, artificial intelligence, automatic control and other technologies and as such is high-tech and complex. It can operate automatically in a specific environment according to the pre-set mode and it can achieve the expected or higher goals without human management.

1.2 New Zealand flax fibre (Harakeke fibre)

In recent years, natural fibre has attracted people's attention because of its lightweight, low price, easy availability and excellent environmental harmony. Among all kinds of natural fibres, New Zealand flax fibre (harakeke fibre) has the advantages of low price, good reproducibility and wide distribution, as well as the benefits of tensile strength, fibre orientation and uniform modulus. It is a high-performance natural fibre [4-6]. At the same time, the microstructure of harakeke fibre is unique, the continuous length is long, and it has excellent processability. The research and development of natural fibre and its products have made early progress in the world [7-8]. At present, a large amount of natural fibre has been used as a substitute for wood and glass fibre, and used as decorative material in the building industry, interior decoration panels in automobile industry, auto parts and other materials. Among them, the application of natural fibre in automotive reinforcement materials has made great progress, and gradually towards industrialization [9-11]. Natural fibre not only has high strength, modulus, low density, low price and abundant sources, but also is an eco-friendly and renewable resource. At the same time, the hollow structure of natural fibre also makes it a sound insulation and heat insulation material. For a long time, natural fibres have served in the decorative, packaging and textile industries. The advancement of people's awareness of environmental protection and the deepening of the concept of sustainable development, natural fibre materials have been rapidly developed and widely used in transportation, construction and other fields. Natural fibre is easy to plant, short growth cycle, low price, biodegradable, easy to recycle, is the preferred material for the pursuit of green environmental protection. Harakeke fibre has abundant resources in New Zealand, which is beneficial to environmental protection and sustainable development as an industrial raw material and has definite social significance. However, the fluctuation of the processing process or the problem of the filament itself makes the mechanical properties of the final harakeke fibre vary greatly, especially the dispersion of the fibre strength. Therefore, strength and elongation of harakeke fibre and its uniformity become one of the important considerations of people's research and conventional measurement. In addition to the internal cause of "fibre internal structure", the factors influencing the tensile performance test results of natural single fibre are also affected by the laboratory temperature and humidity, fixture length, the number of test samples (averaged together), tensile speed and other test conditions. The tensile properties of the same batch of fibres may vary greatly under experimental conditions. In this experiment, the test samples are New Zealand Flax Fibre (harakeke fibre). This material was obtained from the Biopolymer Network Co., Ltd. (BPN) fibre processing unit in New Zealand and stored, in laboratory conditions. This experiment studies the tensile test of harakeke fibre monofilament at different stretching speeds, different spacing length and different fibre thickness. Thereafter, the paper analyses the factors influencing the tensile properties of single harakeke fibres, and obtains the factors influencing the accuracy of the test results, which provides a guide to the significance of the tensile property tests.

1.3 Thesis background

With the continuous development and popularization of modern computer technology, the development of robots has been dramatically increased particularly the intelligence level of robots in recent years, and rapidly changing people's way of life. In the fields of machinery, electronics, metallurgy, transportation, aerospace, national defence and so on, people will use computer technology more widely in daily life, making machines that can replace human labour has always been the dream of human beings, and have been working hard for it. With the progress in the construction industry, the study of construction robots has been more and more concentrated. They are characterised by the ability to perform tasks or work in high-risk environments without human control or through human control. Therefore, in this design, a 3D weaving and feeding robot will be designed. With this basic function, more functions can be added to it and give it more realistic value. An Arduino single-chip microcomputer was selected as the control core and limit switches were used to limit the slide tables working range.

The 3D weaving and feeding robot is a comprehensive system integrating automatic movement, weaving, planning and decision-making, automatic wire feeding and other functions. It concentrates on computer, information, communication, artificial intelligence, automatic control and other technologies and is a case in high-tech complexity. It can operate automatically in a specific environment according to the present mode and it can achieve the expected or higher goals without human management.

Owing to the properties of natural fibre monofilament, the tensile property test results may be affected by various parameters. In this paper, the tensile properties of harakeke high-performance fibre monofilament were compared under different test conditions. The test data of fibre tensile properties were analysed and the factors influencing the accuracy of the test results were achieved.

1.4 Overview of Arduino microcontroller

Arduino is a hardware and software platform built on open-source code. It is built on the simple I/O interface of simple source code and has Processing/Wiring development environment like Java and C languages. It contains two main parts: the hardware part can be used to do a circuit connection and Arduino circuit board; the other is the Arduino IDE, the programming environment on a computer. You write code in the IDE, upload it to the Arduino circuit board, and the program tells the Arduino circuit board what to do [12-15].

Arduino senses the environment through a variety of sensors, and influences the environment by controlling light, motors, and other devices. The microcontroller on the board can be programmed through the Arduino programming language, compiled into binary files, and included in the microcontroller. Arduino is programmed using the Arduino programming language (Wiring) and the Arduino development environment (based on processing). An Arduino-based project can contain only Arduino, or it can contain Arduino and some other software running on a PC, and they can communicate with each other (such as Flash. Processing, MaxMSP) to achieve this. You can make it yourself, or you can buy a kit; the hardware reference design (CAD file) is also available in accordance with the existing open source protocol, and you are free to modify it to suit your own needs.

The Arduino can use developed electronic components such as switches or sensors or other controllers, LED, stepper motors or other output devices. The Arduino can also operate independently as an interface to communicate with the software, such as a flash, processing, Max/MSP, VVVV, or other interactive software. The Arduino development IDE interface is based on open source code and allows you to create more amazing interactive work for free download and use [16].

Why do we use Arduino? There are many SCM and SCM platform is suitable for interactive system design. For example, Parallax Basic Stamp, Netmedia's bx-24, Phidgets, MIT's Handy board and others provide similar features. Arduino also simplifies the working process of single-chip microcomputer but compared with other systems Arduino is more advantageous in many aspects, especially suitable for teachers, students and amateurs. It makes a simple programming environment. It's easy for beginners to learn to utilize the Arduino programming environment while still providing enough advanced applications for power users. For teachers, it is generally convenient to use the Processing programming environment, so if students have learned to use the Processing programming environment, they will feel very similar and familiar when using Arduino development environment [17].

Open source and extensible software - the Arduino software is open-source and can be expanded by experienced programmers. The Arduino programming language can be extended by using the C++ library, and if you want to see the technical details, you can skip the Arduino language and go straight to the AVR-C programming language (because the Arduino language is based on AVR-C). Similarly, you can add AVR C code directly to your Arduino if you need to [18].

Arduino is based on the AVR platform, and the AVR library is the secondary compilation package, the ports are packaged, registers, address pointers and additional basics need not be considered. This greatly reduces the difficulty of software development, ideal for non-professional enthusiasts to use. Advantages and disadvantages exist, because it is a secondary compilation package, the code is not as concise as direct use of AVR code, code execution efficiency and code size are inferior to AVR direct compilation.

1.5 Development status of construction robot

The current state of development in the world is that the intelligence level of the intelligent construction robots in development are not high, but only in the early stages of really intelligent construction robots. The current core issues in the research of intelligent construction robots has two aspects: on the one hand, to improve the autonomy of mobile construction robots, which is in terms of the relationship between intelligent mobile robots and people, that is, to hope that intelligent construction robots can be further independent from people and have a friendly human-machine interface. In the long term, it is expected that the operator will only specify the task to be fulfilled and that the machine will automatically perform the steps of completing the task and finishing it automatically. On the other hand, improving the adaptability of intelligent construction robots, improving the ability of intelligent construction robots to adapt to the changing environment. In terms of the relationship between intelligent construction robots and the environment, the aim is to greatly increase their interaction.

The Intelligent construction robot involves many key technologies that are related to the level of intelligence. Navigation and positioning technology; For the autonomous navigation of the mobile weaving construction robot, it is necessary to determine the current state and position of the robot and any nearby obstacles accurately, in order to complete navigation successfully, obstacle avoidance and path planning and other tasks are required. Path planning technology; The optimal path planning is to find an optimal path from the initial state to the target state and moving and weaving in the assigned workspace according to some optimization criteria. Intelligent control technology; An intelligent control method is needed to improve the speed and precision of the robot. Man-machine interface technology; Man-machine interface technology is the study of how to allow people convenient and natural communication with the computer.

Nowadays, various fields such as intelligent engineering, computer science and mechatronics are discussing automation systems, and peoples demand for automatic machines is getting higher. With the rapid development of artificial intelligence technology, computer technology and automatic control technology, automatic control will usher in a new era in its development. The fusion of computer control and electronic technology brings a broad prospect for enhanced sophistication of automated equipment. Therefore, research into the intelligent 3D weaving and feeding construction robot can only promote the development and innovation of key technologies.

1.6 Research significance and purpose of Arduino 3D weaving machine

With a kaleidoscope of applications, different tools, different motion paths and different program code, the robot will produce various "products". In order to realize the function of automatic guidance and wire feeding, the robot must know how to move and wire feed, and the perception of walking the route is equivalent to giving the robot a visual function. The design of intelligent programming is an important means to achieve an intelligent mobile wire feeding robot. The requirements include high measurement accuracy, painless real-time control and simple calculations to easily achieve the construction of external walls.Given these features it will be commonly used in the process of intelligent building in the future. The future of intelligent 3D weaving robots are an inevitable development in the construction industry, in this case, the study of the application of ultrasound to the intelligent 3D weaving machines obstacle avoidance programming has far-reaching significance, which will play an important role in New Zealand's future research on intelligent building robots in the world's leading high-tech field.

This design focuses on multifunctional construction wire weaving and feeding. The theoretical scheme, analysis method, characteristics and innovative points in this design can provide certain reference significance for the design and popularization of automatic and semi-automatic robots such as mechanized transportation robots. The robot can draw by attaching an airbrush to the end of the arm and matching it with different pigments. If a textile tool is added to the robot, and the corresponding program code is established for it, the robot can also print out a set of incredible clothes for fashion models, realizing economic benefits and forming commercial value.

1.7 The main research content of the project

The design topic is "Automated 3D Weaving Continuous Natural Fibre", which takes an Arduino microcontroller as the control core and mainly studies the wire feeding and weaving function of the machine. First, the weaving pre-processed program was written, and then this Arduino IDE program transmitted to the Arduino microcontroller. When the sliding table of each axis is within the specified working area and in automatic mode, the microcontroller will issue instructions to move the sliding table according to the pre-designed itinerary, and then continue until the entire construction model is formed. The applications of a 3D sliding table such as this are many and varied, and it is equipped with a feeding tool, which allows another path of movement and using different program code, can produce various construction model enclosures or exterior walls.

The high specific strength and high specific modulus of New Zealand flax fibre (harakeke fibre) make it widely used. However, the variables in the processing processes or defects of the filament itself makes the mechanical properties of the final harakeke fibre vary greatly, especially concerning the dispersion of the fibre strength. Therefore, strength and elongation of harakeke fibre and its uniformity become one of the important factors in people's research and conventional measurement. Typically harakeke fibres are very fine (~328 microns), are brittle and have high strength. At the same time, the testing of single filament strength and elongation of harakeke fibre will produce large errors due to numerous factors. In this paper, the factors that may affect the tensile testing of harakeke fibre are investigated and discussed.

2 Chapter 2: Literature Review

2.1 The need for construction robots

Construction is the second most dangerous industry behind the mining industry. The construction industry has the disadvantages of multiple accidents, shortage of labour and low labour productivity. Therefore, a possible and effective way to improve productivity is tantamount to realizing the production of robotic nano-manipulation.

There are many advantages to using robots in the construction industry, and there are four main points:

(1) Human beings can easily extend their construction activities to new places and fields that are not hospitable for human beings, such as underwater, chemically toxic, high temperature, high pressure and other fields, bringing huge economic benefits.

(2) Replacing humans in monotonous and repetitive traditional construction work, such as the laying of external walls on construction sites.

(3) The application of robots can modernize traditional manual processes and improve efficiency.

(4) In the construction industry, the labour costs are high and skilled labour is scarce. Therefore, robots can be used to replace construction workers in some traditional fields. At the same time, more effective robots can be designed in new construction processes to further reduce labour costs.

2.2 Key technical problems of construction robots

The methodological problems faced by construction robots are much larger than those faced by most manufacturing robots. The key technical problems include:

(1) Robot mobility: Mobility requires complex navigation capabilities, including mobile operations in complex environments, obstacle avoidance and accident control algorithms, robot vision systems, new control systems and processing units.

(2) Robot sensors: In the work of a non-structural environment, the construction robot must use a variety of sensors at the same time, the most important of which is pattern recognition and proximity sensors installed at the end of the mechanical arm.

(3) Robot end-effector: In the actual project operation the robot provides the movement, and the specific function tools is added to the robot arm to meet different functional requirements. The robot end tools used in construction which can be installed include an electric drill, welding equipment, cutting knife, laser cutting equipment, etc. according to the different functions to meet different construction requirements.

(4) Control system: The control systems developed at present have serious limitations in correcting the robots actions according to sensor information and as a result cannot effectively complete tasks.

(5) External factors: Severe weather conditions, such as high temperature and extreme temperature, will affect the responsiveness of robot sensors and greatly affect the precision of the robot movement.

2.3 Construction robot market prospects

Among all the engineering practices of human beings, the construction industry has the longest history. Early human beings started a variety of construction practices for the purpose of "weathering the wind and rain, avoiding the cold and heat". With the continuous development of high-rise building construction technology, construction robot technology has emerged.

An intelligent construction robot is an important development direction for the construction industry. At present, the construction of the main building project has realized mechanization. But construction that decorates still relies on handiwork entirely. 2018-2023 industrial robot market monitoring and investment feasibility study report shows that the final implementation of the construction robot idea, for the building decoration industry, will not only greatly improve the work efficiency, reduce labour costs, for the large-scale popularization and application of Internet home decoration also has unusual significance. The market prospects of a construction robot is analysed in four aspects.

First, construction robots will achieve more rapid progress. Construction robots are the most typical electromechanical integration of digital equipment, high technology added value, wide application range, as the support technology for the advanced manufacturing industry and the emerging industry of social information, will play an increasingly important role in the future production and social development. The development prospects of the industry are good.

Second, applications are becoming more prevalent. After more than 40 years of development, construction robots have been applied in more and more fields. The market prospects of construction robots indicates that in the manufacturing industry, especially in the automobile industry, construction robots have been extensively used, accounting for more than 30%. With the development of construction robots in a deeper and broader direction and the improvement of the level of robot intelligence, the application of robots has been expanding and has been extended from the automobile manufacturing industry to other manufacturing industries.

Third, the transfer of production bases. Along with the developing countries such as China and India construction robots expand the market, the international leading nations' industrial robot market sale growth is slowing, international advanced industrial robot manufacturers gradually will develop its business focus to developing countries, to absorb the surplus capacity, in the original market and increase its business profits.

Fourth, industry competition is more intense. At present, industrial robot manufacturing is an area that all the major equipment manufacturers wish to get involved in. Both traditional machinery manufacturers and electrical enterprises hope to take a share in the future industrial robot market. The prospect of the construction robot market foresees that in the future, domestic industrial robot manufacturers will face competition not only from foreign enterprises, such as ABB, FANUC, KUKA and YASKAWA, but also from domestic cross-industry enterprises, and the level of competition in the industry will be more intense.

At present, it seems that construction robots can play a definite role in improving product quality and controlling construction cost. However, the technology is not developed to that extent, and there is no real will yet. No complete project has been constructed by robots. The future of the construction robot market shows that it is difficult to know whether robots working on construction sites will affect the construction cycle, and it is not clear how much it will help developers to collect funds.

2.4 Construction robot technology application and project

1. Wall construction robot

In 2016, an American company launched a brick laying robot named "semi-automatic mason" (SAM100, Figure 1), which can lay 3000 bricks a day (a domestic worker usually has simply 250-300 bricks a day). The world's first fully automated commercial building robot Hadrian X has been created in Australia. It can lay an astonishing 1,000 bricks per hour. Work 7 X 24 hours and sell 2 million dollars at the same time. Instead of using traditional cement, Hadrian X USES building glue to bind bricks, thus greatly increasing the speed and strength of the building and enhancing the ultimate thermal effect of the structure. Hadrian X can handle bricks of different sizes, cut and grind.

Figure 1 SAM 100 claims robot [19]

Developed by Construction Robotics, SAM 100 claims to be the world's first commercial robot for onsite masonry.

Figure 2 Hadrian X, developed by Fast Brick Robotics [19]

In addition, Hadrian X (Figure 2), developed by Fast Brick Robotics, can also 3D print and brickwork, completing the superstructure of a traditional Brick house in just two days.

2. Building demolition robot

Building demolition robots are another kind of building robot that is moving into the mainstream application field. Although they are slower than demolition crews, they are much safer and cheaper to remove concrete and structural parts of a building at the end of its life cycle. Husqvarna DXR series remote-controlled demolition robot is the latest in a series of remote-controlled demolition machines featuring high power, lightweight and functional design. Husqvarna DXR demolition robot can be operated remotely by workers without the need to enter the hazardous demolition site. Brokk has

been engaged in the production and research and development of demolition robot for more than 40 years (Figure 3). Brokk series of 17 demolition robots can adapt to the demolition requirements of different scenes and environments.

Figure 3 Brokk building demolition robot [19]

3. 3D printing construction robot

3D printing robots are part of the most advanced automation applications in the construction industry. It can be divided according to different environments and materials. The 3D printing robot prints the whole structurally safe building through a mobile manipulator, which USES digital pre-programming and instructions to start printing the building according to set style and program after receiving the instructions. This 3D printing robot technology has also brought innovation in building materials. "Semi-automatic" mason and Hadrian X are traditional square brick, but obviously the construction industry and robot research and development institutions are not satisfied with this kind of building material, a team of researchers at the Massachusetts institute of technology have developed a new digital construction of the machine, "print" architecture which uses 3D printing technology, the robots building material is a mixture of foam and concrete, leaving insulative space between inner and outer wall and can be embedded in pipelines.

4. Automatic "Rover" of construction site

Equipped with high-definition cameras and sensors, the automated rover can navigate around the site and is a robot capable of identifying and avoiding obstacles. The "EffiBOT," developed by the French robotics company Effidence, can follow workers and carry tools and materials (Figure 4).

Figure 4 EffiBOT [19]

2.5 Research Pavilion 2014-15: Interactive Panorama

The institute for computational design (ICD) and the institute for architectural structure and structural design (ITKE) continues to use their research venue series in the new ICD/ITKE institute at the University of Stuttgart, 2014-15 [19]. These prototypes explore the potential of different computational design, simulation, and manufacturing processes in architecture. The pavilion is developed in the interdisciplinary areas of research of the two institutes and their collaborative teaching in the context of the interdisciplinary and international ITECH Master of Science program. The prototype project is the product of a year and a half of development by researchers and students in architecture, engineering and the natural sciences. It shows the architectural potential of a modern architectural method inspired by the construction of underwater nests of water spiders. Through a novel robotic manufacturing process, the original flexible pneumatic templates were gradually hardened by strengthening them from the inside with carbon fibre. The resulting lightweight fibre composite shell forms a pavilion of unique architectural quality and an efficient material structure (Figure 5).

The water spider spends most of its life underwater, building a reinforced bubble to survive. First, the spider creates a horizontal web of thin plates and places bubbles underneath. In a further step, the bubbles need to be strengthened in turn by layering a layered structure of fibres from within. The result is a stable structure that can withstand mechanical stresses, such as changing water flow, to provide a safe and stable habitat for spiders. This natural manufacturing process demonstrates how adaptive manufacturing strategies can be used to create inexpensive fibre reinforced structures.

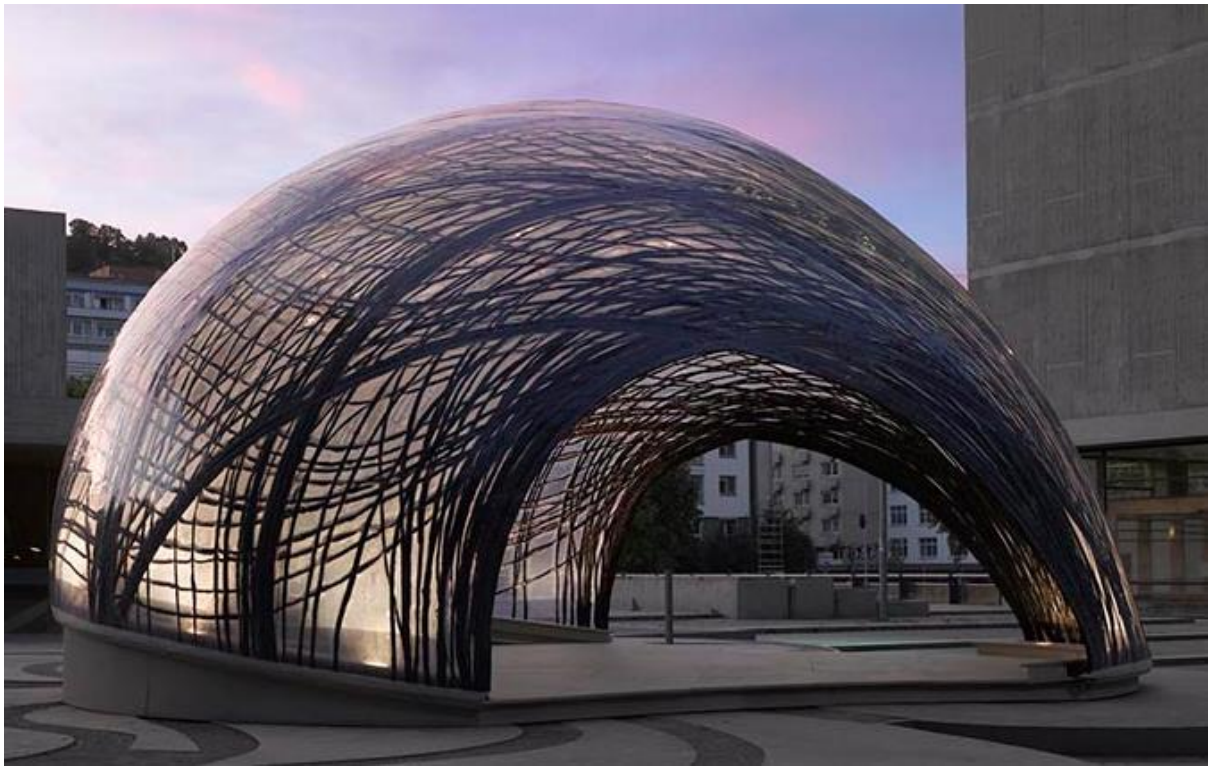

Figure 5 The ICD / ITKE Research Pavilion [20]

The design is built on the biological construction technology of fibre reinforced structure. These processes are relevant to applications in architecture because they do not require complex templates and can accommodate the unique requirements of a single structure. Biological processes for custom fibre reinforced structures in a highly materialized and functionally integrated manner. In this regard, the web weaving process of Agyroneda Aquatica has proved particularly interesting and useful for the robot weaving machine design. The article cited studies the weaving process of water spiders, analyses, and abstracts and transforms the potential behaviour patterns and design rules of a water spider.

In order to translate this biogenetic sequence into architectural applications, an industrial robot was designed to be placed inside an air support membrane made of ETFE (Figure 6). The expanded soft shell is initially supported by air pressure, however, by mechanical strengthening of the interior with carbon fibre, it gradually hardens into a self-supporting monomer structure. Carbon fibre is used selectively only when structural strengthening is required, while pneumatic formwork is used as a functional integrated skin of the building. This leads to an efficient build process resources.

2014-15 ICD/ITKE research centres cover an area of about 40 square meters, with an internal volume of about 130 square meters, a span of 7.5 meters and a height of 4.1 meters. The total weight of the structure is only 260 kg, equivalent to 6.5 kg/m^2 (Figure 5).

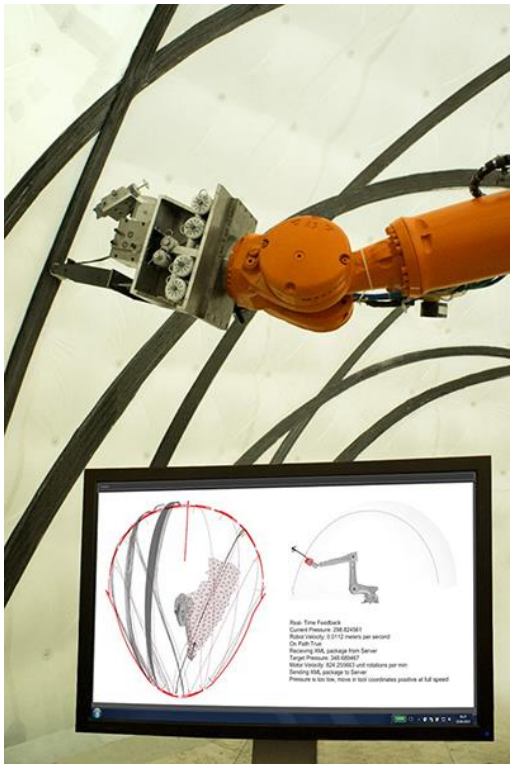

Figure 6 Feeding arm [20]

The following figure (Figure 7) shows the computational system for all the machine. Corresponding to the adaptive computing design strategy, a prototype robot manufacturing process for carbon fibre reinforced on a flexible membrane was developed. In order to be adapted to these parameters in the production process, the current position and contact force are recorded by an embedded sensor system and integrated into the robot control in real time. The development of this network physics system allows for continuous feedback between actual production conditions and the numerical generation of robot control code. ETFE is considered a suitable material for pneumatic formwork and integrated building casings as it is a durable external wall material with mechanical properties that minimizes plastic deformation during fibre placement. A high degree of functional integration is done by using ETFE film as pneumatic formwork and building enclosure. This saves material consumption of traditional template technology and the additional external wall installation. The composite binder provides the appropriate adhesion between ETFE film and carbon fibre. During the production process, nine pre-impregnated carbon fibre roving yarn is placed in parallel. This additive process not only allows for the stress orientation placement of the fibre composites but also minimizes the structural waste associated with the usual subtraction of the construction process.

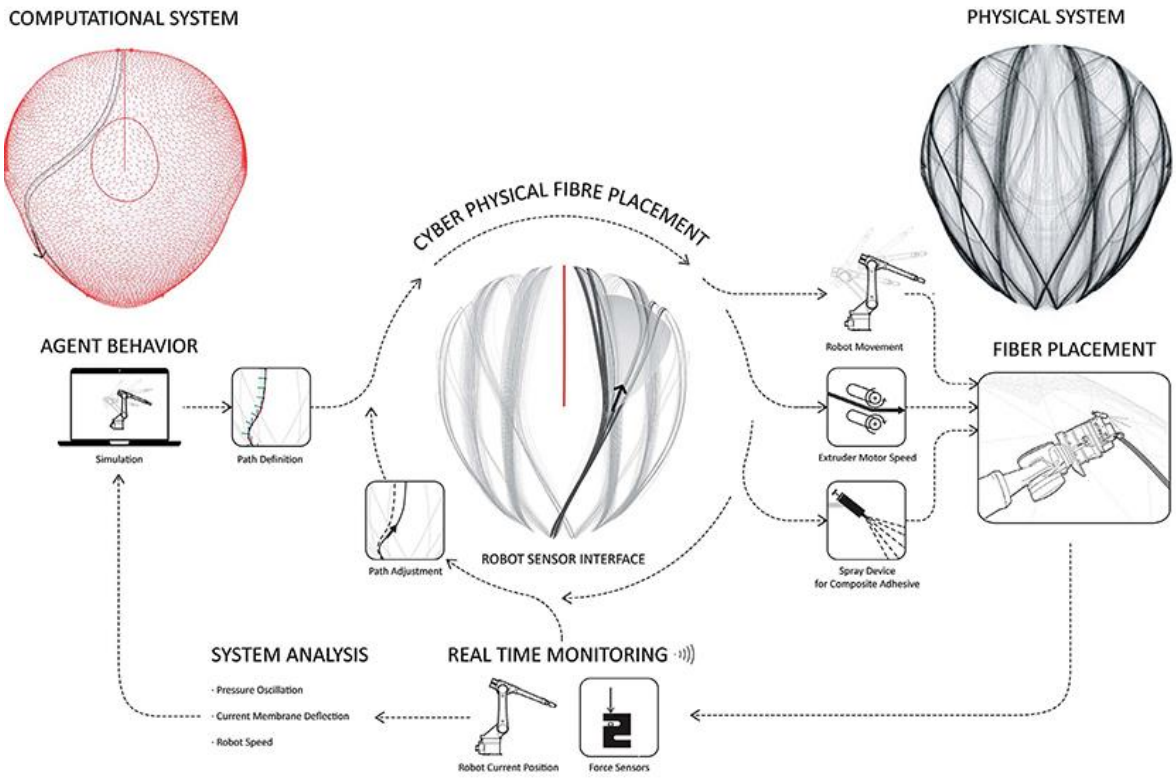

Figure 7 Computational system [20]

The following figure (Figure 8) shows the feeding station for the whole machine. The four sets of carbon fibre material will be attached to the spools. The stepper motor will control the fibre feeding speed of the Arduino when the machine is running. At the end of the wire feeding mechanism, the composite binder provides the appropriate adhesion between the ETFE film and the carbon fibre. The application of this wire feeding system will be implemented in this thesis project design.

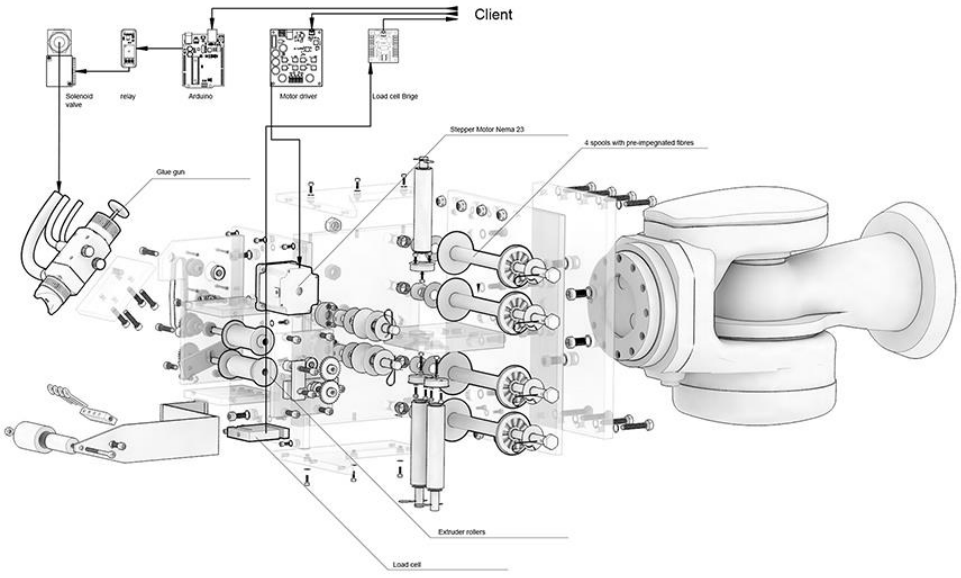

Figure 8 Feeding unit diagram [20]

ICD/ITKE research institute 2014-15 demonstrated the innovative potential of interdisciplinary research and teaching as a demonstrator of innovative computing design, simulation and manufacturing technologies. The prototype expresses the anisotropic characteristics of fibre composites as architectural quality and reflects the underlying processes in novel textures and structures. The result is not only a particularly effective structure, but also an innovative architectural demonstration [20].

2.6 The development of robots in architecture colleges

Exploration of the former robot in architecture is still preliminary, but the development speed is very rapid. The main reason is that digital design is more and more introduced into actual project design by designers, which lead to a problem of digital construction. CNC, laser cutting technology, 3D printing, mechanical arm and other industrial design technologies and equipment have been introduced and applied to numerical construction. However, the role of mechanical arm is not limited to the construction field, but also can be combined with related disciplines, such as visual art, material science, intelligent technology, etc., to expand thinking, make bold attempts, and explore new possibilities of architectural design.

Many architecture schools and research and development teams around the world have carried out the application research of robotic arm and established corresponding robot laboratories, including world-class architecture schools. For example, Harvard school of architecture (GSD), ETH Zurich federal institute of technology (ETH), MIT MEDIA LAB, university of Michigan school of architecture (UMICH) and southern California school of architecture (sci-arc) all have robot LABS. Among them, the research of the department of architecture of the federal institute of technology in Zurich and the school of architecture of the University of Michigan mainly focuses on the construction of mechanical arms, including the cutting, milling, bending and clamping in construction of materials, which have completed many project practices. Research at the MIT media lab and the southern California school of architecture focuses on exploring new design practices that combine robotic arms with materials and technology to explore different design possibilities. Among them, sci-arc has introduced six siX-axis robots to build a robot laboratory. The laboratory is divided into two areas. One is the computer program control area, and the other is the robot experiment area. Among them, five big mechanical arms are fixed installation, respectively, two sets of one and three sets of one, easy to cooperate with each other, the other small mechanical arm can move flexibly according to the needs, to meet various design possibilities [21].

2.7 Exploration of robots in architectural design

Undoubtedly, the application of robots overturns the traditional construction model and provides strong technical construction support for digital design. It can even be combined with 3D printing, CNC machine tools and laser cutting to create a whole new set of construction techniques and technology. At the same time, through the control of the robot, combined with modern materials, use design technology and the robotic arm in combination, in virtual reality to explore different design possibilities [22].

2.8 Robot and digital construction

With the support of robots, the process of digital architecture from "generation" to "construction" is expected to be completed. By means of milling, hot wire cutting, bending, clamping and other construction methods, the material is digitized and finally completed. Since in the digital age, an exhibition booth may be composed of thousands of materials of different sizes and shapes, the traditional construction methods are no longer able to complete such complex material cutting and final construction, but the whole process of construction can be easily completed by robots and an downloaded digital program. For example, we use carbon fibre and glass fibre as materials, attached to a pre-designed steel structure. In the computer, the trajectory and sequence of motion of the robot arm are organized in advance and then converted into robot code. The end of the robot arm is equipped with weaving tools, and the movement of the robot arm is used to leave the skin texture, which is constructed like "weaving cloth" [23].

2.9 The robot combined with new materials

When robots are combined with materials, especially intelligent materials, they can "make" products directly by operating the movement of the mechanical arm. The 2012 Gehry award was awarded to SCIARC students Kyle and Liz Von for their graduation project, PHANTOM, which uses a liquid epoxy resin that solidifies under laser light. Designers take advantage of this feature, and on the end of a mechanical arm is installed liquid silicone acrylic in a transparent vessel, in the bottom of which is set up a laser device, the device is controlled through an ARDUINO controller (a platform based on open source software and hardware, the hardware platform is can be connected by various sensors to perceive the environment, also can connect all kinds of LED's, or motors as an output device, the software platform can be connected to PC, on which the programme is written in the ARDUINO language. It can also connect the PC to all kinds of interactive software, such as PROCESSING, GRASSHOPPER, FLASH, etc.). It is connected to a computer to control the timed change of laser shape. The designer must go through repeated experiments to obtain such parameters as solidification time and material thickness of liquid silicon under the action of the laser. They designed the general shape in MAYA software and cut the section of the model according to the thickness of the material. After cutting the section the liquid silicon was solidified by the laser according to the shape. At the same time, the trajectory curve of the robotic arm is obtained at the midpoint connecting each section, and the corresponding movement time is given to the movement curve according to the solidification time of the material. Finally, all the files are imported into the program interface of the machine for code translation. After repeated proofreading and trial and error, the robot arm was finally used to "make" a work like the stalactites in a karst cave. This project uses the same effect as 3D printers, all the clever use of the solidification of the liquid silicon and the laser. The advantage is that due to the good use of the movement of the mechanical arm, the 3D printer is able to print the objects size requirements by adhesion, and print the object directly hung up, no need to support the external medium [24].

2.10 Combination of robot and technology

When robot and technology are combined, virtual reality can be combined with visual media art to explore different design possibilities. The following is an example of two robot experimental research projects conducted by team members Brian Harms, Haejun and Vince Huang during their study SCIARC. The relative movement of laser and mirror, three mirrors with three terminals fixed to a mechanical arm, one of the mirrors a hidden laser pen is aimed, the movement of each mechanical arm drives the movement of the mirror, the effect of the light reflection of the laser between the three-mirrors, at the same time, by setting different trajectories, the mechanical arms forms a protean light path.

At the end of the robot arm, the robot can draw by installing an air gun and different pigments. The robot can also "print" an incredible suit of clothing for a fashion model if it is fitted with textile tools and programmed to do so. With the ever-changing application of robots, different tools, different motion paths and different programming code, it will develop a variety of "products" [25].

2.11 Natural fibre

Natural fibres are predominantly composed of cellulose, lignin, hemi-cellulose, pectin, wax, and minerals. Different types of natural fibre chemistry the composition is shown in Table 1 [26, 27]. Cellulose is the most important component in natural fibres. Cellulose is a macromolecular polysaccharide composed of β-1,4 glycoside bonds in D-glucose, and the degree of polymerization is about 10,000. Each repeating unit has three hydroxyl groups, which also determines the strong water absorption of natural fibres and brings about its poor interface properties as a reinforcing material for composites.

Table 1: Chemical composition of natural fibres

Fibre	Cellulose (%)	Lignin (%)	Hemi-cellulose (%)	Pectin (%)	Wax (%)
Jute	61-71.5	12-13	13.6-20.4	0.4	0.5
Flax	71	2.2	18.6-20.6	2.3	1.7
Hemp	70.2-74.4	3.7-5.7	17.9-22.4	0.9	0.8
Kenaf	31-39	15-19	21.5	/	/
Sisal	67-78	8-11	10-14.2	10	2
Cotton	82.7	/	5.7	/	0.6
Ramie	68.6-76.2	0.6-0.7	13.1-16.7	1.9	0.3
Henequen	77.6	13.1	4-8	/	/
Coir	36-43	41-45	0.15-0.25	3-4	/

The mechanical properties of natural fibres are largely determined by the structure, chemical composition, helix angle, and cell size defects of natural fibres (Figure 9).

By establishing a model of natural fibre microstructure, the effects of helix angle, cellulose content, and geometric parameters of the fibre cross-section on the mechanical properties of the fibre were investigated. It was noted that: (1) If the arrangement of microfibrils is at an angle to the fibre axis, then natural Fibres exhibit a certain degree of toughness, otherwise they are rigid. (2) The higher the cellulose content, the better the mechanical properties of natural fibres. Usually, the helix angle,

cellulose content, etc. will be influenced by factors such as the region, the stage of growth, and the harvest season. Therefore, the mechanical properties of natural fibres can have large dispersions.

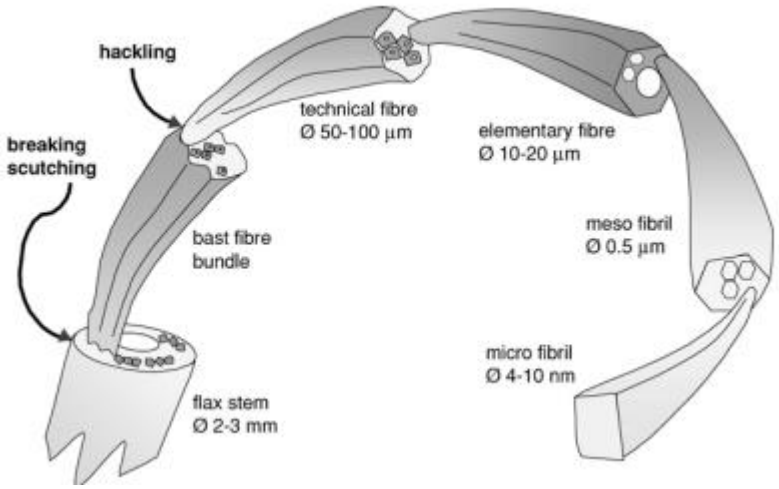

Figure 9 Schematic representation of the microstructure of flax fibre [28]

The mechanical properties of different types of natural fibres are shown in Table 2.

Table 2: Mechanical properties of natural fibres compared with synthetic fibres [28]

Fiber	Density (g/cm^3)	Elongation at break (%)	Tensile Strength (MPa)	Tensile Modulus (GPa)	Spiral Angle (°)
Ramie	1.5	3.6-3.8	400-938	44-128	8
Sisal	1.45	2.0-2.5	511-700	3.0-98	20
Flax	1.5	1.4-1.5	345-1500	10-80	10
Jute	1.3-1.45	1.5-1.8	270-900	10-30	8
Cotton	1.5-1.6	7.0-8.0	287-597	2.5-12.6	20-23
Kenaf	/	2.7	427-519	23.1-27.1	6-10
Hemp	1.48	1.6	270-900	20-70	6
Coir	1.15	15-40	131-175	4-6	30-49
E-glass	2.5	2.5	2000-3500	70	/
S-glass	2.5	2.8	4570	86	/
Aramid	1.4	3.3-3.7	3000-3150	63-67	/
Carbon	1.4	1.4-1.8	4000	230-240	/

2.11.1 The performance of natural fibre

The name of this plant is harakeke as called by Maori. The earliest European traders referred to it as "flax" because its fibres were similar to real flax in the rest of the world. Although today we call it flax. Harakeke is P. Gerbeaux, really a lily. Flax is a unique New Zealand plant and one of our oldest plants. Harakeke is the name of the indigenous Maori plant of New Zealand, commonly known as New Zealand flax or New Zealand Tenex. In this case, however, the name "flax" is inappropriate because harakeke is not biologically related to European flax. Derived from harakeke leaves, long fibre bundles have a long history of being used in the production of clothing, canvas, and rope. In the early 1920s, harakeke products accounted for a significant portion of New Zealand's total export revenue of about 20 percent. However, due to the decline in sales in the 20th century due to the presence of synthetic fibres and the expansion of the sisal industry, the harakeke currently used is largely confined to arts and crafts [29]. Harakeke fibre is believed to have similar properties to sisal fibre - another leaf fibre [30, 31] widely used to strengthen polymer composites [32, 33]. Therefore, harakeke fibres will also have the potential to enhance polymers.

2.11.2 Harakeke/New Zealand flax fibre

The microstructure of the natural fibre is unique. Its cross section is the lumbar circle or polygon with a hollow cavity, longitudinally has transverse section and vertical grain. The chemical composition of natural fibre is mainly cellulose, hemicellulose, lignin, pectin, water soluble, fat, wax, ash and so on.

Ramie fibre's cross section is a hollow waisted circle, longitudinally it has striations and horizontal grain. Its mechanical properties are extremely good for natural fibre. The cross section of flax fibre is a pentagonal or hexagonal shape, which is not easily rotted in water and it is waterproof. It has the characteristics of resistance to friction and high temperature, fast heat dissipation, difficult to ignite and acid and alkali resistant. Jute fibre has the characteristics of solid, high strength and wear-resisting. It has excellent water absorption (it can absorb up to five times its own weight) and oil absorption. Sisal fibre has many excellent properties such as long fibre, high toughness, elasticity, strong tensile strength, friction resistant and acid and alkali resistance.

Natural fibre has the characteristics of high moisture absorption, fast drying, high strength and low elongation. The structure of natural fibre shows typical composite material characteristics.

2.11.2.1 Harakeke fibre introduction

Harakeke is produced in New Zealand, from sea level to about 1,300 meters above sea level. It is generally found in lowland wetlands and coastal areas along rivers and estuaries, dunes and cliffs. A hundred years ago, harakeke was rich resource in many areas, but today's large wild forests are disappearing and dispersing. Harakeke is often found in gardens, widely used in landscaping projects and wetland restoration, as well as on farmland.

Harakeke is said to be indigenous also to Norfolk Island, though may have been introduced by Māori. The harakeke found on the sub Antarctic Campbell and Auckland islands was taken there by Māori and sealers in the 1800s [34].

Flax is the most important fibre plant in New Zealand (Figure 10, a. harakeke plant; b. extracted fibres; and c. unidirectional non-woven harakeke). Each marae usually has a 'PA harakeke' or linen plantation. Unusual varieties are grown especially because of their strength, softness, colour and fibre content.

Figure 10 Harakeke/New Zealand Flax Fibre [35]

2.11.2.2 The Purpose of the Flax Fibre

The use of flax fibre is varied. Clothes, cushions, dishes, baskets, ropes, birdcages, binding wires, fishing lines and nets are composed of flax leaves. Floating objects or rafts are comprised of bundles of dried stems. Flax rich nectar is utilized to sweeten food and drink. Flax also has many medicinal USES. Sticky liquid or flax produced gum is used for boiling wounds and for toothache. Flax leaves are invoked as dressings for binding broken bones and lustrous leaves. Flax root sap is usually applied to wounds as a disinfectant [34]. Although structurally harakeke is no better than other existing natural fibres such as sisal or hemp, it has a unique property that sets it apart. It stands out among other natural fibres because harakeke produces colour and beauty in a way no mass-produced fibre composite can.

Innovative methods of using this fibre, include fabricating fibre mat composites, decorative tiles, harakeke fibre surfboard prototypes (adding fibre through decorative mat panels) and fibre-reinforced bioplastics. Existing composite industrial methods, such as resin transfer moulding, protrusion moulding, and compression moulding, use the best fibre. Sample prototypes include pull rods, smooth harakeke fibre wall tiles, natural fibre wall tiles (showing the beautiful texture of harakeke), a decorative harakeke fibre laminate (containing harakeke fibre paper), a harakeke fibre target board, and a sturdy harakeke fibre briefcase.

The research in this thesis begins with the industrial extraction of fibres at the history museum of the Templeton linen factory in Riverton, the only genuine linen factory in New Zealand operating from its original site. The museum retained the ability to peel and clean the fibres and continued to sell flax, which was later used for research into new industrial products.

2.11.3 Application of natural fibre composite materials.

2.11.3.1 Natural fibre material products.

The development of natural fibre materials is understandable, which is inseparable from its wide application field. Natural fibre composite materials are used in automobile, construction and transportation.

Natural fibre reinforced materials processed by different processing methods have different uses:

(1) Materials produced by contact forming method can be used for washbasins and other containers, bathing facilities in cruise ships and so on. This kind of compound material commonly uses linen for the reinforcing material, some surfaces have glass fibre, some surfaces do not have the glass fibre; also some surfaces have polyester resin gel with pigment mixed in.

(2) Pipe fittings are usually processed with winding technology. The twisted linen material can be used, untwisted yarn, felt and fabric. Its products are primarily used in various transmission pipelines and industrial pipelines, such as fibre winding thermosetting resins. Fibre winding reinforced thermosetting resin mortar tubes and fittings etc.

(3) Extruding can produce various kinds of workpieces with different applications and intricate shapes. The natural materials used in extrusion are also as stripped, yarn, non-woven felt and fabric. Because the structure of the natural fibre is very loose, and the fibre is in a single direction, it must be very carefully extruded to avoid tangling. Bidirectional materials can be made with felt and fabric.

2.11.4 Natural fibre material application

The application of natural fibre materials has become a hot spot of research by scholars all over the world. The research on the application of natural fibre has achieved great development and is gradually moving towards industrialization, even forming an industrial chain from planting to harvest, to fibre processing, to material moulding.

2.11.4.1 Construction industry

The application of natural fibres in architecture and civil engineering has a long tradition. The excavation of the ruins of Banjo village in Xi 'an proves that as early as 5000 BC, Chinese people began simple processing of natural fibres, which is also considered to be the earliest example of using natural fibres as building materials.

In recent years, due to the progress of technology, in all aspects of the natural fibre material cost, quality and performance (including mould and moth-proofing, sound insulation, heat insulation, mechanical properties and stability of the product, etc.) were significantly improved, the natural fibre also gradually entered the building and civil areas and has become the first choice for green building materials.

Natural fibre's hollow structure makes it have good sound insulation and heat insulation performance. Therefore, natural fibre sprayed products such as insulation sound-absorbing material used in building

interiors are favoured by people. With natural fibre as raw materials, with resin or inorganic gelled material man-made board using adhesives is a comprehensive utilization of timber and is an effective means of utilising agricultural by-products, and making cost savings and also is an effective measure to create new products instead of using traditional wood.

In 2008, housing minister Caroline Flint officially unveiled the Barratt Green House, Britain's first zero-carbon home, which met the government's sustainable housing standard at level 6. In 2009, the Renewable House, designed by Archial Architects in the innovation park of the architectural research institute in the UK, also unveiled the house, as shown in Figure 11. The roof is of natural fibre insulating blanket, the carpet is made from natural fibres, and the outer wall used a new material called Hempcrete. Hempcrete is composed of hemp fibre and lime glue adhesive creating a compact lightweight material, having a good heat insulation performance and has useful application prospects. It also allows renewable houses to meet the UK government's sustainable housing at level 4 standard, which is almost carbon-free [36].

Figure 11 Renewable house located in the BRE Innovation Park [36]

3 Chapter 3: 3D Weaving Construction Using Continuous Natural Fibres

3.1 The overall design of the continuous natural fibre 3D weaving machine

3.1.1 Design principles and methods

The movement of the 3D weaving machine depends upon the three stepper motors of the slide table for positioning. At the same time the wire feeding system feeds continuous fibre to generate the product under construction. The main functions of the control system for the stepper motors in this design include accelerating and decelerating the stepper motors, setting the speed of each motor and intelligently controlling of the motors conveniently and with precision. The main circuit consists of a progressive motor control module for each axis. What the stepper motor driver receives is an impulse signal. The driver will give the motor a pulse to turn the motor around by a fixed angle. In this way, the acceleration and deceleration of the stepper motor, as well as the forward and backward rotation of the motor can be controlled, and the speed of the motor can be adjusted to facilitate the judicious control of the motor. An adjustable pulse width signal is generated by the Arduino microcontroller and input to the TB6600 motor driver chip to control the stepper motor.

3.1.2 The hardware design

The hardware part of the 3D weaving machine is divided into several modules: fibre feed motor and motor driver, Arduino microcontroller, power supply, three stepper motors, three stepper motor drivers and a three-axis slide table. The power supply is connected to the stepper motor driver to power the entire machine and the Arduino is powered by the USB cable from the computer. The 3D weaving machine takes the Arduino microcontroller as the core, and connects to each axis' motor driver to control the operation of the stepper motor for that axis, thus actuating the sliding table to control the movement of the overall machine in 3D space. Limit switches are attached to both ends of the slide table (for each axis) to prevent the slide table from moving beyond the allowable range. When the slide touches the maximum limit switch of the maximum distance, feedback is provided to the microcontroller to reverse the motor direction and return the slide to the minimum limit switch. Another stepper motor in the wire feeding mechanism controls the fibre feeding movement. The hardware frame figure is shown in Figure 12.

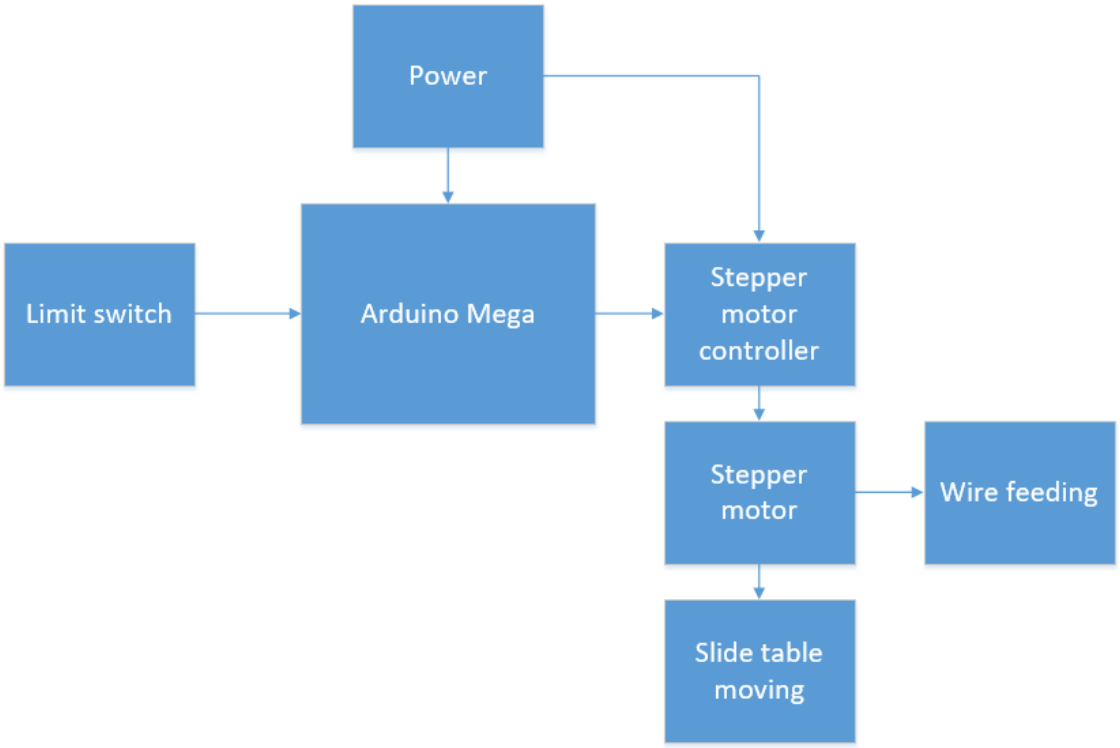

Figure 12 Hardware design framework

3.1.3 The software design

3.1.3.1 The language of Arduino

Arduino is based on the open source simple I/O interface and has a Processing/Wiring development environment that uses code similar to Java and C programming languages. It mainly comprises two parts: The hardware part is the Arduino circuit board which can be used for wiring connections; the other is the Arduino IDE, which is the programming environment on the computer. The user writes code in the IDE, uploads it to the Arduino board, and the program tells the Arduino board what to do. Arduino is able to perceive the environment through a variety of sensors. By controlling light, motors and other devices, Arduino can feedback and influence the environment. The microcontroller on the board can be programmed using Arduino's programming language, compiled into binary files and burned into the microcontroller. Arduino-based projects can either contain only Arduino, or they can contain Arduino and additional software running on a PC that communicates with each other (such as Flash memory, additional processing, MaxMSP etc.) [38].

Arduino is not only the most popular open source hardware in the world, but also an excellent hardware development platform and the current trend in hardware development. Arduino's simple advanced methods enables developers to pay more attention to creativity and implementation and complete their own project development faster, which greatly saves the cost of learning and shortens the development cycle [38].

Arduino features:
1. Open source circuit diagram design, program development interface is a free download and can also be modified according to the need of the user.

2. Low price micro-processing controller (AVR series controller) can be powered through the USB interface, no external power supply is needed, and external 9 VDC input can also be used.
3. The Arduino module circuit diagram is available in the Eagle CAD PCB and SCH format

4. A complete micro processing control module can be built that operates independently which can be easily connected with sensors and various electronic components (e.g. infrared rays, ultrasonic waves, thermistors, photosensitive resistors, servo motors, etc.)

5. Supports a variety of interactive programs, such as Flash, Max/Msp, VVVV, PD, C, Processing, etc.

6. In terms of application, Arduino can break through the interactive limitations of devices that can only be input by mouse, keyboard, CCD and other devices in the past, and achieve interaction of single or multi-player game more simply.

3.1.3.2 Arduino IDE

The Arduino IDE is developed based on the processing IDE. For beginners, it's easy to master and flexible. Arduino language is developed based on wiring language, which is a secondary packaging of the avr-gcc library. It does not require too much single-chip microcomputer foundation or a programming foundation. After simple learning, it can also be developed quickly.

The following figure (Figure 13) shows the Arduino operational interface. Arduino IDE is a professional Arduino development tool, mainly used for the preparation and development of Arduino programs. With open source circuit diagram design, supports ISP online burn, while supporting Flash, Max/Msp, VVVV, PD, C, Processing and other compatible features of a variety of programs.

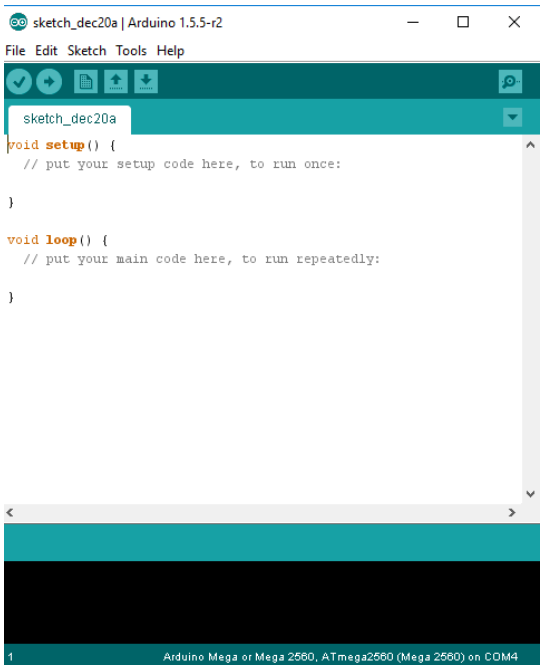

Figure 13 Arduino operational interface

When the program is completed and ready, click Update, and the IDE compiles and uploads the program to the Arduino board. Figure 14 is a screen shot of the serial port monitor, which is relatively

simple in function compared with the numerous serial debugging software circulating on the Internet. The correct baud rate, for both receiver and transmitter must be the same, or garbled code will be received.

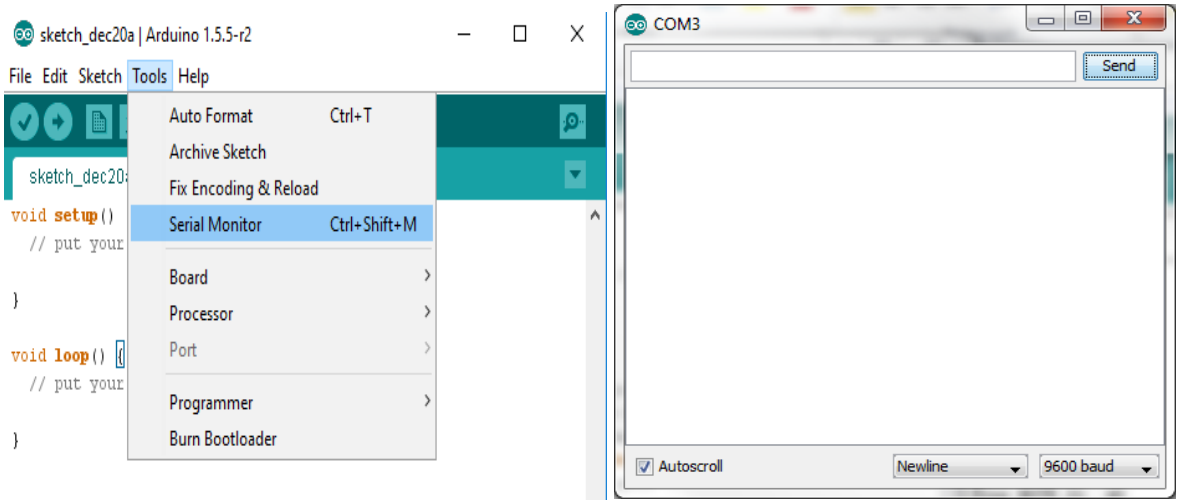

Figure 14 Arduino IDE Serial Monitor

In this project, the user needs to open the program and connect to the Arduino via USB. Upload the file and open the serial port monitor according to the user instructions to control the movement of the 3D weaving machine.

3.1.4 Equipment preparation

The components list for building the 3D weaving machine is as follows:

4 × stepper motors
4 × stepper motor driver
1 × switching power supply
2 × synchronous belt linear guide module (X-axis)
1 × synchronous belt linear guide module (Y-axis)
1 × synchronous belt linear guide module (Z-axis)
1 × breadboard
An amount of DuPont equipment wire
1 × power cord
1 × Arduino Mega 2560
5 × belt linear guide base
3 × stepper motor direct connection seat
5 × coupling unit
1 × coupling rod
6 × inductance link pieces
6 × limit switches
1 × L-shaped side bar
A number of M3 screws and nuts
A number of M5 screws and nuts
Number of MDF laser cut parts
Number of polymethyl methacrylate laser cut parts
Number of 3D printing parts

3.2 Hardware module of the 3D slide table

3.2.1 The basic performance of each module

3.2.1.1 Arduino microcontroller module

The 3D weaving machine control system adopts Arduino microcontrollers. Arduino is a convenient, flexible and convenient fit to the open source electronics prototyping platform. Because of the Arduino's easy programming, and the use of its more modular components it is easy to control all the motors running in accordance with the requirements. Three distinct types of Arduino models can be used in the design: Arduino Uno, Arduino Mega and Arduino Nano. The comparison of the functions is illustrated in Table 3 below. Arduino Mega is deemed to be the best single chip microcomputer to control all components by comparing various models of Arduino single chip microcomputer. It has enough space and the required pins for the components of the machine needing to be used, such as motors and all the sensors.

Table 3: Arduino Models functional comparison

	Arduino Model		
Feature	Arduino MEGA 	Arduino Uno 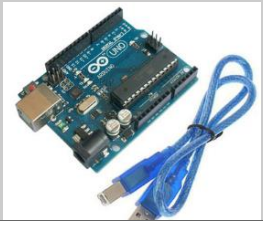	Arduino Nano 
Operating Voltage	5V	5V	5V
Input Voltage(recommended)	7-12V	7-12V	7-12V
Input Voltage (Limits)	6-20V	6-20V	6-20V
Digital I/O Pins	54	6	14
Analog Input Pins	16	6	8
DC Current per I/O Pin	20mA	20mA	40mA
Clock Speed	16MHz	16MHz	16MHz
Flash Memory	256KB	32KB	32KB
SRAM	8KB	2KB	2KB
EEPROM	4KB	1KB	1KB
Dimensions	53.3mm x 101.52mm	53.4mm x 68.6mm	18mm x 45mm
Power	P = IV = 50mA*5V = 250mW	P = IV = 46.5mA*5V = 232.5mW	P = IV = 2.4mA*5V = 10.8mW
Weight	37g	25g	5g

3.2.1.2 Motor and motor driver module

A stepper motor is an open-loop control motor that converts an electrical pulse signal into angular displacement or linear displacement. The motors speed and stop position depends only on the pulse signal frequency and number of pulses, it is not affected by load change. When the stepper driver receives a pulse signal, it drives the stepper motor according to the set the direction at a fixed angle, known as the "step angle". Its rotation is based on the angle of the fixed step. The angular displacement can be controlled by controlling the number of pulses, which achieves an exact angular location; at the same time, the speed and acceleration of motor rotation can be controlled by controlling pulse frequency, to achieve speed regulation.

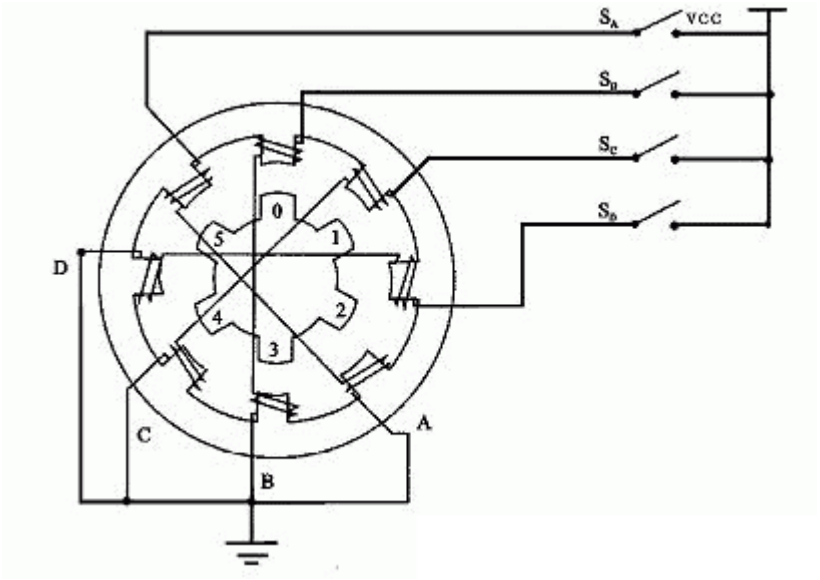

Figure 15 Stepper motor schematic diagram

As shown in Figure 15, there are many pairs of magnetic poles inside the stepper motor. If the energized state remains unchanged, the stepper motor will remain at a certain fixed position. Only by constantly changing the energized state of each magnetic pole pair, can be the stepper motor keep rotating. Therefore, stepper motors cannot be directly connected to dc or ac power supply to work, a special drive power supply (stepping motor driver) must be used. The controller (a pulse signal generator) can control the angular displacement by monitoring the number of pulses. Therefore, to achieve accurate positioning, the speed and acceleration of motor rotation can be controlled by controlling the pulse frequency, and to achieve speed regulation. The stepper motor is the main actuator in innovative digital program control systems, which are extremely widely used. Unless overloaded, the motor speed and stop position only depend on the frequency and pulse number of the pulse signal.

3.2.1.2.1 NEMA23 stepper motor

This is an independent motor drive system, one stepper motor is used to drive the movement of each sliding table (one per axis). The rotation of the motor will drive the movement of the sliding table forward or backwards. Controlling the rotation direction and steps of each motor controls the movement distance of each axis of the sliding table. This design is very close to that used in many 3D printers. The machine also controls the maximum number of rotations of the motor to prevent the sliding platform from exceeding its own movement limit. The advantage of using a single motor for a

single slide table is that it is the simplest and cheapest design, which requires only one motor and one slide table to complete the movement of a single axis. Therefore, it takes just three stepper motors and three slides table to get three dimensions of motion. The overall system configuration has a very minor impact on the environment as fewer components are required. The power consumption of the motor is lower than that of three or four actuators. This also saves space, since only one motor is required to drive the slide plate. However, it lacks a comprehensive design that is operable and flexible. In the case of composite wire feeding movement, the path may be beyond the range of movement of the machine, so the number of revolutions must be limited to control the movement range of the sliding table. But these benefits outweigh the performance disadvantages. The following figures 16-18 show the dimensions and the internal structure of a stepper motor.

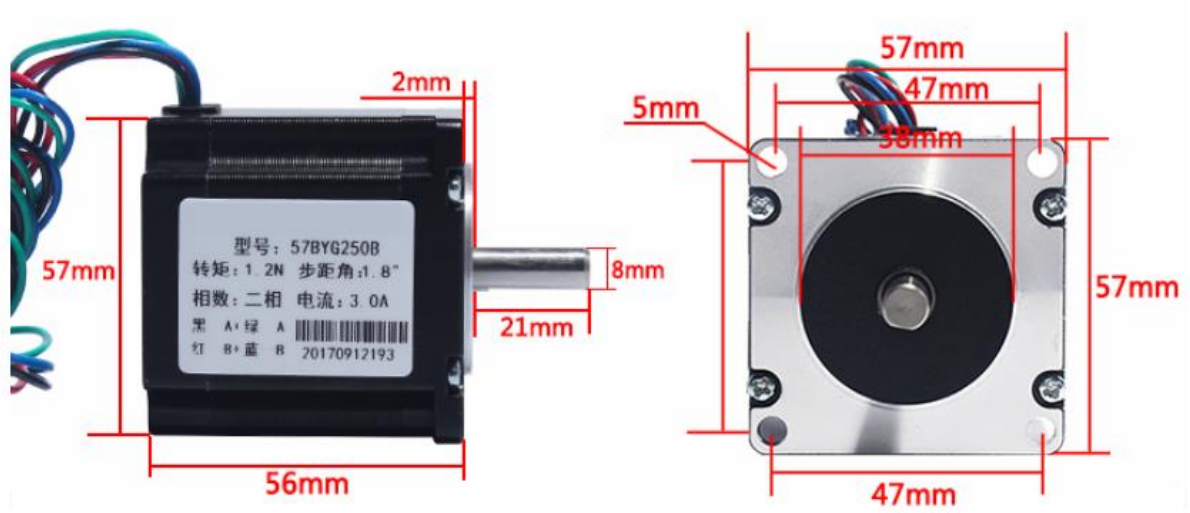

Figure 16 Stepper motor dimensions

Figure 17 Internal structure of stepper motors

Model	NEMA23 Stepper Motor
Size	57*57*56 mm
Maximum Torque	1.2 Nm
Phase	2
Step angle	1.8°

Figure 18 Specifications of the stepper motor

3.2.1.2.2 Stepper motor driver

The stepper motor driver is an electronic actuator that converts electrical pulses into angular displacement (Figure 19). When the stepper driver receives a pulse signal, it drives the stepper motor to rotate at a fixed Angle (called "step Angle") in the set direction. Its rotation is performed step by step at a fixed Angle. The angular displacement can be checked by controlling the number of pulses to achieve accurate positioning. At the same time, the speed and acceleration of motor rotation can be controlled by controlling the pulse frequency, to achieve speed regulation and positioning. The stepper motor driver designed in this project is a TB6600 (Figure 20). Since a stepper motor does not directly operate on a dc or ac power source, a dedicated drive power supply (stepper motor driver) must be utilized. The controller (a pulse signal generator) can control the angular displacement by controlling the number of pulses to achieve accurate positioning; at the same time, the speed and acceleration of rotation of the motor can be controlled by controlling the frequency of pulses so as to achieve speed regulation.

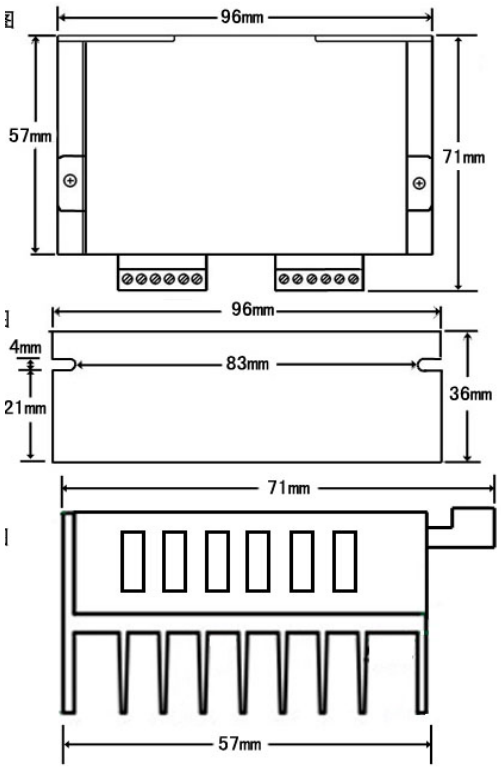

Figure 19 Stepper motor driver dimensions

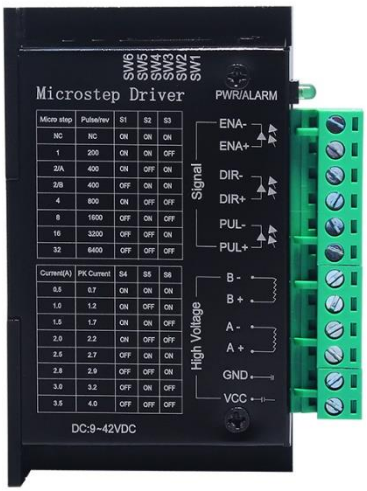

Figure 20 Stepper motor driver connections

3.2.1.3 Power supply module

The power supply of the 3D weaving machine in this project is an S-150 single output switching power supply. Figure 21 indicates the size of the power module. Single output switching power supplies are characterised by high efficiency, high reliability and low cost. In order to ensure a reliable power supply, 230V AC input voltage and 12V DC output voltage are used for the power supply to the motor system and motor driver system. The 230V AC input voltage of the power supply will be connected to the ac outlet and the 12V DC output voltage will be connected to the motor drivers. (Figure 22).

Figure 21 Size of power supply

The Model	S-150-12
DC OutPut Voltage	12V
AC Input Voltage	230V
Overload Protection	115%-135% Protection: cut off output
Working Temperature	-10℃ - 50℃

Figure 22 Power supply specifications

3.2.1.4 Continuous Fibre feeding module

A wire feed mechanism is utilized to feed the long and continuous fibre to the wire feed terminal, and the wire feed needs to be smooth and reliable. European natural flax fibres have been selected for this study as the raw thread generally has a diameter of 1-2 mm. The reason why New Zealand natural fibre (harakeke fibre) was not selected was the raw material was currently not available as a long and continuous yarn so it does not meet the material requirements of this study. Therefore, in this study the material selected was the available European flax fibre. The wire feeding mechanism is comprised of a stepper motor, which can control the wire feed speed, opening and closing at any time by the command of the control module. The wire feeding mechanism and wire feeding terminal adopt a combination mode of pushing, to ensure that the wire feed is stable and reliable and avoid the fibre being broken or misfeed.

The wire feed mechanism is composed of a laser cut polymethylmethacrylate frame and 3D printed ABS parts. Figure 23 shows the 3D SolidWorks design of the designed continuous fibre feeding module.

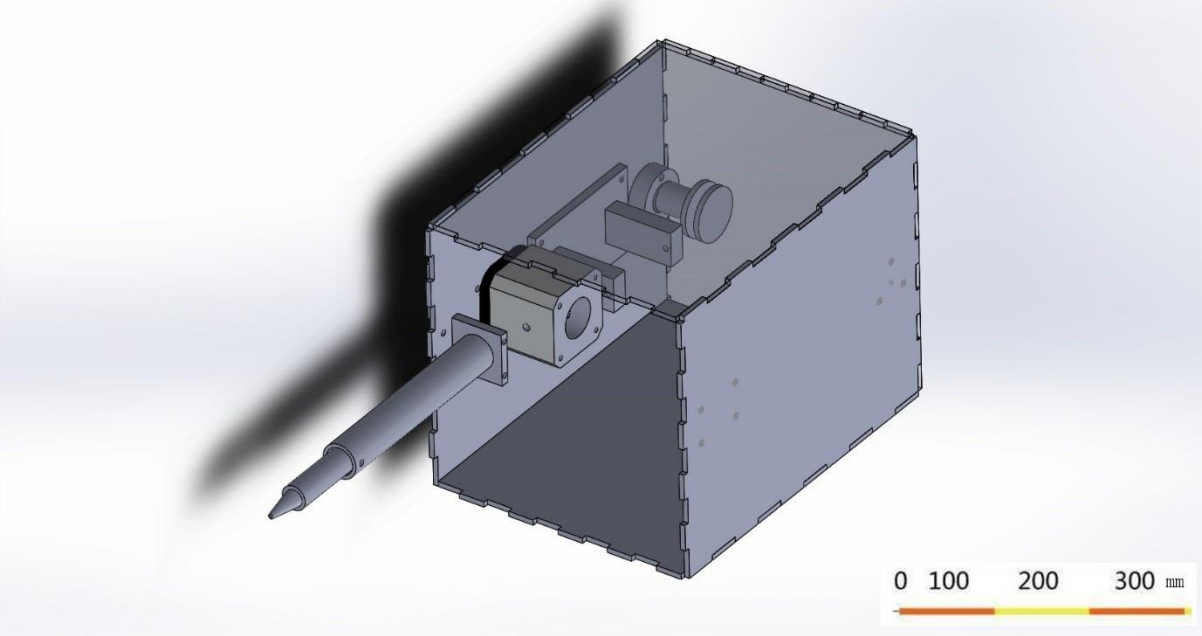

Figure 23 3D model of the continuous fibre feeding module

(1) Continuous fibre spool station

The first station of this prototype is the feeding module responsible for controlling the delivery of the European flax fibre to the construction module. To control the speed of the feed of flax fibre into the feeding nozzle includes providing a means for moving the fibre yarn through the stepper motor and keep the yarn straight, to make sure the fibre yarn will not be damaged during the transition. The fibre feeding speed of this system needs to be coordinated with the translational speed of the sliding platform, so as the platform moves the fibre can be feed simultaneously and synchronise with the movement.

The design of this station for controlling the spool of fibre yarn allows for a spool of any continuous fibre yarn to be easily removed and replaced with a new spool. The spool used was an empty Mark One 3D printing spool, wrapped with the long and continuous natural fibres. The spool is attached to the station by the 3D printed shaft. The shaft is designed with an outer diameter that allows for the

shaft to fit within the hole in the spool. Also, at the end of the shaft there was a space designed for a magnet to be positioned between the shaft and the acrylic walls. When the spool was connected to the shaft, a steel pin will be put through the shaft and locks the spool onto the shaft due to the magnet. Figure 24 shows the fibre spool station.

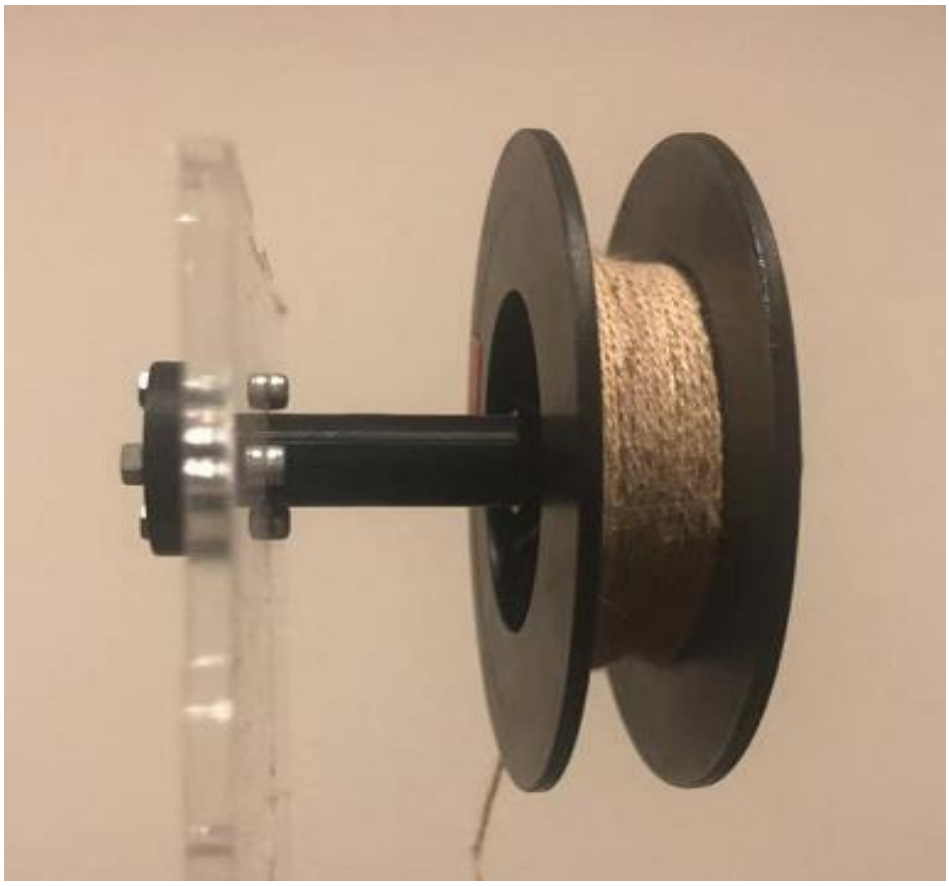

Figure 24 Continuous Fibre Spool

(2) Straightening station

Before the continuous fibre material enters the wire feeding motor, it has to be straightened with a straightening device. The wire straightening device from an existing factory design generally adopts the use of three straightening wheels with grooves, one straightening wheel above and two straightening wheels below. The wire goes through the grooves between the straightening wheels to achieve straightening of the wire. As the straightening wheel of the wire straightening device mentioned above is fixed and installed on the rack, the wheelbase cannot be adjusted and cannot been adjusted to wire of different diameters, nor the straightening effect can be adjusted.

Therefore, an adjustable “wire” straightening device is designed in this project, which includes a bracket and 3D printed shaft. The 3D printed shaft was connected to the acrylic walls of the housing. The feature of the bracket is that there is a slide-way and a straightening hole in the fixed bracket. The straightening bracket is fixed on the 3D printing shaft with a retaining nut, and a slider on the bracket is locked with the nut. The two brackets are attached to the 3D-printed parts and can be adjusted to align it to the straightener hole through a transverse slide-way to adjust the direction of the fibres from the spool to the wire feeding motor. The universal model has the characteristics of good, effective and high adaptability. Figure 25 shows the straightening station.

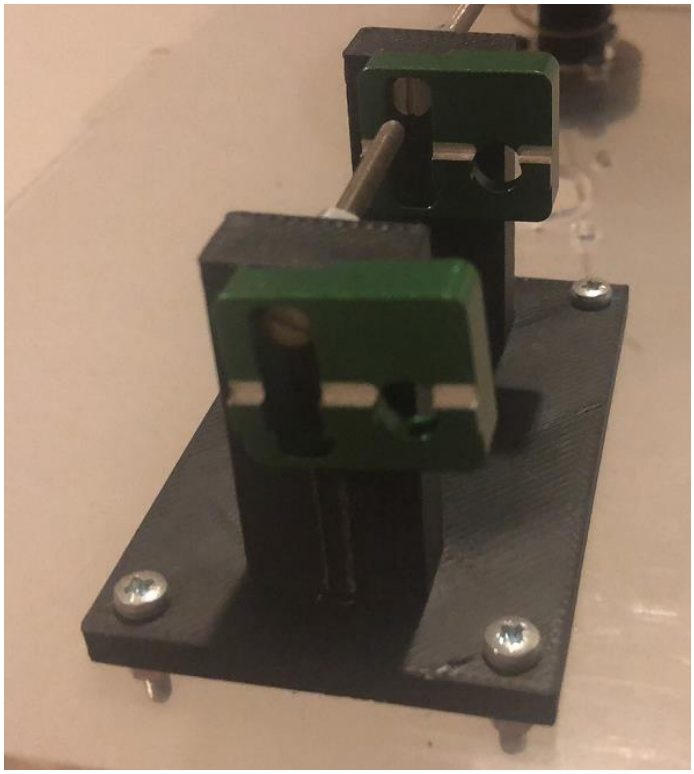

Figure 25 Primary Straightening station

There is another straightening station positioned between the feeding station and the nozzle station. The following figure shows the second straightening station. All the composition of this station is made up of 3D printed components. It consists of a balance of the hole and another roller wheel. The function of this mechanism is to ensure a balanced condition between the wire feed mechanism and the nozzle mechanism. Figure 26 shows the subsequent straightening station.

Figure 26 Secondary straightening station

(3) Feeding station

The wire feeding station and its system are essential components of the whole wire feeding mechanism. It is designed to have a novel spring support for a spring structure with v-shaped grooves, and it has the characteristics of auto-adjusting to the fibre monofilament, which will ensure the accuracy and stability of the feed. The wire feeding mechanism's primary requirement is to feed the fibre smoothly

and reliably to the nozzle. The wire feeding station of the wire feeding mechanism adopts a pair of wire feeding wheels for wire feeding, one of which is the driving wheel, it connects to the rotary shaft of the transmission, and the other rotary shaft of the transmission is coupled to the rotary shaft of the driving motor to receive power transmission. The other is the compression wheel (the passive wheel), which rotates by friction with the driver and the filament, thereby transmitting the filament.

The main function of the driving wheel is to directly transfer the power of the wire feeding motor to the natural fibre monofilament, so that it can be propelled forward, and continuously send the natural fibre monofilament into the nozzle until the construction in the working area is completed. One of the characteristics of direct transmission of power to natural fibre monofilament is that greater power can be obtained from natural fibre monofilament. In order to make the power transfer between the driving wheel and the natural fibre monofilament more sufficient and increase the contact and friction between the two, the driving wheel is fixed in two v-shaped grooves, in which each v-shaped groove is equidistant from the wheel edge. The purpose of this is to replace the natural fibre monofilament with other diameters due to the type of wire feeding work to be done, and to use natural fibre monofilament of different sizes by changing the driving roller. Figure 27 is a schematic diagram of the wire feeding wheels. The type of groove on the surface of the driving roller is very important, as it affects the efficiency of wire feeding. Because the diameter of the fibre has a certain variation in size, a U-type groove is not suitable. If the size of a single fibre is too large, it may not be transported into the groove or it may need much conveying tension, then it would possibly slip in the groove, and unable to ensure accurate wire feeding speed. In this design, the fibre can be driven by a larger force, and the wire feeding speed accuracy and stability can be maintained.

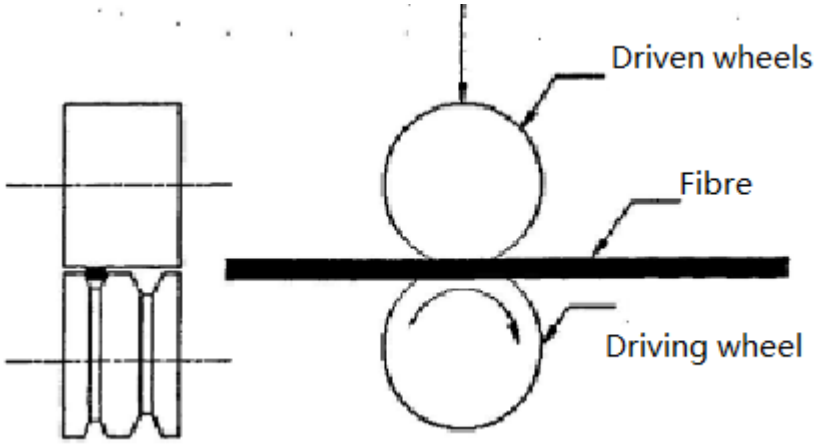

Figure 27 Wire feeding wheels

As can be observed in Figure 28, the feeding unit will use a spring to hold the roller of the upper and lower parts, mainly to allow the gap between the rollers to automatically adapt to natural fibre monofilament of different thicknesses. After comparison, a 3 mm diameter tension spring was selected. When using the thicker natural fibre monofilament, the natural fibre monofilament is transported by the wire feeding wheel with greater pressure on the spring, and the spring automatically expands outward under the external pressure to adapt to the thickness of the natural fibre monofilament, and then forms a greater reaction force on the natural fibre monofilament, so that it does not slip and offset. This achieves the automatic adjustment of the natural fibre monofilament pressure, which will ultimately guarantee the accuracy and stability of the delivery speed and controlled.

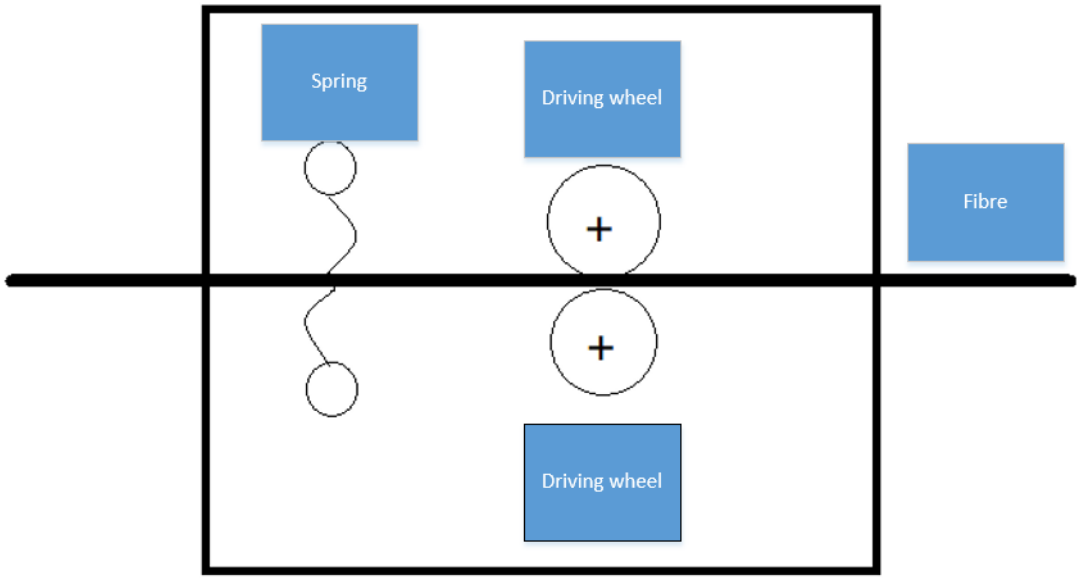

Figure 28 Wire pressure stage

Figure 29 below shows how the feeding mechanism was constructed in the feeding station.

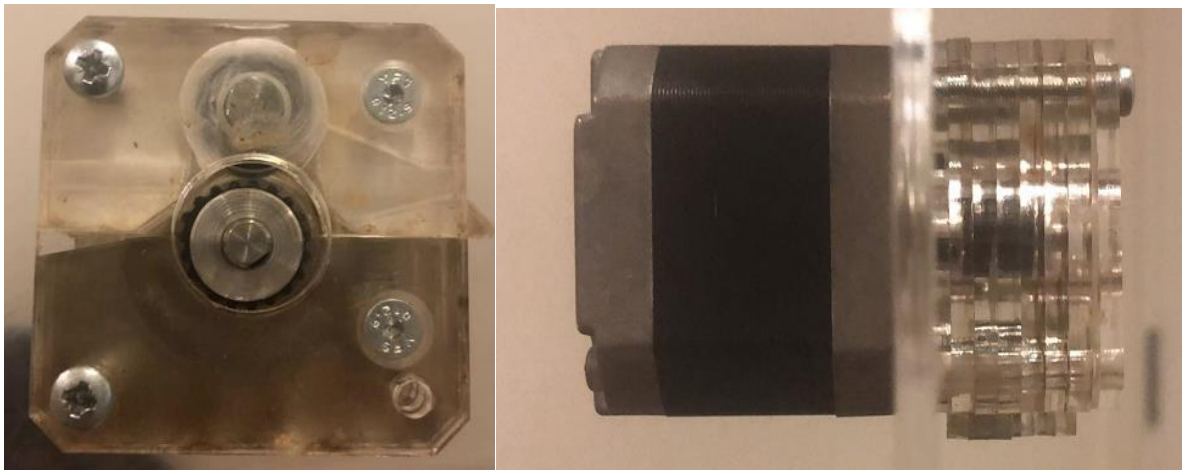

Figure 29 Feeding station

(4) Nozzle station

The nozzle system is mainly made up of the following parts: The bottom conveying nozzle, the spring chamber, the top fixer and the upper connecting parts. The 3D SolidWorks model in Figure 30 shows the components of the entire nozzle system. All the parts of the nozzle system were made using the 3D printing material.

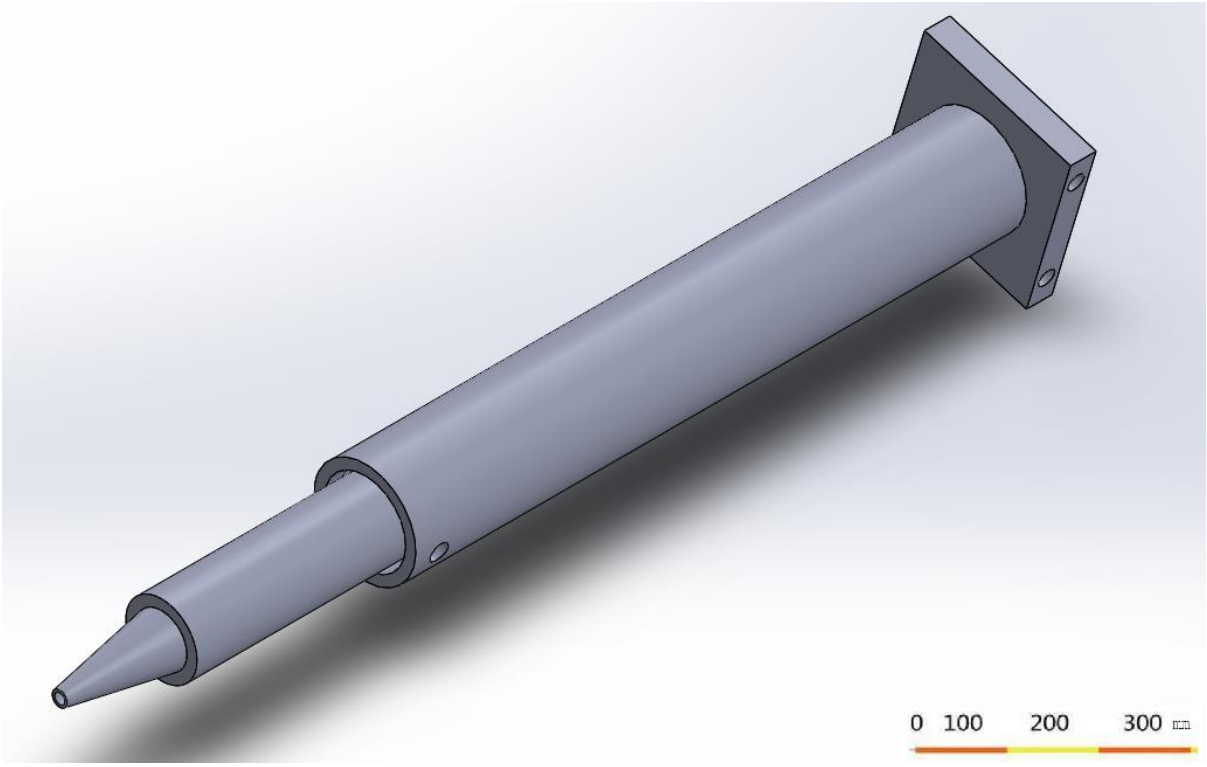

Figure 30 3D model of the nozzle station

The nozzle system is made up of five parts. Natural fibre monofilament material passes through all the components. And the bottom of the nozzle station has a design is similar to a nozzle, and the spring gives the nozzle a certain amount of pressure to extrude the natural fibre monofilament (Figure 31 and Figure 32). The nozzle header will extrude material along the required cross-sectional design profile and orbital trajectory motion of the construction. Initially testing on the x-y plane, the fibre material has been sent out of the nozzle and has been used to travel back and forth along the designed path, to achieve the diverse architectural shapes and images that need to be produced. The technique used is similar to the technique used in wrapping yarn around a board of nails. Under the control of the computer, the nozzle system can move freely in the x-y plane, and its feeding and retracting are controlled by the stepper motor. It will be next fixed to the Z-axis, which will control the lifting and lowering of the nozzle. When working, first the spacing of each nail or the spacing and width of each bracket is determined and then the corresponding information is entered into software. In this way, the nozzle can be controlled to move along the path, and the natural fibre monofilament will be bonded to the pre-designed template. As a result, the fixed pins will be found repeatedly until the last point, and all the winding patterns will form the required solid model (Figure 32).

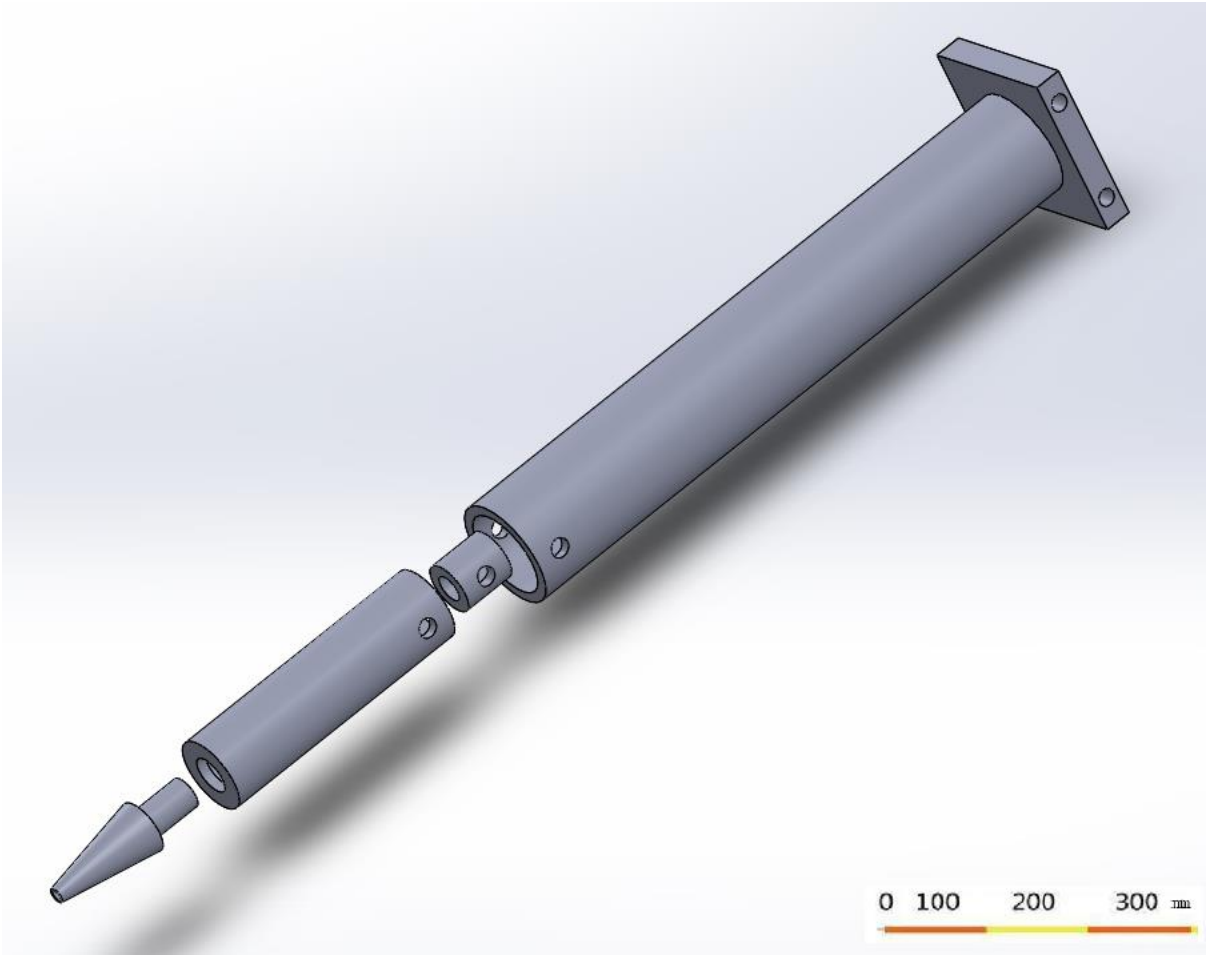

Figure 31 3D Exploded drawing of nozzle station

Figure 32 Components of nozzle station

After designing the wire feeding mechanism, it was found that the pressure at the nozzle of the wire is still not enough to affix the single natural fibre material on the plane in the process of wire feeding without fixed nails. Therefore, a pressure roller was added to the wire feeding station composed of a spring loaded castor to increase the pressure of the natural fibre monofilament to the work plane, which will allow the material to be attached to the plane. This pressure roller was designed in two parts, the 3D printing C-shape with the spring and the bottom castor wheel (Figure 33). When the C-shape connect to the feeding system, the computer will control the height of the Z-axis and give sufficient pressure between the material and the plane. If the pressure is too low, the material will not adhere to the plane. If the pressure is too high, the castor wheel will stick to the plane, which may damage the operation of the whole system.

Figure 33 Pressure roller

The following figure (Figure 34) shows in the overall design of the wire feeding module. The wire feeding mechanism is mainly composed of a stepper motor. Under the command of the control module to the motor driver, it can repeatedly control the start and stop of wire feeding at any time.

Figure 34 Continuous fibre feeding module

3.2.1.5 Composition of X-Y-Z axis sliding table (3D sliding table)

The linear sliding table is a type of mechanical structure that can provide linear motion. It can be used horizontally or vertically or combined into a definite motion mechanism -- that is, in the automation industry, it is usually called XY axis, XYZ axis and other multi-axis motion mechanisms. This mechanism is used in different industries and have unique names, more common names are: linear sliding table, electric cylinder, electric sliding table, mechanical arm, manipulator and so on. The linear sliding table is usually used in conjunction with the power motor, and other required workpieces are installed on its sliding block to form a complete motion conveying system component for automatic cycling of the workpiece or reciprocating movement.

There are for two types of linear sliding tables widely used at present, synchronous belt type and ball screw type. The 3D weaving machine in this project utilized a synchronous belt type linear sliding table. Its main components are constructed, including a linear guide rail, an aluminium alloy profile, a coupling, a motor, and a photoelectric switch (Figure 35). The working principle of the synchronous belt type is that the belt is installed on the transmission shaft on both sides of the linear sliding table, which serves as the power input shaft, and a slider is fixed on the belt to mount the workpiece or other equipment. When there is input, the slider moves by driving the belt. This design makes reference to rapid prototyping technology, which is the principle of any complex three-dimensional parts into a planar graphics stack. The x-y axis linkage effects the movement of the wire feeding mechanism to the contour plane, while the Z-axis drives the height direction of the wire feeding mechanism to realize feed and the control of the graph composition. The motion mechanism is

composed of x-y-z stepper motors and synchronous belt transmission mechanism. The control module controls the motor motion to complete the plane movement of the x-y axis and the height feeding of the Z-axis. The Z-axis direction adopts a reduced motion speed to ensure the accurate feeding of the Z-axis. The plane motion of the x-y axis uses a higher speed to ensure the reduction of working time and the still maintain sufficient accuracy of motion.

There are four limit switches built on each end of the X-axis and Y-axis slide table. A limit switch is an electrical switch used to limit the movement position of motorized equipment. Limit switches are contactless and non - contactless. This product type has contact limit switches. On both sides of the slide table, the travel switch is installed, and the limit position stop block is installed on the fixed point of relative movement. When the mechanical contact of the travel switch hits the block, the control circuit is switched off (or changed), and the slide stops or changes operation. Due to mechanical inertia, this travel switch has a definite "over-travel" to protect the switch from damage.

All parts of the sliding table used in this project are customized by the Wanxin Tai hardware machinery co., LTD. which includes 2 * 800 mm X-axis slide tables, 1 * 600 mm Y-axis slide table, 1 *600 mm Z-axis slide table and other accessories. All the platforms cost about $700 in total.

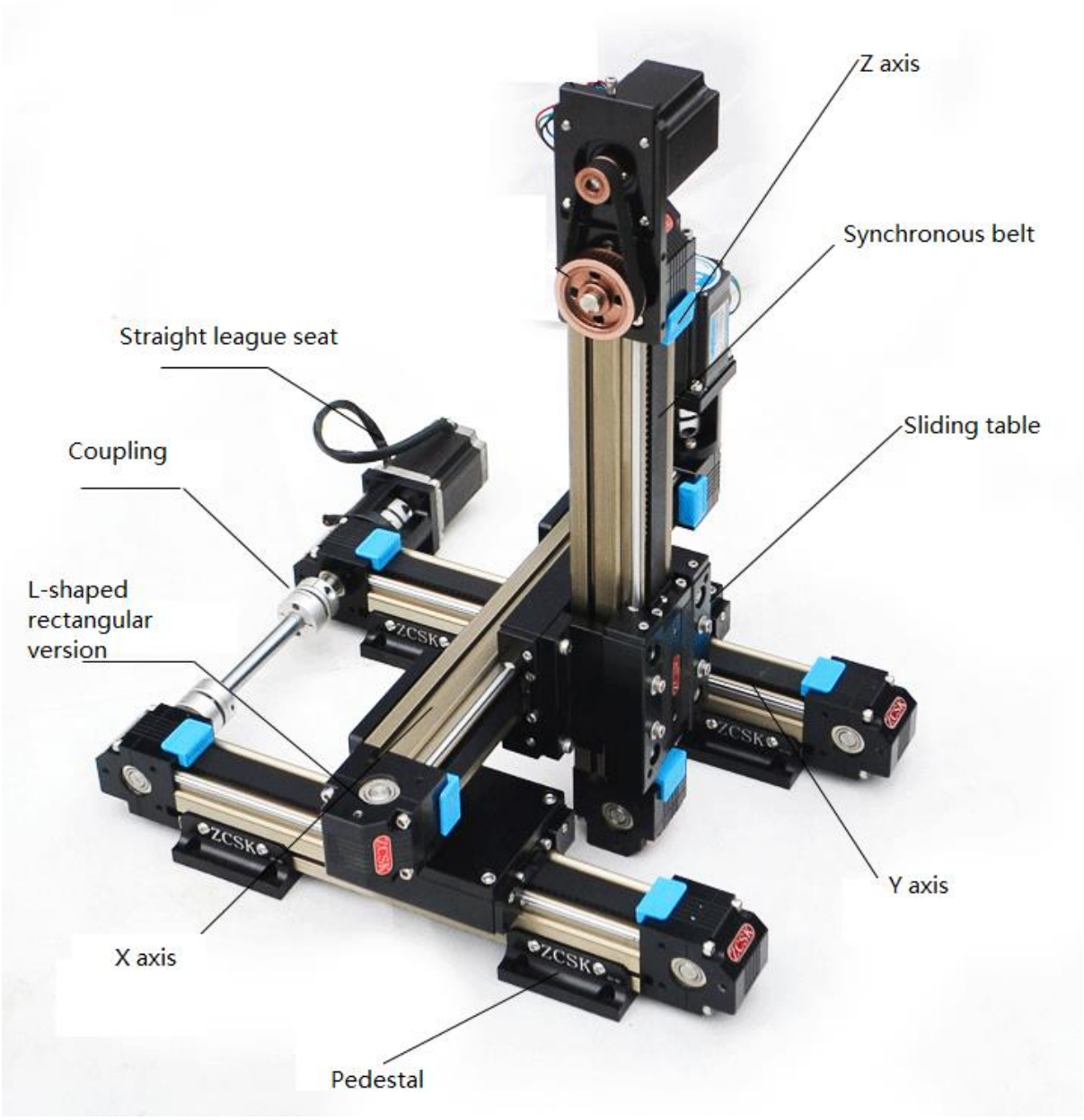

Figure 35 3D slide table

Assembly of the 3D slide table:

A laser cutter was used to cut the 3 mm medium-density fibreboard (MDF) material and the four surfaces joined with hot glue, and linked to the roof plate according to the mounting holes (Figure 36).

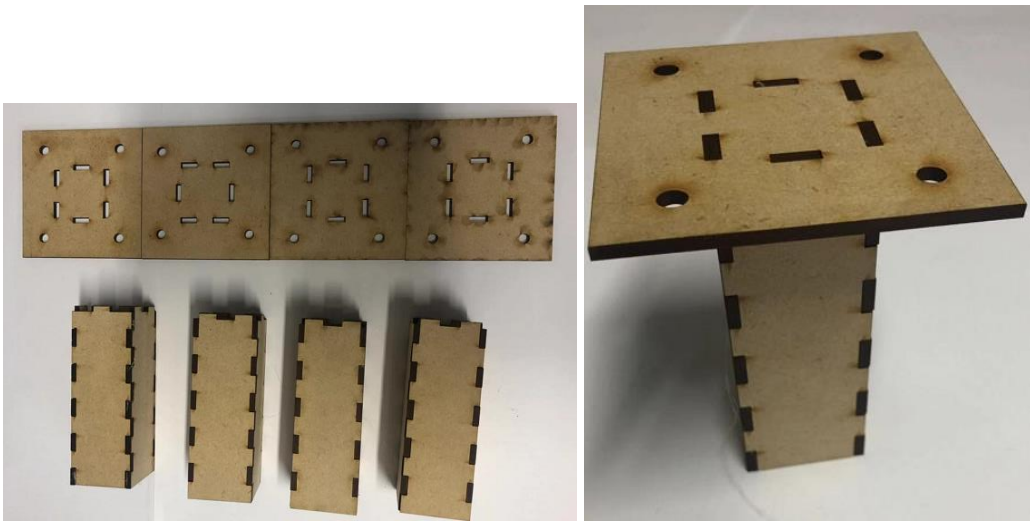

Figure 36 Slide table pedestal

Connect two of the pedestals to the X-axis slide table using four M5 screws and nuts (Figure 37).

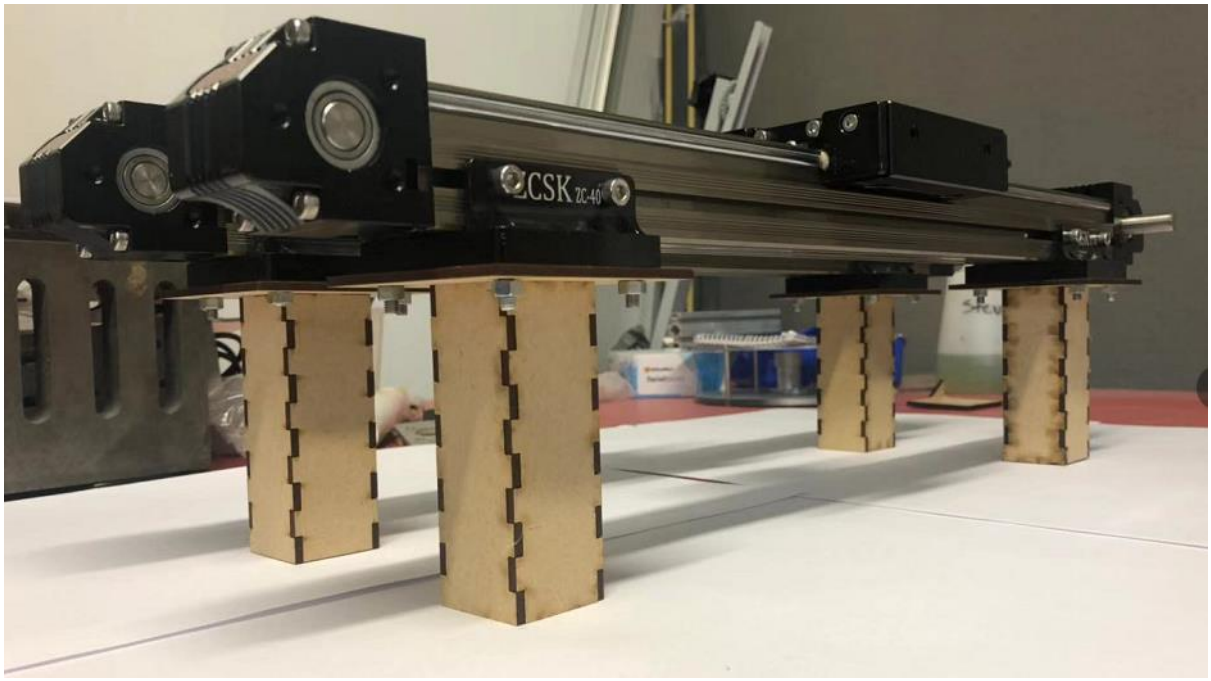

Figure 37 The base connection to the X-axis

First, secure one end of each of the two couplings on the x axis, then connect the other end of the couplings to the two x-axes with an aluminium shaft (Figure 38).

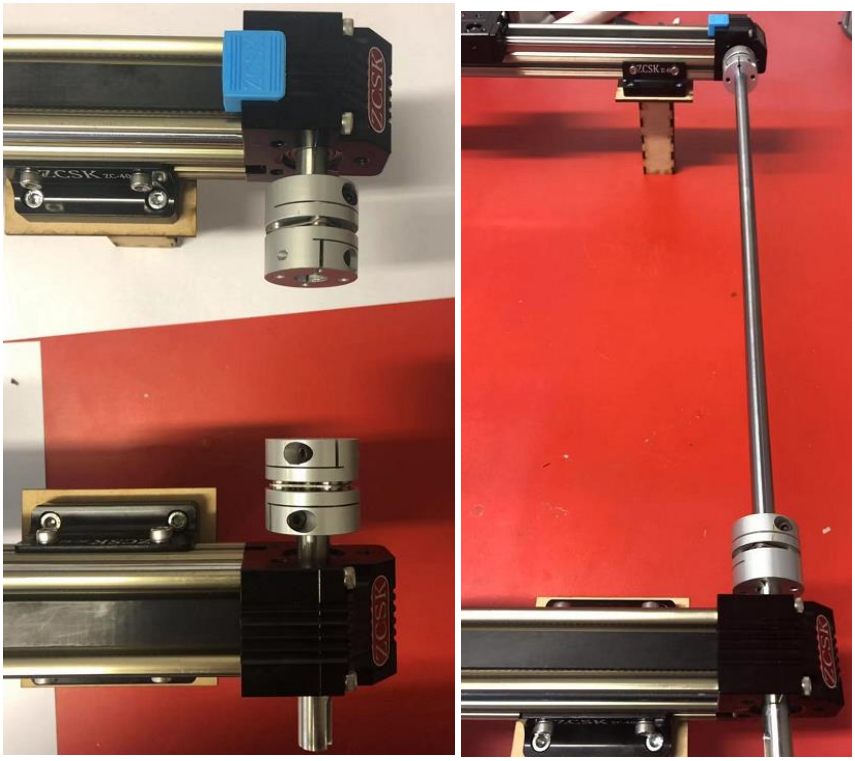

Figure 38 Connecting the shaft couplings

Connect two L-shape brackets to the X-axis slide table (Figure 39).

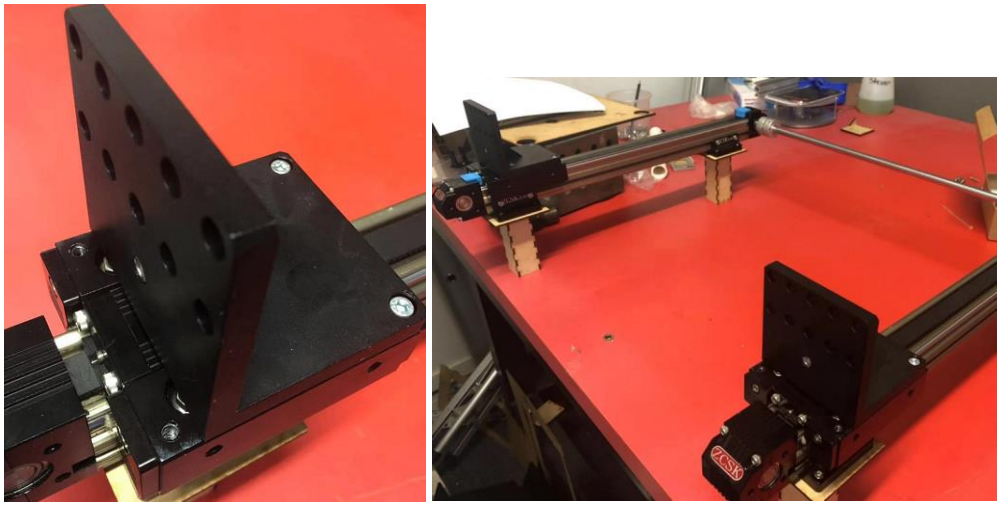

Figure 39 L-shape brackets

Connect the Y-axis slide table to the L-shape brackets (Figure 40).

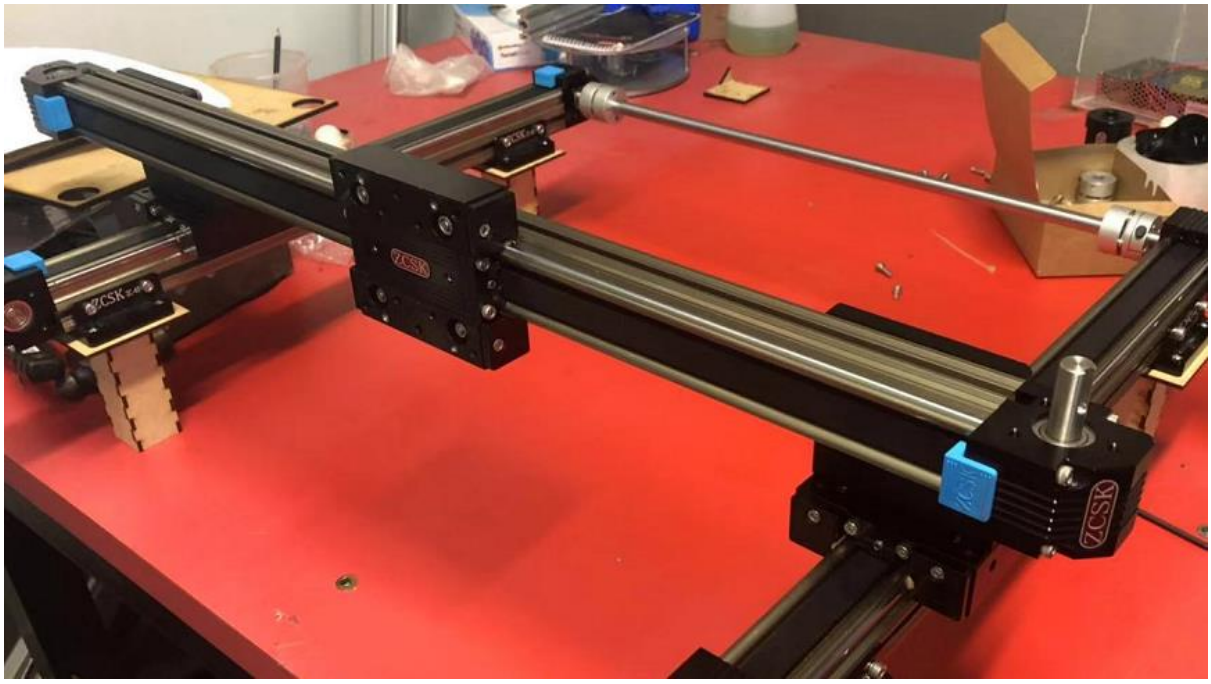

Figure 40 Connecting the Y-axis slide table

Connect the Z-axis to the Y-axis slide table (Figure 41).

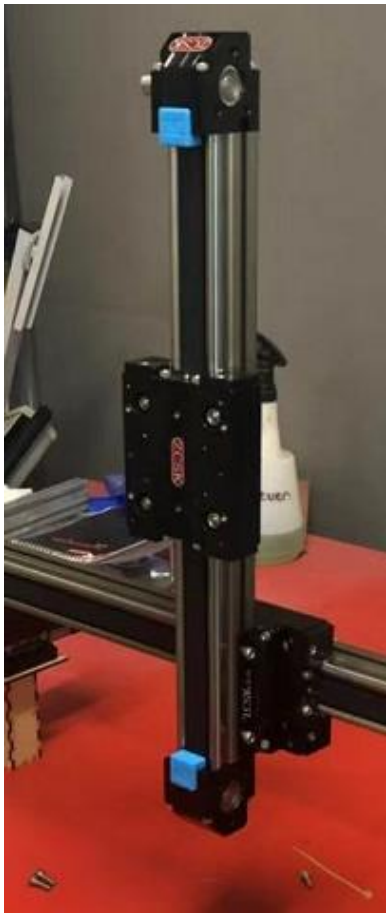

Figure 41 Z-axis connection

Next link each shaft to the stepper motor. First, connect the motor fixed base to the sliding table, then connect one end of the link shaft on the slide table, and then connect the other end of the link shaft to the stepper motor and connect the motor on the fixed base (Figure 42).

Figure 42 X, Y and Z-axis stepper motor assembly

Follow the above steps to connect three stepper motors on all the sliding tables. After that, all the 3D slide table connections have been completed. Figure 43 shows the prototype of the 3D slide table.

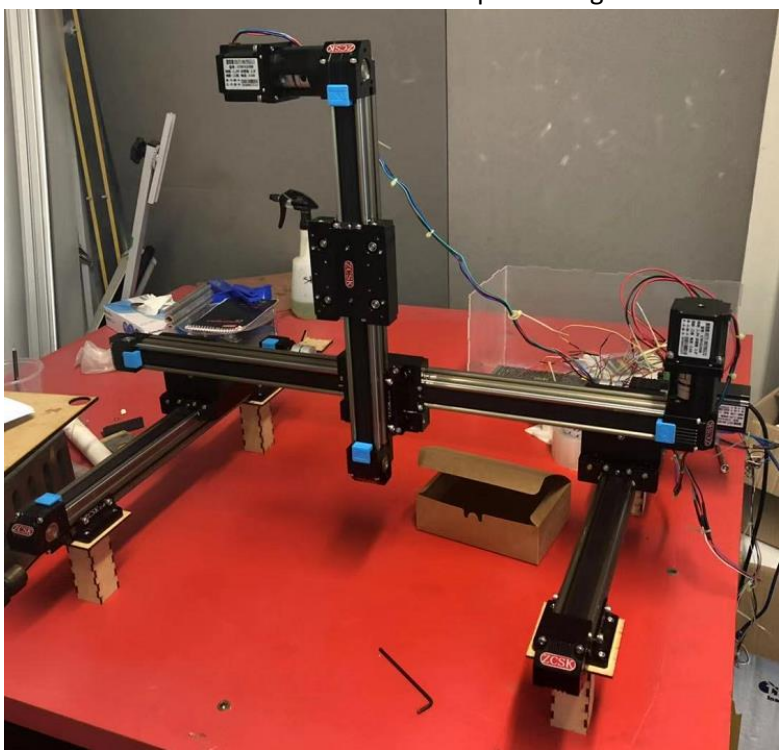

Figure 43 Slide table assembly

3.2.2 Connections for the 3D slide table machine

The electronics for this prototype utilise many peripheral electronic components to enable control using a microcontroller. The Arduino Mega2560 was selected for the microcontroller for this prototype.

3.2.2.1 Connection of the motor and motor driver

1. Stepper motor

The stepper motor has of four different coloured wires, which are black, green, red and blue. These wires are the positive and negative of phase a and b of the motor and are connected to the controller as required. The following figure (Figure 44) shows the connections of the stepper motor:

A+: Black

A-: Green

B+: Red

B-: Blue

Figure 44 Motor connections

2. Microstepping configuration

Physically the stepper motor has 200 steps to turn a full circle (360° divided by 1.8°/step). i.e. One pulse moves the rotor 1.8°. The driver can subdivide this by 1, 2, 4, etc. up to 32 to increase the number of steps per revolution using electronics.

200 steps using a subdivision of 1, 400 steps for a subdivision of 2 and 800 steps using a subdivision of 4 etc. As a result, the resolution of rotation can be increased. However, this also affects the speed at which the motor can be driven. In this prototype the subdivision of 4 was selected giving 800 pulses per revolution, which means the dip switch at sw1 is on and for sw2 and sw3 off. Figure 45 shows how the subdivision of the motor driver is configured.

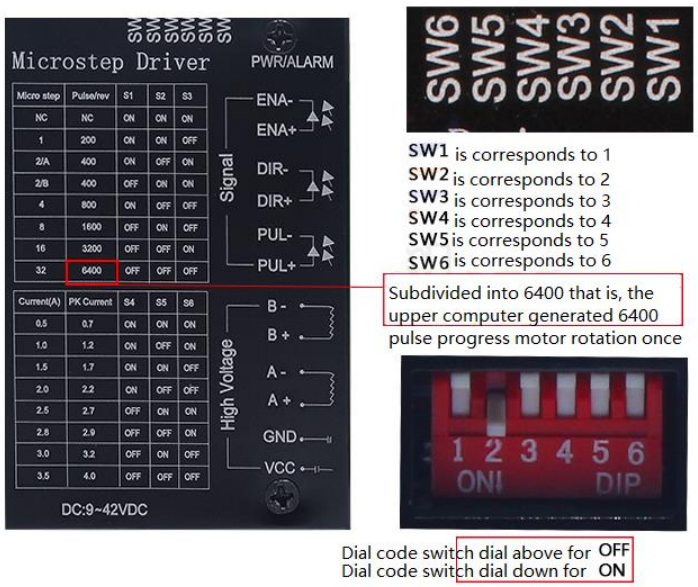

Figure 45 How to configure the subdivision of the motor driver

3. The connection between the motor driver and the power supply

The power supply module uses 230V alternating current (ac) and supplies 12 volts DC to the motor drivers. Live (phase), Neutral and Earth need to connect to the correct colour wires in the supply plug. The ground terminal of the motor driver needs to connect to the negative pole of the power supply (com) and the VCC terminal of the motor driver will need to connect the positive terminal of the power supply (+V) (Figure 46).

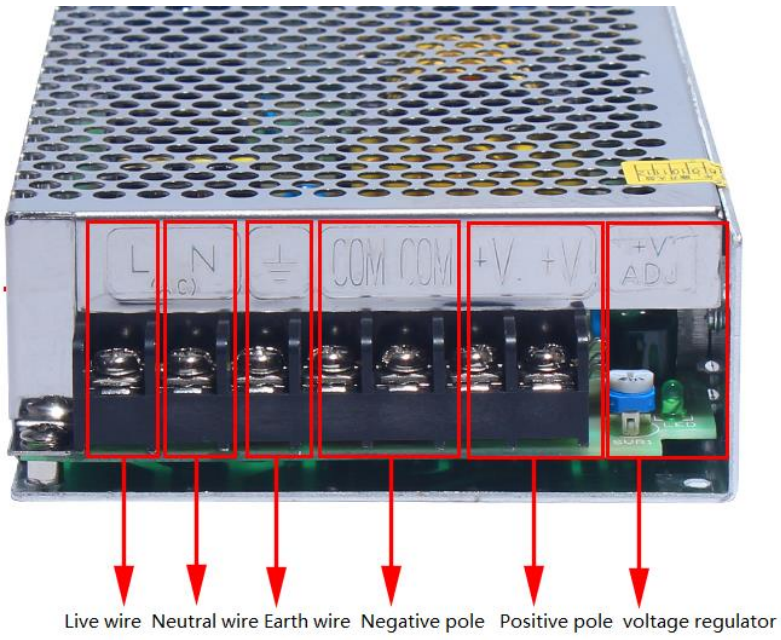

Figure 46 Connection of the power supply

4. The connection between the Arduino and the motor driver

There are three kinds of input signals from the motor driver (1) stepping pulse signal PUL+, PUL-; (2) direction level signal DIR+ DIR-; (3) offline signal EN+, EN-. The common cathode connection method is adopted in this product type:

The X-axis slide table motor:

PUL-, DIR-, EN- connects to ground terminal of the Arduino

EN+: off-line signal, grounded or disconnected, interface 4

DIR+: control rotation direction, high level forward rotation, interface 5

PUL+: control pulse, interface 6

The Y-axis slide table motor:

PUL-, DIR-, EN- connect to ground pole of Arduino

EN+: off-line signal, grounded or disconnected, interface 7

DIR+: control rotation direction, high level forward rotation, interface 8

PUL+: control pulse, interface 9

The Z-axis slide table motor:

PUL-, DIR-, EN- connect to ground pole of Arduino

EN+: off-line signal, grounded or disconnected, interface 10

DIR+: control rotation direction, high level forward rotation, interface 11

PUL+: control pulse, interface 12

This prototype used the breadboard to connect all the negative terminals to the Arduino. The following figures (Figure 47 and Figure 48) show the actual wiring connections.

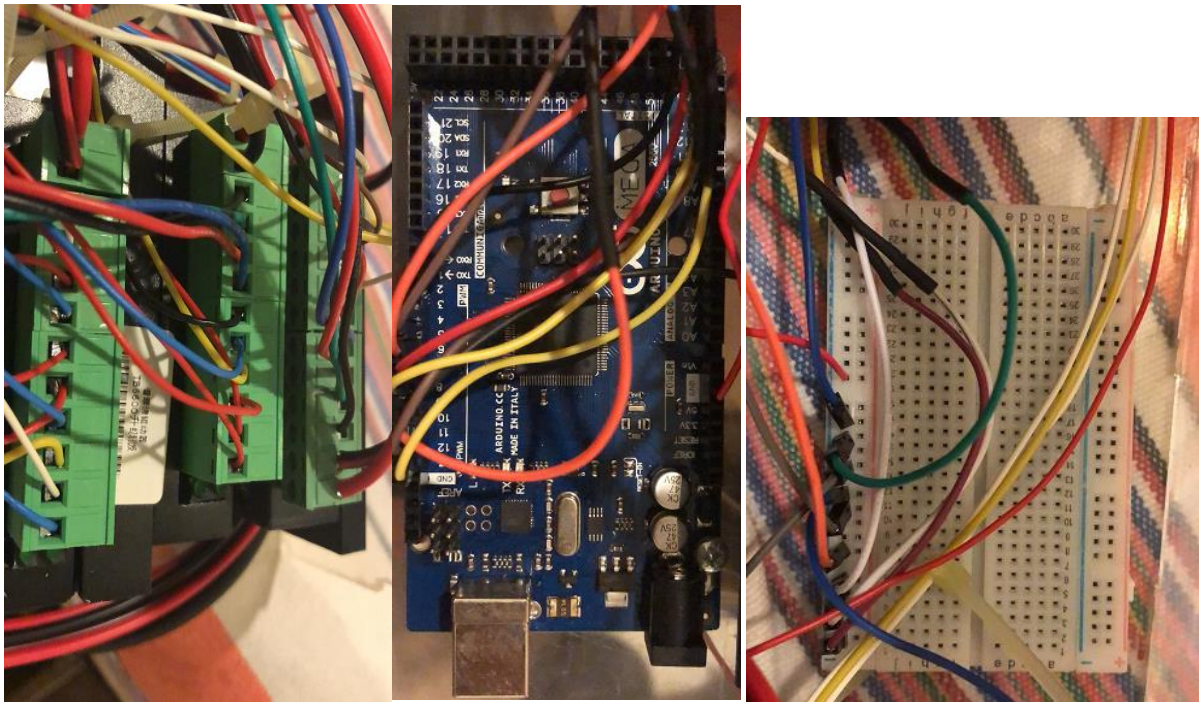

Figure 47 Actual wiring connections (1)(2)(3)

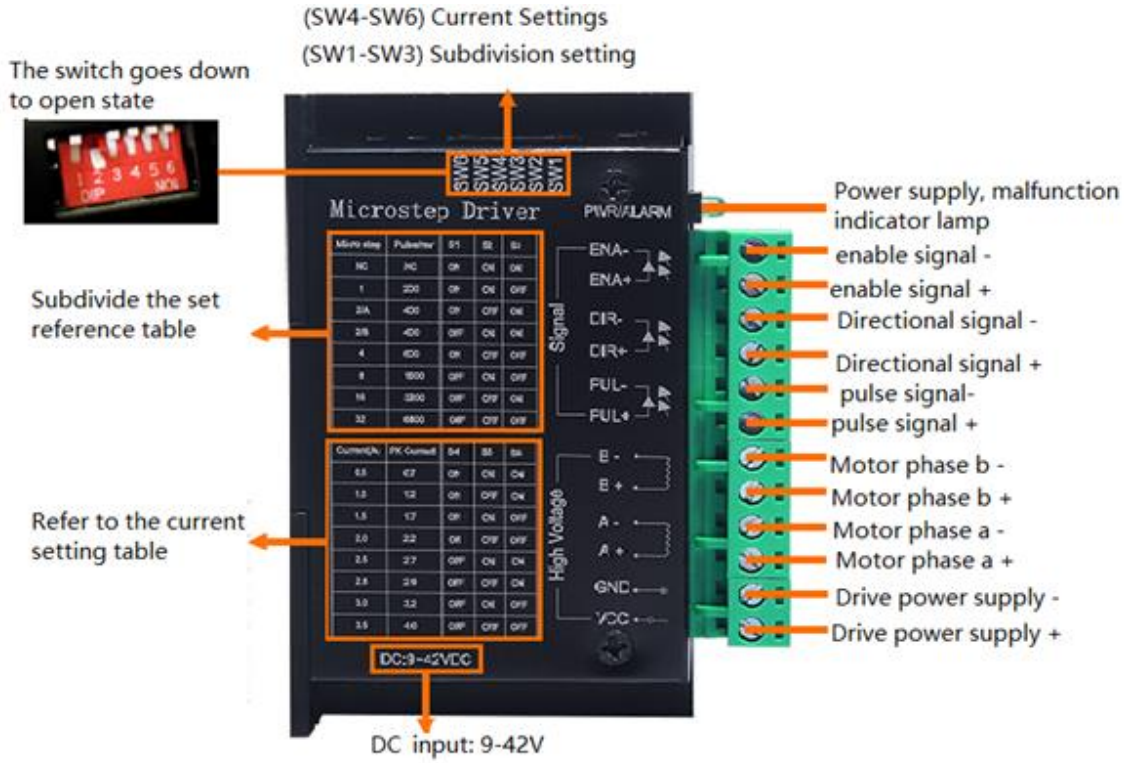

Figure 48 Motor driver connections

3.2.2.2 The connection of the feeding module

On the feeding station there is just one stepper motor and this motor will be connected to another Arduino as shown in the previous step above. This is a different microcontroller than the stepper motor feeding the natural fibre. There are also three push button switches to control the stepper motor moving forward, backwards or stop. The following diagram (Figure 49) shows how each component is connected to the Arduino.

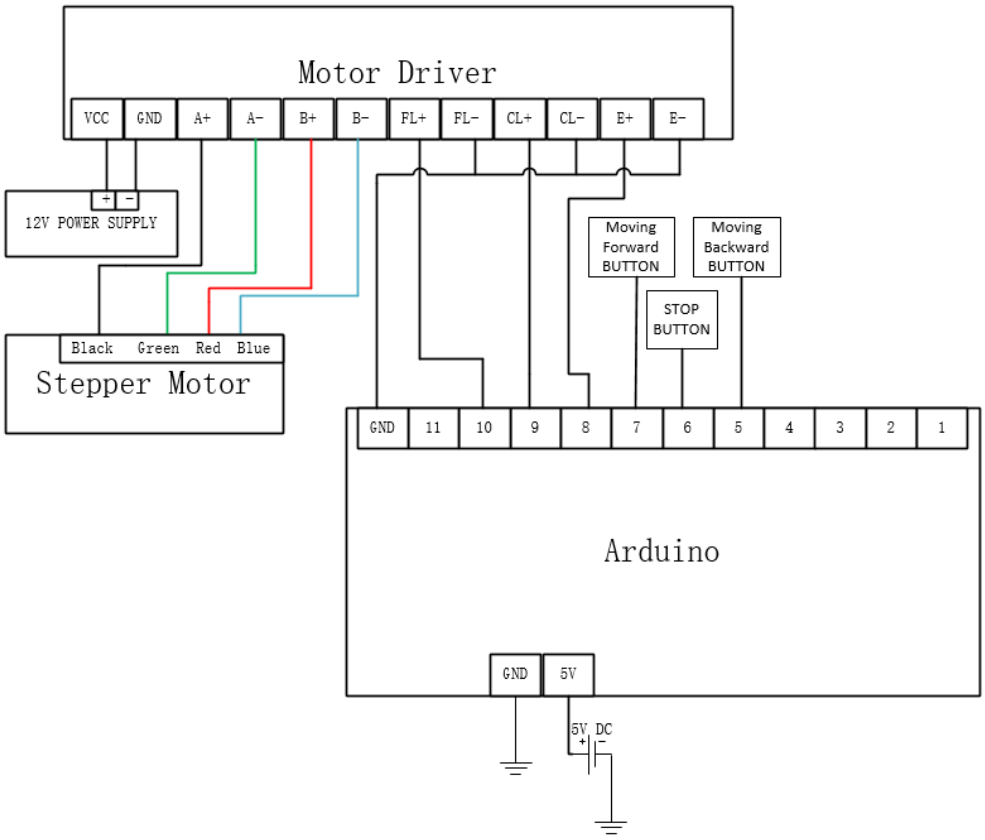

Figure 49 Feeding station connection diagram

3.2.2.3 The connection of the limit switch

Limit switches are used to make physical restrictions on the working area and provide the initial position for the original regression (Figure 50). Proper connection of the limit switches can improve the reliability of GRBL, because the input pin of the MCU can easily receive noise interference.

Normally Open end switches (NO) - switches are attached in parallel, if the head hits one of the switches the resistance becomes low (Less than 10 Ohms). The wiring is simple but there is no indication if one of the switches becomes disconnected (broken wire etc.).

Finally, the prototype will connect limit switches on the x, y and z axes to the Arduino port 1, 2 and 3. If the slide table touches a limit switch it will stop the stepper motor and move back to the original position (Figure 50).

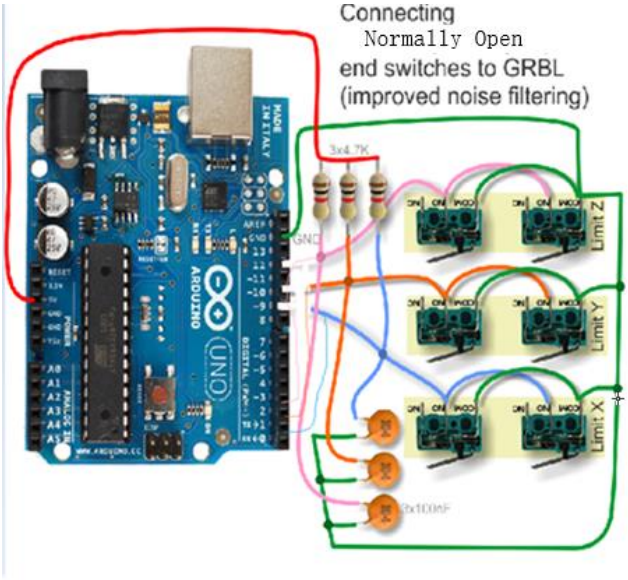

Figure 50 Limit switch connections to the Arduino

3.2.2.4 General connection diagram for 3D weaving machine

The stepper motors of the three sliding tables are connected to their respective motor driver. The stepper motor driver and limit switches are directly connected to the Arduino microcontroller board and the power module supplies power to each motor driver. The Arduino board is powered and controlled by a computer (Figure 51).

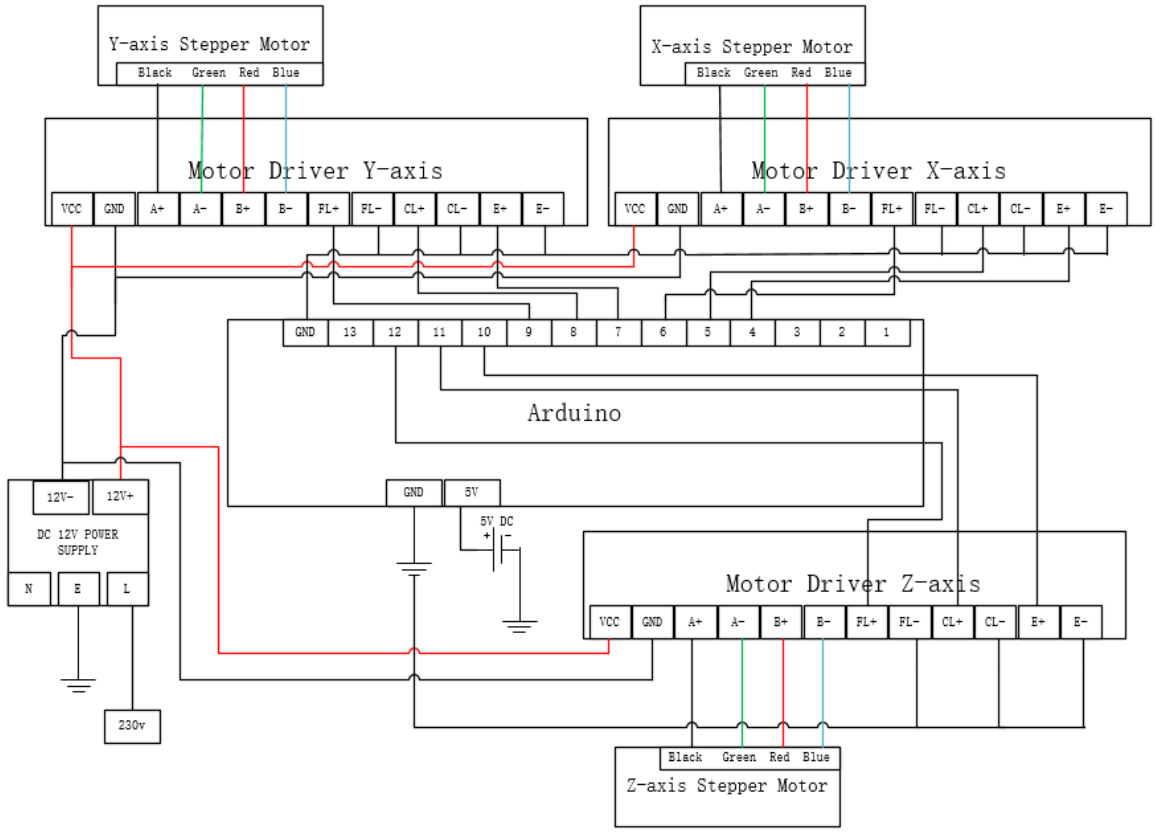

Figure 51 General connection diagram for the 3D weaving machine

3.3 Software module for the 3D slide table

The software design is the most critical part of the whole machine. It must correctly direct the movement of the hardware body according to the users input.

The microcontroller selected for this machine is Arduino mega, with an ATmega328 chip and the programmer used is Arduino 1.0.5-r2. Its programming language is based on c/c++, which is the basic c language. The Arduino language is a simplified function set with some parameter settings related to the AVR MCU (microcontroller), without the need for the user to understand its underlying code, so that the difficulty of programming is greatly reduced. It looks like the c language and it is object-oriented programming. It is programmed in the Arduino IDE programming environment, using the modular programming method which has many advantages:

1. It is convenient for users to write and debug, and the program structure is clearer.

2. Modules can be repeatedly invoked, which improves the processing rate and work efficiency of the program.

3. Simplified programming ideas, so that the programmer is not required to consider the whole program but focus on one program node, so that program editing is more refined.

This machines system software adopts a modular structure, which is composed of the main loop program, automatic wire feeding program and the directional control motion subroutine.

3.3.1 Main loop programming

The main program flow chart is shown below (Figure 52):

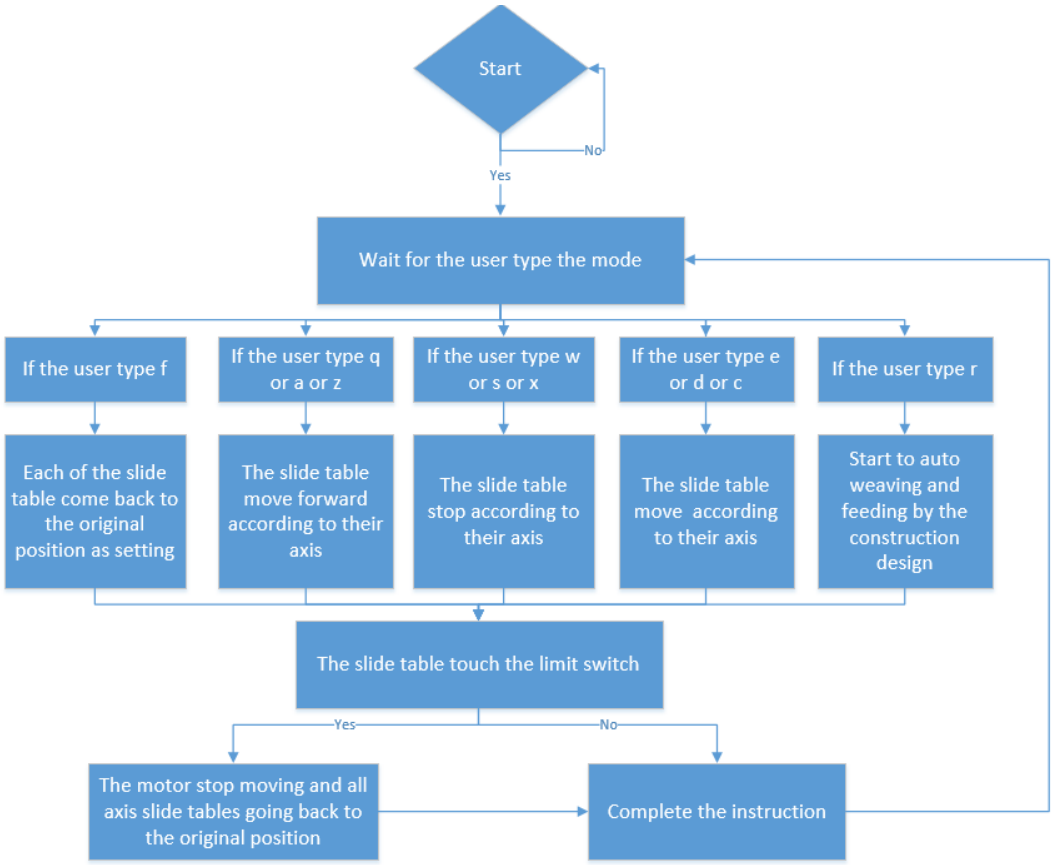

Figure 52 Main loop programming flow chat

According to the main flow diagram, when the 3D weaving machine receives an action instruction issued by the user, the processor needs to accurately find the corresponding subroutine from many corresponding subroutines, so here, the programming will use if statements to achieve this function.

The following figure (Figure 53) show the Arduino IDE programming environment of the main program related code:

```
void loop() {
 if(Serial.available()){
   // when it is turn on the power
    user_input = Serial.read();
    Serial.println(user_input);
 // if the user type a word flowing the user instuuction
 // which is manual mode
    if((user_input =='q')){//move the x-axis slide table forward
        eject();
    }if(user_input == 'w'){//move the x-axis slide table backward
      eject1();
    }if(user_input == 'a'){//move the y-axis slide table forward
      eject2();
    }if(user_input =='s'){//move the y-axis slide table backward
      eject3();
    }if(user_input == 'z'){//move the z-axis slide table forward
      eject4();
    }if(user_input == 'x'){//move the z-axis slide table backward
      eject5();

    // The flowing function is auto mode
    }if(user_input =='e'){
      //atuo to weaving with construction wall model
      eject6();
    }if(user_input == 'r'){
      //atuo to weaving with Winding model one
      eject7();
    }if(user_input == 't'){
      //atuo to weaving with Winding model two
      eject8();
    }
    if(user_input == 'y'){
     //auto mode to move to the origional point
     // move x-axis to origional point
```

Figure 53 Main loop program code

3.3.2 Directional motion subroutine

There are a total of 11 subroutines concerned with motion control of the slides. Nine of them control the movement of each axis manually, one returns the slides to the origin and lastly automatic mode to automatically weave the programmed path. They are all called by the instruction lookup of the main program. Table 3 shows the input character and corresponding function description. The program listings are detailed in Appendix 2.

Table 3: Instruction - program corresponding table

Function Description Table	
Instruction Character	Function Description
q	x forward(): X-axis slide table move forwards
w	x stop(): X-axis slide table stop moving
e	x backward(): X-axis slide table move backwards
a	y forward(): Y-axis slide table move forwards
s	y stop(): Y-axis slide table stop moving
d	y backward(): Y-axis slide table move backwards
z	z forward(): Z-axis slide table move forwards
x	z stop(): Z-axis slide table stop moving
c	z backward(): Z-axis slide table move backwards
r	auto(): auto weave flowing the set course
f	original(): Return to the original position

3.3.3 Limit switch subroutine design

The limit switch subroutine follows the design of the flow chart below. While the stepper motors are running if a limit switch is triggered the motor will either stop or automatically return to the origin (Figure 54).

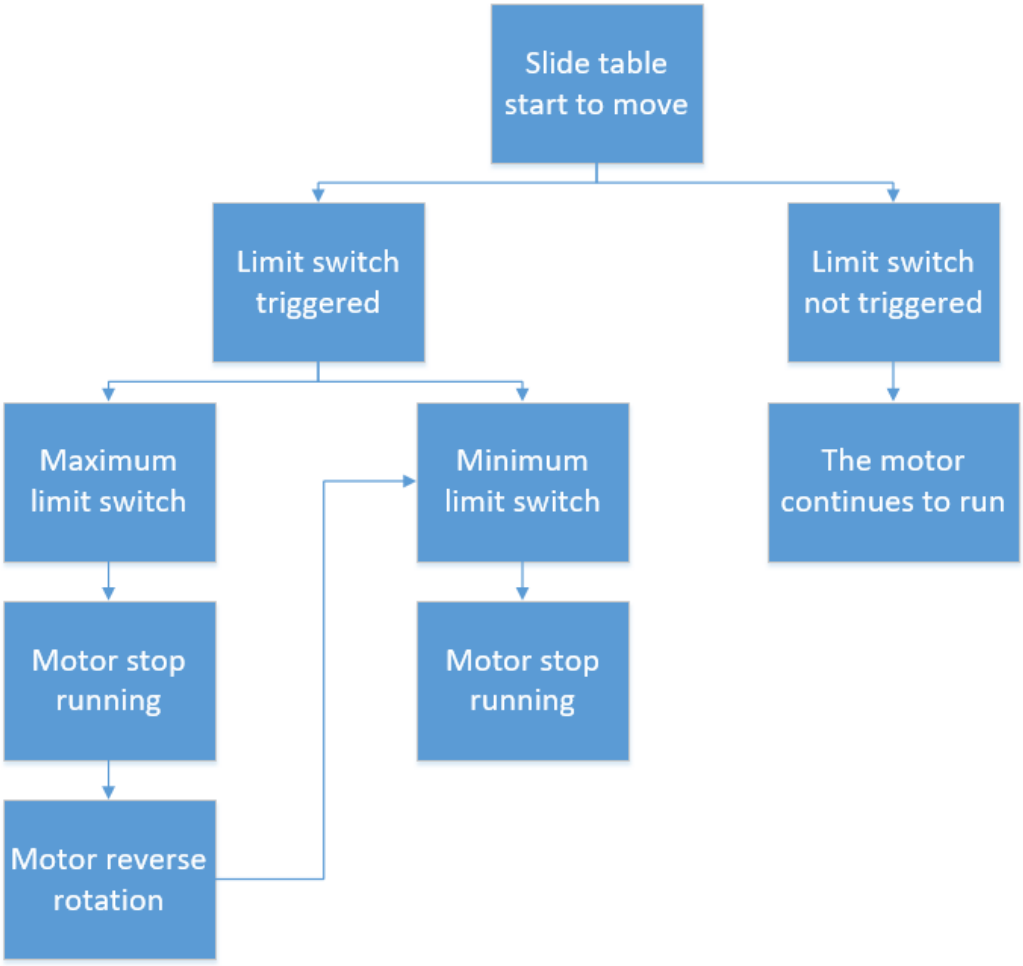

Figure 54 Flow chart of limit switch subroutine design

The limit switch subroutine listing is shown in Appendix 2.

3.4 Machine Testing and results analysis

3.4.1 Expected goal

Overall, the aim of this machine has been achieved.

(1) The 3D weaving machine can weave and feed the long and continuous natural fibre automatically within a specified range.

(2) When the machine is commanded to run in automatic control mode, the machine can weave and feed the fibre automatically according to the path planned in the program, and form the desired external structure of the construction model.

However, the machine has several shortcomings to be overcome. For example, the outer wall can only be formed in one direction. If the direction of motion has to be reversed, the material can easily become knotted, and the product will fail. In future designs, a custom robotic tool could be prepared that allows fibres to be placed based on integrated sensor data and provide appropriate bonding between the model and the fibres using a composite adhesive. In this way allowing a reciprocating motion or reversal to be possible without tangling problems.

3.4.2 Problems encountered and solutions

When the topic of a 3D weaving machine was initially determined, I initially adopted the RAMP1.4 (RepRap Arduino Mega Pololu Shield) board as the controller for the machine. Due to the low voltage output of the RAMP1.4 controller, it could not supply the requirements of the motor. Then, I decided to try to build the intelligent 3D weaving machine using the Arduino chip as the controller and TB6600 motor drives to drive the stepper motors. Initially I was not clear about the principles of the hardware operation, did not know which documents to use, and the curriculum design guide book was not detailed enough, so I spent a lot of time consulting various texts in the library. Only after further understanding of the pinouts, circuit design and other aspects of the Arduino control board, stepper motors and motor driver, the assembly of the robot could begin.

In terms of building the model, after the program is downloaded and the units powered on, the slide table remained in situ. After observation, I found that the motor has no electrical connection problems. The problem is present in the coupling of the motor to the sliding table, and the screws on the coupling were not tightened properly. I screwed all the coupling screws tight, and that resolved the problem.

In terms of software and hardware debugging, I also encountered some problems. First, how to control the rotation angle of the motor to be 45 degrees to control the wire feeding unit to increment by 10 mm. Maybe because of the friction of the sliding table, the moving of the sliding table could not reach the 10 mm position I set. Later, I improved the program and set the rotation angle a little more than 45 degrees, and the movement of the sliding table was nominally in place. Another problem was the case that the motor of the fibre feeding module sometimes gets stuck, which often caused the machine to get stuck. This is easily the biggest problem I have encountered. I made a great effort to debug this problem, but I could not achieve the desired result. In the subsequent experiments, I intend to try to improve the fibre feeding module further.

3.4.3 Hardware debugging and integration

3.4.3.1 Debugging methodology

The 3D weaving machine designed in this thesis has two major modules. They are the sliding table drive module and fibre feeding module. When I was debugging, I debugged the two major modules separately, and finally combined all the modules and hardware together for the final debugging of the whole machine. This debugging idea worked well.

3.4.3.2 Sliding table drive module debugging

On the motor drive board there are three kinds of input signals to the motor driver (1) stepping pulse signal PUL+, PUL-; (2) direction level signal DIR+ DIR-; (3) offline signal EN+, EN- and through PWM the motor speed can be controlled, high level active. After I finished writing the program and energised it, the X-axis motor kept rotating, and I discovered a wiring error. I modified the wiring of the motor controlled by the X-axis driver, and this problem was resolved.

3.4.3.3 Fibre feeding module

On the feeding module there is just one stepper motor and this motor is connected to another Arduino as the step shown above which is another microcontroller to control the stepper motor to feed the natural fibre. There are three push button switches to control the stepper motor to run forwards, backwards or stop. The following diagram shows how each component is connected to the Arduino. Another problem is that the motor on the fibre feeding module sometimes gets stuck. Even after I made a great effort debugging the program for this problem, I could not eliminate it. In the subsequent experiments, I intend to try to improve the fibre feeding module.

3.4.4 Demonstrating the winding results

The first product is used as a model exterior wall built around four aluminium columns (Figure 55). The continuous fibre material selected is European flax fibre. The second product uses a nail plate as the base of the winding (Figure 56). The fibre winding is fixed on the nail and finally forms an artwork (Figure 57). From the attachment of the program code, you can see the code for construction wall model, model1 and model2. To weave the corresponding model, the user needs to open the program and enter "e", "r", "t", so that the machine can weave the model according to the corresponding instructions.

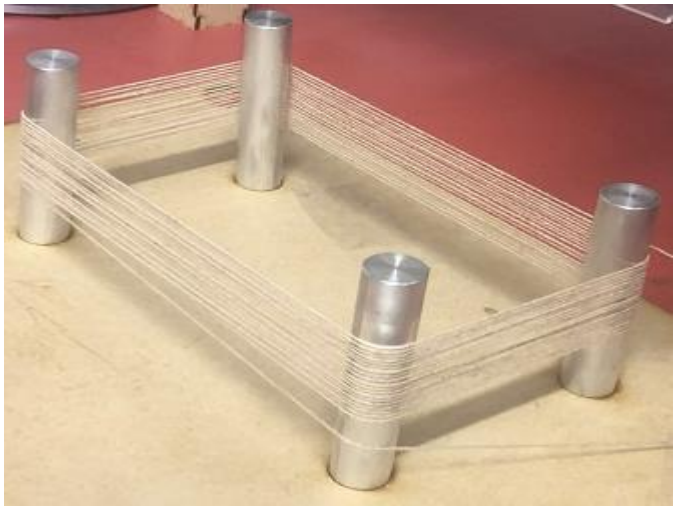

Figure 55 Construction wall model

Figure 56 Winding model one

Figure 57 Winding model two

3.5 Chapter conclusions

Through this project, I learned a lot of automation knowledge, and improved my ability to learn unfamiliar hardware. For example, I had never heard of ramp control before this project and had to find information about it and learn how to use it properly. Slowly I became familiar with it and later skilled in its application. I met a lot of unfamiliar hardware in the course of the project and gradually improved my ability in its use as the project progressed.

The practical nature of the project also strengthened my practical ability, especially the ability to analyse and resolve problems. I believe the improvement in these abilities will be of great help in my future work.

(1) The most attractive prospect of this intelligent 3D continuous natural fibre wire feeding system is that it can be used in the up and coming construction industry. When robots are combined with materials, especially intelligent materials, they can "make" products directly by operating the movement of the mechanical arm. In this machine, I use continuous European flax fibre as the material, attached to a pre-designed steel and screw plate structure. On the computer, the track and sequence the sliding table takes are designed in advance and then converted into Arduino code. The end of the robot arm is equipped with weaving and feeding tools, and the movement of the robot arm is used to apply the skin texture, which is constructed like "weaving cloth". With the ever-changing application of robots, different tools, different motion paths and different programming code, it will produce a massive variety of "products". Intelligence is also the general trend in future society, and a kind of indispensable part of this is intelligent building robots. Artificial intelligence is widely involved in computer vision, automatic control, precision instruments, sensing and information and a series of innovative research disciplines, its research results can be widely applied to the actual field in the construction industry. In our future work and life, more and more robots will be needed to replace humans to work and accomplish some difficult or laborious tasks, and the demand for these practical robots will also be increasing. Therefore, the prospect of robot research and development is immeasurable.

（2）The 3D weaving machine designed in this paper is not very perceptive. It does not possess the ability to learn and control itself independently, and it can only weave using the wire feeding system by manual control or pre-programmed form. Construction site preparation and module assembly are operations that need to be completed in the field in the construction process, and it is also very difficult for robots to achieve automation of the whole process at present. The main reason this is the case is that the construction of the plant involves a wide variety of materials and tools and the robot adaptability requirements are very high. This may be applied in the impending construction industry. The main obstacle is the development of computer software to control the construction robots. Therefore, the design of this machine in the future can pay greater attention to the development and design of intelligent software.

The second project training impressed me the most: as an electronics enthusiast, no matter what problems and difficulties you encounter in electronic production, you should have a calm heart and a persistent spirit, an impetuous heart will not reach the other side of success. This course design gives me more of a modular idea. The modular nature of the system according to the functions we need and the functions the system can provide will make our work clear at a glance and neat. For example, the 3D weaving machine at this time can be divided into the wire feeding module, motor drive module and the core module of the single chip microcomputer. Each of the three parts performs its particular

duties and can clearly distinguish their functions between hardware and software, which is conducive to the connection of hardware and programming.

4 Chapter 4: Test method for tensile strength of New Zealand flax fibre monofilament

In the evaluation of the tensile properties of natural fibres, the conventional method of bundle fibre tensile testing is used. However, it is just an indirect method to characterize the tensile mechanical properties of fibres by the tensile properties of a bundle of fibres. Therefore, the conclusions reached by this method do not objectively and accurately reflect the actual performance of the fibre. The fibre bundle is a group of single fibres. But it has the benefit of less testing and easy operation. In order to evaluate the tensile properties of natural fibre objectively and accurately, it is necessary to develop a scientific and reasonable test method for the tensile properties of a single fibre. In addition to the internal causes of the "fibre internal structure", the factors influencing the tensile performance test results of natural single fibre are also affected by the laboratory temperature and humidity, fixture length, the number of specimens, tensile speed and other test conditions. The tensile properties of the same batch of fibres may vary greatly under different experimental conditions. In this research, test samples are of New Zealand Flax Fibre (harakeke fibre). This material was obtained from the Biopolymer Network Co., Ltd. (BPN) fibre processing unit in New Zealand and stored, in laboratory conditions. This research studies the tensile testing of harakeke fibre monofilament at different stretching speed, different spacing length and different thickness of the fibres. Finally, the paper analyses the factors influencing the tensile properties of single harakeke fibres, and obtains the factors influencing the accuracy of the test results to provide a guide as to the significance of the effect each makes on the tensile property tests.

Because of the brittle and fibrous nature of harakeke, tensile testing requires special consideration in regard to securing the fibre in the machine to prevent fracturing in the jaws. The usual jaws for testing materials clamp the specimen, however these are unsuitable for monofilament type materials as the jaws damage the material while clamping and cause premature failure within the jaws and inaccurate results.

In this study, tensile modulus, ultimate strength and failure mode were used to identify the single fibre strength of harakeke fibre. Upon investigation, the international standard organization (ISO) has no industry standard for tensile testing of natural fibre monofilament nor do other countries. Therefore, the experiment followed the American Standard ASTM D3379-75 “Standard Test Method for Tensile Strength and Young's Modulus for High Modulus Single Filament Fibres” and discussed many fibres for statistical analysis.

4.1 Tensile test

4.2 Experimental principles

A single harakeke fibre is stretched to fracture on an iso-elongation tensile tester, an Instron 5967, under specified conditions. The tensile properties such as tensile strength, load force and tensile modulus were obtained from the load elongation curve and data acquisition system.

4.3 Experimental material

The Biopolymer Network Co., Ltd. (BPN) has the harakeke fibre stripping and cleaning capabilities, which are used for later research on new industrial applications. Every test sample was extracted from the fibre bundle. The length of each sample is about 500 mm.

All the experimental harakeke fibre was placed in an environment chamber set to a temperature of 20°C ± 2%, relative humidity 65% ± 3% standard atmospheric conditions for 24 hours. Sticky tape was used to help attach the harakeke fibre to the tensile fixtures, to maintain the fibre vertically and lightly stretch tight. Then the harakeke fibre was clamped and the edge of the intersection covered with adhesive. The harakeke fibre tensile samples are shown below in Figure 58.

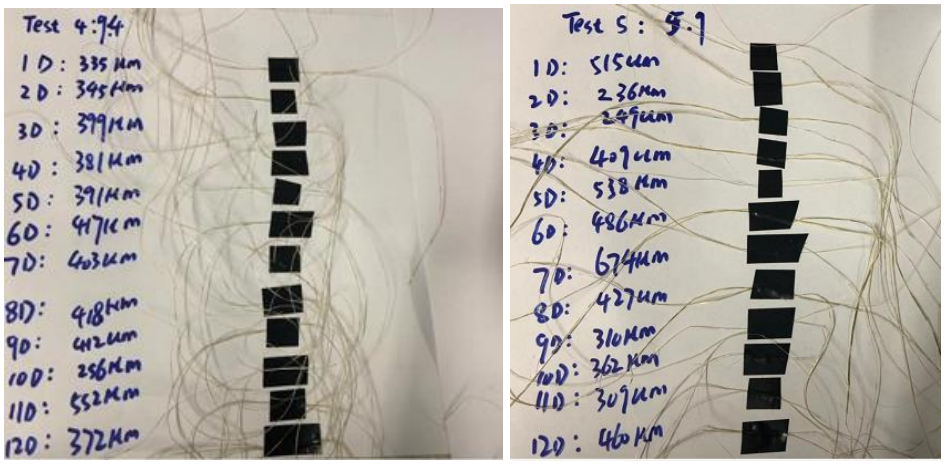

Figure 58 Harakeke fibre tensile samples

4.4 Experimental equipment

The test equipment was an Instron 5967 Universal testing machine, with strain gauge type load cell. The diameter of the samples was measured by a scanning electron microscope (SEM), a HITACHI TM3030Plus. This is a form of electron microscope that produces images of a sample by scanning the surface with a focused beam of electrons [39].

4.5 Diameter and Cross-section of the sample

4.5.1 Determine the diameter measurement technology

Natural fibre density can be measured using one of the following five methods: (1) the diameter and linear density, (2) the Archimedes Principle, (3) helium pycnometer (4) gradient column (5) liquid displacement method. In this thesis, the method selected was the diameter and linear density to determine the density of the harakeke fibres. The traditional method to work through this problem is to measure the average fibre diameter at five different random positions under an optical microscope. The apparent cross-sectional area of each fibre is then calculated by assuming a circular cross-section using the average fibre diameter. This method is considered as a reasonable approximation. The purpose of this study is tantamount to study the influence of gauge length on tensile properties. However, a more detailed study to improve the accuracy of fibre cross-section measurements, considering the existence of hollow structures (cavities), is under development [40-43].

4.5.2 SEM Measurement Procedure

(1) Starting the Instrument

First power up the machine using the power switch on the right-hand side of the machine. After that, when the EVAC LED flashes blue, it will automatically begin to evacuate. The yellow LED lights up and press the EVAC / AIR switch to start. At the end of the evacuation, EVAC LED lights up in blue. Then power on the computer and start the TM3030Plus application.

(2) Preparing the Specimen

First from the prepared harakeke fibre monofilament samples one single harakeke fibre is selected. Then a fibre sample of approximately 10 mm length is cut from both ends of the fibre. Samples of the 10 mm single harakeke fibre are shown in Figure 59. The samples are then placed on top of conductive tape.

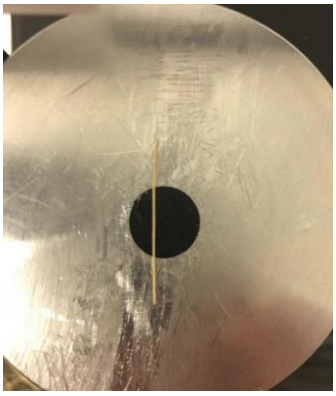

Figure 59 Preparing the Specimen for SEM Testing

Next the distance between the test platform and the measuring rod must be measured, the distance between them should be about 1 mm. This is required to bring the camera into the focal range for accurate measurement. Not doing so can lead to damaging test samples, damage to the camera, or unmeasurable samples.

(3) Mounting the Specimen

Press the EVAC/AIR switch to introduce air into the specimen chamber. When the yellow light stops blinking the air introduction is complete. Draw out the specimen stage slowly and set the specimen holder. Then push the specimen stage back to the SEM machine, the next stage is pushing the start button to run the SEM machine.

(4) Start the Observation

On the computer click the “start” button at the top left corner of the window. This automatically runs and displays the image. Then using the X, Y knob on the mobile platform, set up the required view and frame the test samples to display on the screen. Adjust the magnification, review the settings and magnification. Then click the automatic B/C to adjust the brightness and contrast and perform an auto focus (Figure 60).

Figure 60 TM3030Plus application

(5) Saving the Captured Image

Finally, after the image is displayed as required, click on the save button to capture the image. The "save image" dialog will display. Enter the desired file name and save the image. Next click the edit menu and select measure the image on the top of the application. The range tools are used and I selected five diameters along the harakeke fibres in the image to insert them on the image. The figures below (Figure 61 and Figure 62) show a sample image, with (Figure 62) and without (Figure 61) the diameter measurement of the sample.

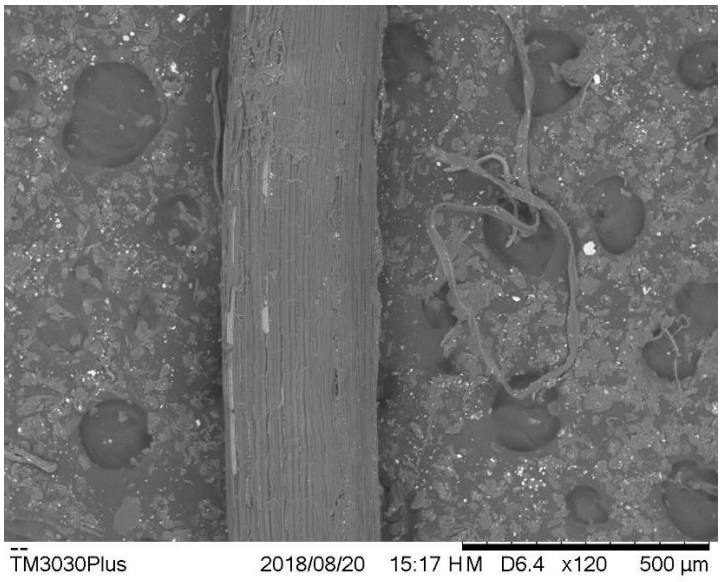

Figure 61 SEM Harakeke Fibre bundle surface

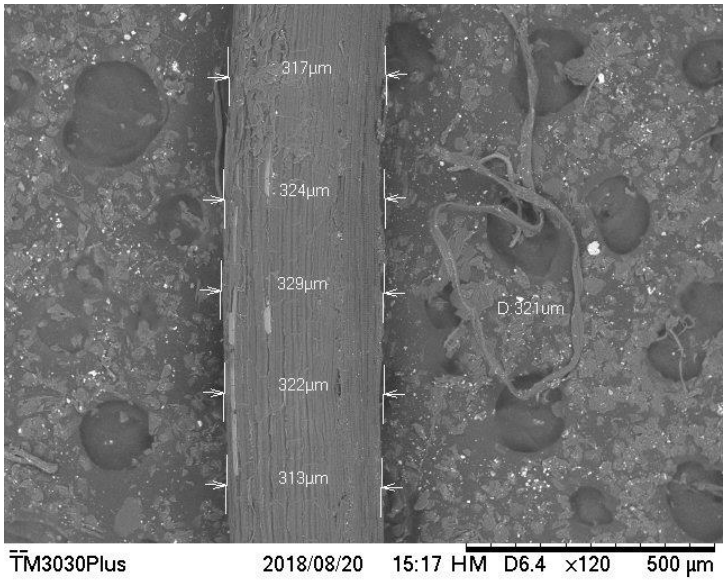

Figure 62 Diameter measurements of the harakeke Fibre

(6) Stop the Observation

Click the "stop" button at the top left corner of the window. Press the EVAC/AIR switch to introduce air into the specimen chamber and then, wait for the yellow light to stop blinking. Draw out the specimen stage and remove the specimen holder. Close the specimen stage and shut down the main power of the machine.

4.5.3 Calculate the diameter of the sample

The approximate diameter of each fibre specimen was measured by the SEM machine. Each specimen was measured in five locations along its length. The average diameter of the five sections was calculated. Table 4 below indicates the diameter distribution of one set of the samples. As in all the experiments undertaken, there are nine sets of samples, the average diameter of ten specimens in each group is shown in Table 5 below.

	Test 2 (UNIT: µm) (length 100 mm)
1	302
2	321
3	346
4	350
5	360
6	365
7	371
8	377
9	386
10	389
	356.7
Average Diameter	0.3567 mm

Table 4: Specimen diameter data for the second sample

	Average Diameter (mm)
Test 1	0.254
Test 2	0.357
Test 3	0.448
Test 4	0.361
Test 5	0.377
Test 6	0.306
Test 7	0.350
Test 8	0.365
Test 9	0.285

Table 5: The average diameter of all nine samples

4.5.4 Calculate the cross section of harakeke fibre

In this experiment, the diameter of each harakeke fibre specimen is assumed to be constant. The samples diameter has been established using the electron microscope. The tensile fracture strength and modulus need to be calculated, however calculation of fibre tensile strength and tensile modulus require the fibre cross-sectional area. Generally, there are three methods used to calculate the cross-sectional area of the fibre:

(1) The microscope method

The microscope method assumes the cross section is circular, and its diameter is uniform everywhere, under the microscope. The diameter is measured using a graticule. This diameter is used to calculate the cross-sectional area.

(2) The linear density method

This method uses the linear density of the fibre divided by the density of the fibre to obtain the cross-sectional area.

(3) The scanning electron microscopy method

A scanning electron microscope is used to measure the cross-sectional area.

The three methods assume homogeneous fibre diameter. The first approach assumes that the fibre is spherical in cross-section, but the harakeke fibre has a polygonal cross section, this calculation method is accurate enough. The second method needs to be calculated using fibre density, which increases the inaccuracy. The third method is to randomly select a plurality of position measurement diameters on a length of fibre, and take the average diameter to calculate the cross-sectional area of the fibre. In combination, the basic method is easy to test, and the average cross sectional area of the fibre is obtained by calculating the average sectional area of the fibre. The comparison is representative, and this method is selected for calculation. Calculated using the experimental data of each harakeke fibre's cross-sectional area, the specific results are shown in Table 6. Calculation of the circular cross-sectional area will use the following formula to compute the area of the samples.

$$A = \pi r^2$$

Table 6: The cross-sectional area of the nine samples

	Average Diameter(mm)	Radius(mm)	Cross-section Area(mm^2)
Test 1	0.254	0.127	0.0507
Test 2	0.368	0.184	0.1062
Test 3	0.448	0.224	0.1576
Test 4	0.361	0.180	0.1021
Test 5	0.377	0.188	0.1116
Test 6	0.306	0.153	0.0738
Test 7	0.350	0.175	0.0964
Test 8	0.365	0.182	0.1046
Test 9	0.325	0.162	0.0829

4.6 Tensile testing the samples

4.6.1 Designing the test procedure

The experiment will follow the steps below:

Selection of independent variables
Selection of the number of level settings for each independent variable
Selection of the table of samples
Set up all the samples
Finish the tensile test for all the samples
Analyse the data
Summary

The details of the above steps are given below.

4.6.1.1 Selection of independent variables

In this experiment, three sample variables were chosen as independent variables, namely, the tensile speed, the length between the two clamps and the cross-sectional area of harakeke fibres. All samples in a test use the same settings. This experiment selects three independent variables to control the strength of the samples in this experiment. For tensile speed, there are three different speeds: 1 mm/min, 3 mm/min and 5 mm/min. For the length between the two clamps (gauge length), five different distances were selected: 50 mm, 60 mm, 80 mm, 100 mm and 120 mm. For the cross-sectional area of the harakeke fibre, the diameters selected were: 0.250 mm, 0.350 mm and 0.450 mm, and their corresponding cross-sectional areas are: 0.05 mm^2, 0.10 mm^2 and 0.16 mm^2 respectively.

4.6.1.2 Selection of the number of level settings for each independent variable

For tensile speed, there were three different speeds selected, namely 1 mm/min, 3 mm/min and 5 mm/min for each set of samples. The reasoning for selecting these three speeds is as follows. If the machine speed is too fast, the sample harakeke fibre will fracture outside the gauge length, rather than in the middle. This will influence the tensile strength of the fibre monofilament and the accuracy of the data. Therefore, the maximum tensile test speed selected for the experiment is 5 mm/min. The Instron machine minimum crosshead speed is 1 mm/min. Therefore, 1 mm/min was chosen as the minimum tensile speed in the test. Finally, 1 mm/min, 3 mm/min and 5 mm/min were chosen as the tensile test speeds.

For different lengths between the two clamps (gauge length), five different lengths being, 50 mm, 60 mm, 80 mm, 100 mm, and 120 mm were chosen. The maximum length between the two clamps selected for the experiment was 120 mm. This is because each length of the fibre monofilament is about 500mm. If this distance between the two clamps is too long the fibre will not be able to be very well fixed on both sides of the clamps which means the fibre cannot wind many wraps around the clamps and it is easy to create slack in a way which affects the accuracy of the fibre stretch test results. Therefore, the maximum distance between two clamps of 120 mm was selected. For the minimum distance between the two clamps, 50 mm was selected. This is the minimum distance between the two clamps and if the distance is too small the two clamps will make contact. Therefore, 50 mm was chosen as the shortest distance between two clamps in the experiment. Finally, 50 mm, 60 mm, 80 mm, 100 mm, 120 mm were selected as the distance between the two clamps.

In the diameter measurements, the monofilament harakeke fibres have a slight variation in diameter, which is about 0.250 mm, 0.350 mm and 0.450 mm. Therefore, the implementation chose these three different ranges of fibre monofilament diameters for the tensile strength tests.

4.6.2 Tensile Test

4.6.2.1 The testing processes

The Instron testing machine loaded the fibre samples at the different selected speeds. In order to prevent the fibre from being unevenly loaded, both sides of the fibre should be very firmly fixed to the clamps. This ensures that the test sample remains stable during the tensile test. The figure below (Figure 63) shows the set up ready to start testing.

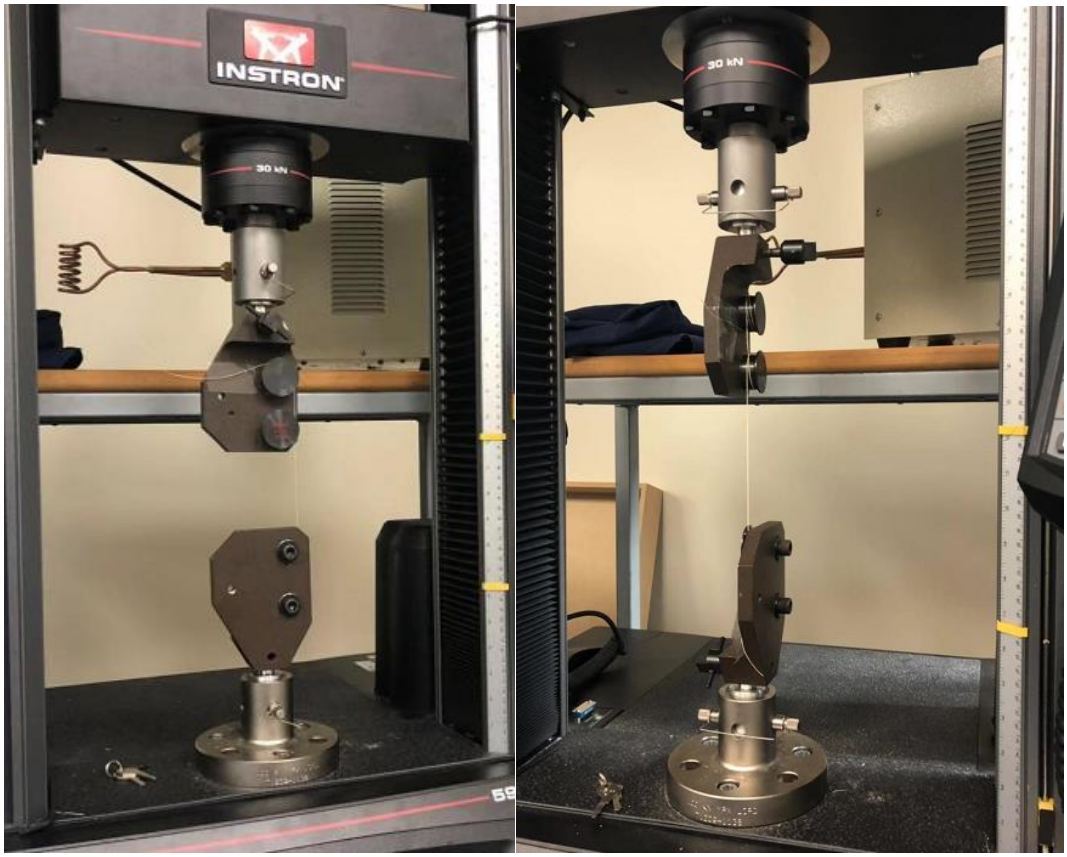

Figure 63 The harakeke fibre set up for testing

Figure 64 shows how the fibre sample is wound on the clamps. The harakeke fibres are wound around the upper and lower cylinders to hold the filaments firmly to the clamps. The free end is then fastened to the clamp with transparent sticky tape.

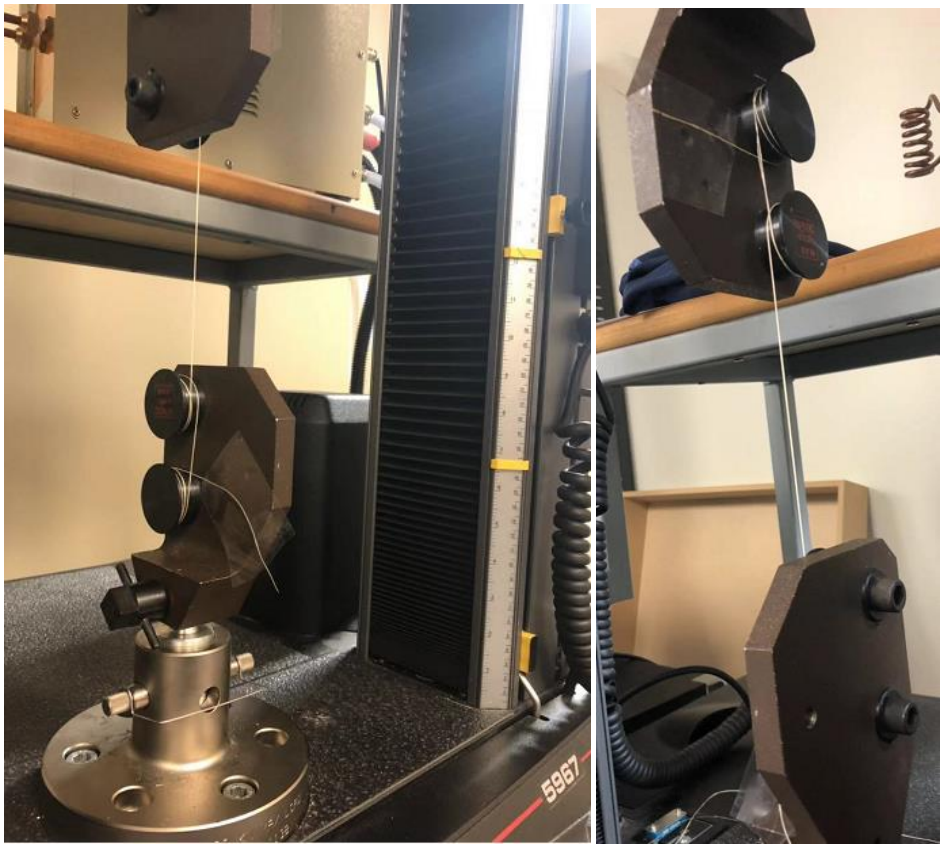

Figure 64 How the fibre specimens are attached to the clamps

4.6.2.2 The test phenomenon

During the loading process, the fibre makes an intermittent cracking noise until suddenly a louder snap at the failure point. From Figure 65, it can be seen that the test specimen has a very clean break in the middle. For most harakeke fibre samples, the fracture sites are concentrated in the middle of the samples during tensile testing. However, a small number of test samples did not break very cleanly, the reason may be that the fibre is not completely secured to the fixture, the test sample was slipping during the tensile test or a defect in the fibre. As a result, the stretching force graph of the sample appears uneven, and it does not show a clean break. After the completion of the tensile test, a partially fractured sample was also selected for observation in the scanning electron microscope.

Figure 65 Tensile test of Harakeke Fibre with clean break

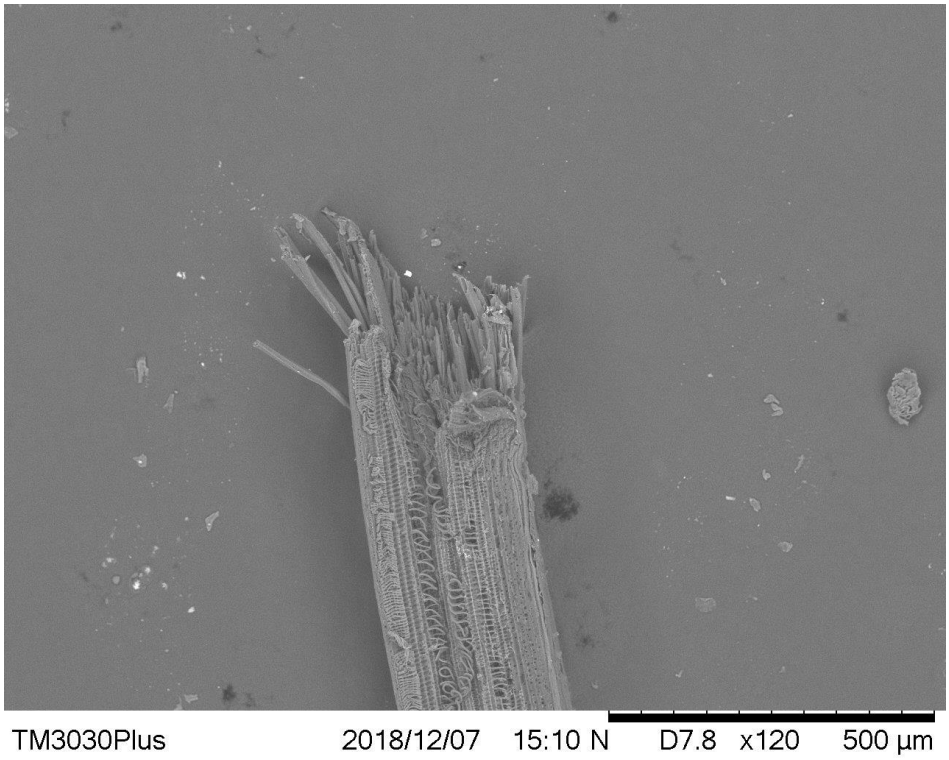

Figure 66 Harakeke fibre fracture with clean break observed in the SEM

The cross-sectional shape as shown in Figure 66, from specimens of the harakeke fibre presented a very good fracture section under the electron microscope. The specimen fracture is ordered and is truncated from a complete monofilament into a number of slender fibrils. The result shows the fibre retention at the bonding point was better when the harakeke fibre was broken. However, this does not have a great impact on the test results for the whole sample. The test results are within the control range.

4.6.2.3 Calculate the tensile stress at tensile strength of harakeke fibre

For metals the tensile stress strain curve changes from a linear shape in the elastic range to a curve peaking to maximum stress during the plastic deformation stage, which is the classic metals tensile strength or maximum load carrying capacity under static stretching. Tensile strength is characterized by the largest resistance to plastic deformation. Typically, before the maximum tensile stress, the deformation is uniform, but beyond, metal begins to show the necking phenomenon, namely centralized deformation; For brittle materials there is little or no uniform plastic deformation, which reflects the fracture resistance of materials [43-45].

The stress (σ) is the maximum force (Load Force) that the material undergoes at fracture during the stretching process divided by the original cross-sectional area (Area), called the tensile strength or strength limit, in units of N/m x 10^6 (MPa). It represents the maximum ability of a material to resist damage under tensile forces. The equation is show below:

$$\text{Stress}(\sigma) = \frac{\text{Load Force (N)}}{Area(mm^2)}$$

From the equation: Load force-- the maximum force sustained when the sample was pulled apart, unit: N (Newton); Area -- the original cross-sectional area of the sample, unit: mm^2.

Tensile strength (Rm) relates to the material before the fracture at maximum stress. When steel yields to a certain extent owing to internal grain rearrangement, a renewed ability to resist deformation is shown, deformation while developing rapidly at this time, but only with the increase of stress, and reaches maximum. From then, the steel has a significantly lower resistance to deformation, and large plastic deformation occurs in the weakest place, the specimen cross-section shrinks rapidly and necking occurs until the fracture failure. Steel tensile fracture before the maximum stress value is known as the ultimate strength or tensile strength. The following table (Table 7) shows the average value of maximum load and cross section area of each set of samples. The tensile stress of each specimen is then calculated.

Table 7: Tensile stress of harakeke fibre

	Maximum Load (N)	Cross-section Area (mm^2)	Stress (MPa)
Test 1	12.1	0.0507	237.9
Test 2	14.2	0.1062	133.9
Test 3	16.4	0.1576	104.2
Test 4	20.5	0.1021	200.6
Test 5	21.3	0.1116	190.8
Test 6	18.1	0.0738	245.4
Test 7	21.4	0.0964	222.1
Test 8	22.2	0.1046	212.5
Test 9	18.8	0.0829	226.7

4.6.2.4 Calculating the tensile strain at tensile strength of harakeke fibre

Extension and the original length are referred to as the ratio of strain, which is the ratio change in length and the original length, which is the distance between two clamps, it has no units, because it is a ratio of two lengths measured in metres. The equation for calculating the tensile strain is shown below:

$$\text{Strain} = \frac{extension(\Delta L)}{Length(L)}$$

From the equation: Extension – the extension at yield, which is the change in length, unit: mm; minus original length, which is the distance between two clamps, unit: mm. The following table (Table 8) shows the average length of extension at yield (Zero slope) and the sample length of each set of samples. From this the tensile strain of each set of tests is calculated.

Table 8: Tensile strain of harakeke fibre

	Extension at Yield (Zero slope) (mm)	Length (mm)	Strain
Test 1	6.77	100	0.0677
Test 2	5.36	100	0.0536
Test 3	6.73	100	0.0673
Test 4	7.72	80	0.0965
Test 5	9.56	50	0.1912
Test 6	7.54	60	0.1256
Test 7	8.32	120	0.0694
Test 8	9.278	100	0.0928
Test 9	9.181	100	0.09181

4.6.2.5 Stress-Strain graph for harakeke Fibre

The relationship between the stress (force per unit area) and strain (resulting in compression/stretching, known as deformation) that a material displays is known as that material's stress–strain curve. It is specific for each material and is found by recording the amount of deformation (strain) at distinct intervals of tensile or compressive loading (stress). These curves reveal many of the properties of a material (including data to establish the Modulus of Elasticity, E) [46]. Stress-strain curves vary a lot between various materials, and different tensile tests of the same material produce different results, depending on the sample temperature and loading rate [47].

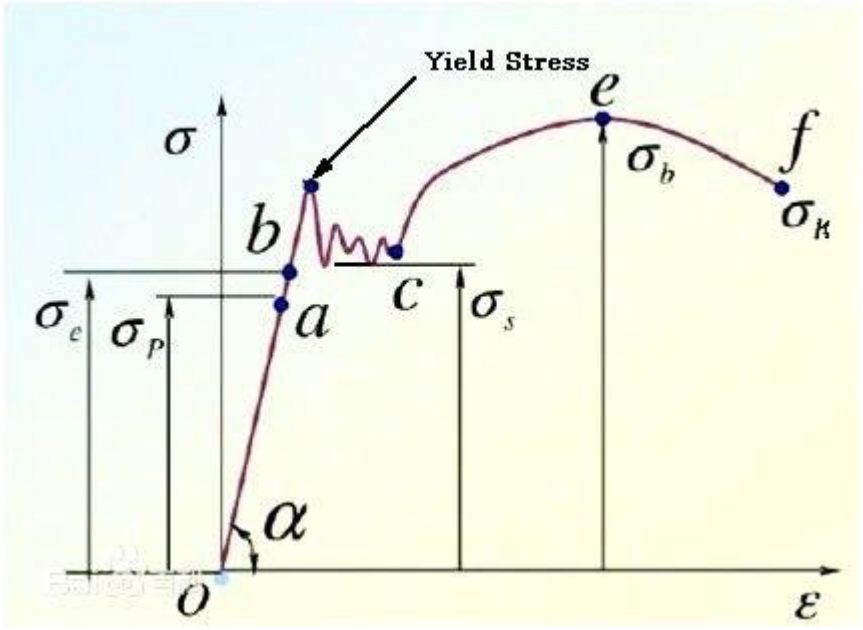

Figure 67 Stress-Strain curve (for mild steel)

From Figure 67 for mild steel, the process of tensile testing harakeke fibre has the following similar characteristics:

1. While the stress falls below σe, the stress depends on the test sample, if the stress is removed, the deformation disappears. This means the sample is in the elastic phase of the elasticity, and σe is the elastic limit of the material, and represents the maximum stress on the material to be fully flexible.

2. When the stress exceeds σe, the linear relationship between the stress and the strain ends, and the yield plateau begins. If unloaded, the deformation of the sample can be partially recovered, while some residual deformation, namely plastic deformation, is retained, which indicates that the deformation of the material has exceeded the yield point (yield stress) and entered the elastic-plastic range. The σs is called the lower yield point of the material.

3. When the stress exceeds σs, the test piece is plastically deformed significantly and homogeneously. If the strain of the test piece is increased, the stress value must be increased, which is called the process hardening or deformation strengthening with the increase of elastic deformation. When the stress reaches σb, the equal-deformation phase of the sample is terminated, the maximum stress σb is called the tensile strength of the material or the ultimate tensile strength, and it represents the resistance to the maximum uniform plastic deformation.

4. After σb, the sample starts to have an inhomogeneous plastic deformation that causes a contraction or neck, the load drops, and the final stress is a simple fracture at σk. This is the stress at fracture, which means the material has reached the ultimate force of plasticity.

The stress and strain in the above stress-strain curve are calculated on the basis of the initial size of the sample. In fact, the size of the sample is constantly changing during the stretching process. At this time, the actual stress S should be the instantaneous load (P) divided by the instantaneous cross-sectional area (A) of the sample, that is, S=P/A. Similarly, the true strain e should be the instantaneous elongation divided by the instantaneous length DE =dL/L. The figure below (Figure 68) is the instantaneous load force-extension of a harakeke tensile test sample. Unlike the stress-strain curve for metal, it does not decline after the load reaches its maximum value but continues to grow until it breaks.

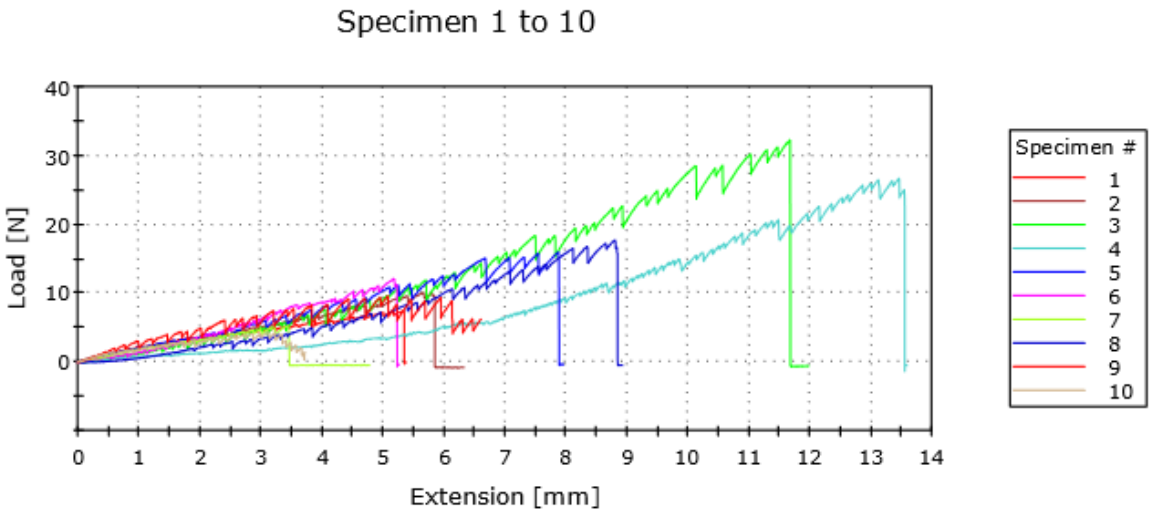

Figure 68 Load force vs. extension graph of a Harakeke sample

4.6.2.6 Calculating the Elastic Modulus (Young Modulus) of harakeke fibre

Elastic modulus is a key performance parameter of engineering materials. From a macro point of view, the elastic modulus is used to describe the size of the object's resistance to elasticity. In the microscopic view, it reflects the bonding strength between atoms, ions, or molecules. All factors that influence the strength of the binding, affect the elasticity of the material, the bonding method, the crystal structure, the chemicals, the microstructure and the temperature. Because of different alloy composition, different heat treatment state and different cold plastic deformation, Young's modulus for metals will fluctuate by 5% or more. However, the elastic modulus of a metal is an index of mechanical properties that are not sensitive to the structure, alloy, heat treatment, cold plastic deformation and other mechanical properties. The elastic modulus is not influenced significantly by the temperature, loading rate or external factors, so the elastic modulus is considered constant for a particular material in general engineering applications [48-49].

The modulus of elasticity can be seen as a measure of the degree of elasticity of a material's elastic deformation. The greater the value for the material, the greater the elastic deformation stress of the material, that is, the greater the stiffness of the material, the smaller the elastic deformation under a specified stress. Elastic modulus E refers to the stress required for the material to produce elastic deformation of the element under the action of external force. It is just an index of the materials resistance to elastic deformation. Figure 69 is a stress strain curve, it shows the proportional nature of stress and strain. The gradient of this line is young's modulus. E. The elastic modulus is constant, for a given material does not change. It represents the "stiffness" of material properties. Young's modulus of dissimilar materials is usually in the form of a table column in reference books, for scientists and engineers to refer.

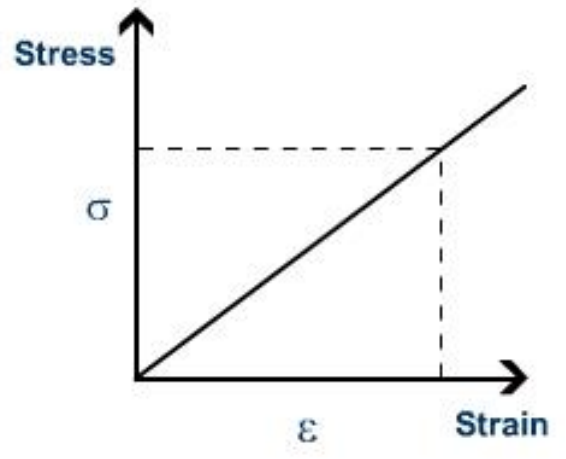

Figure 69 The linear trend line in Stress vs. Strain

The equation to calculate the Elastic Modulus is show below:

$$Elastic\ Module(E) = \frac{Stress(\sigma)}{Strain}$$

$$E = \frac{\sigma}{\varepsilon} \qquad \text{and} \qquad \sigma = \frac{F}{A}$$

$$\text{So}, E = \frac{F}{A\varepsilon} \qquad \text{and} \qquad \varepsilon = \frac{e}{l_o} \text{ so } \frac{1}{\varepsilon} = \frac{l_o}{e}$$

$$\text{So}, E = \frac{F\, l_o}{A\varepsilon}$$

Units of Young's modulus (E): Pa. More practically MPa or GPa

Shown by the following Figure 70, experiment set one and set seven, the modulus of elasticity is greater than 3000 MPa, which is 3 GPa. That's a lot more than the set of samples two and five. It can also be seen in the data that the Young's modulus value is higher when the test piece has a larger gauge length. The lower the modulus of elasticity, the greater the deformation. The smaller the stiffness, the more resilient the material is. The higher the modulus of elasticity, the smaller the deformation of the elastic modulus of the material, the higher the stiffness, the smaller the deformability of the material, and the higher the brittleness. Thus, unique natural materials can be chosen according to the areas in which they need to be used.

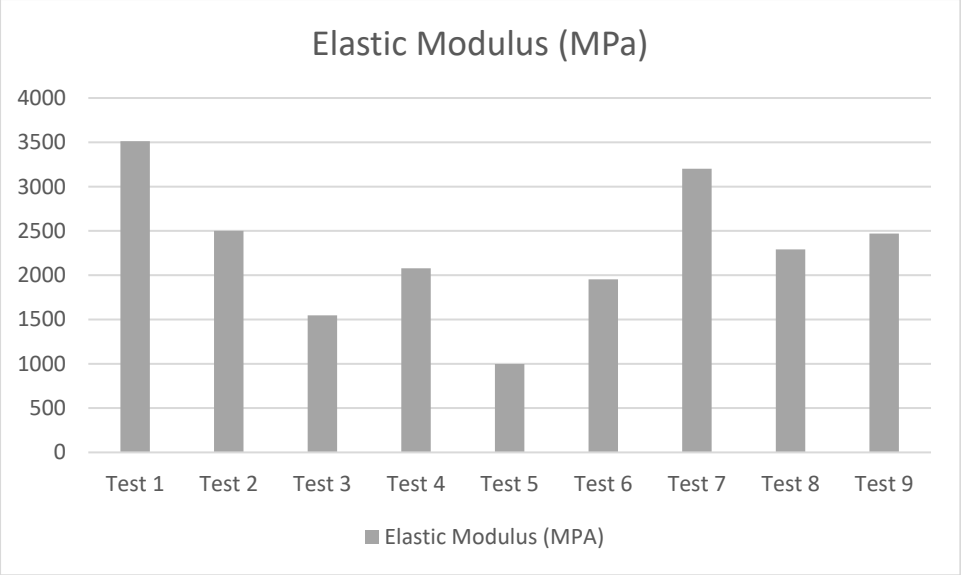

Figure 70 The Elastic modulus of each set of the test samples

4.6.2.7 Analysing the data

Harakeke fibre test results are shown in Table 9 and Figures 71-73.

Table 9: Harakeke fibre tensile test results

	Specimen Variable					
	Distance bwtween the clamp(mm)	Stretching speed(mm/min)	Average diameter of samples(mm)	Maximum Load Force(N)	Strain	Stress(Mpa)
Test 1	100	1	0.2540	12.1	6.770E-02	237.9
Test 2	100	1	0.3677	14.2	5.360E-01	134.0
Test 3	100	1	0.4479	16.4	6.730E-02	104.2
Test 4	80	1	0.3607	20.5	9.650E-02	200.6
Test 5	50	1	0.3770	21.3	1.912E-01	190.8
Test 6	60	1	0.3065	18.1	1.256E-01	245.4
Test 7	120	1	0.3503	21.4	6.940E-02	222.1
Test 8	100	3	0.3650	22.2	9.278E-02	212.5
Test 9	100	5	0.3250	18.8	9.181E-02	226.7

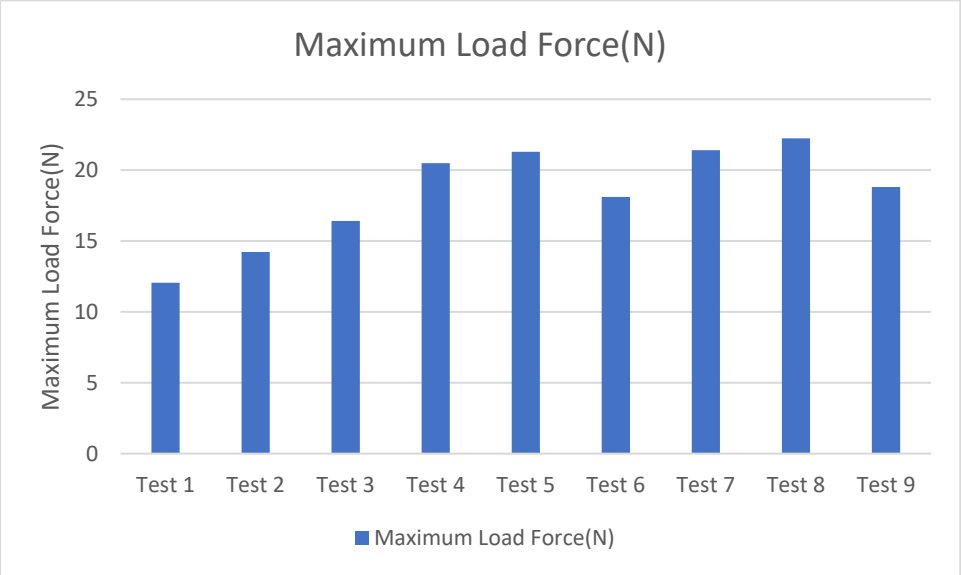

Figure 71 Harakeke Fibre -The load force results

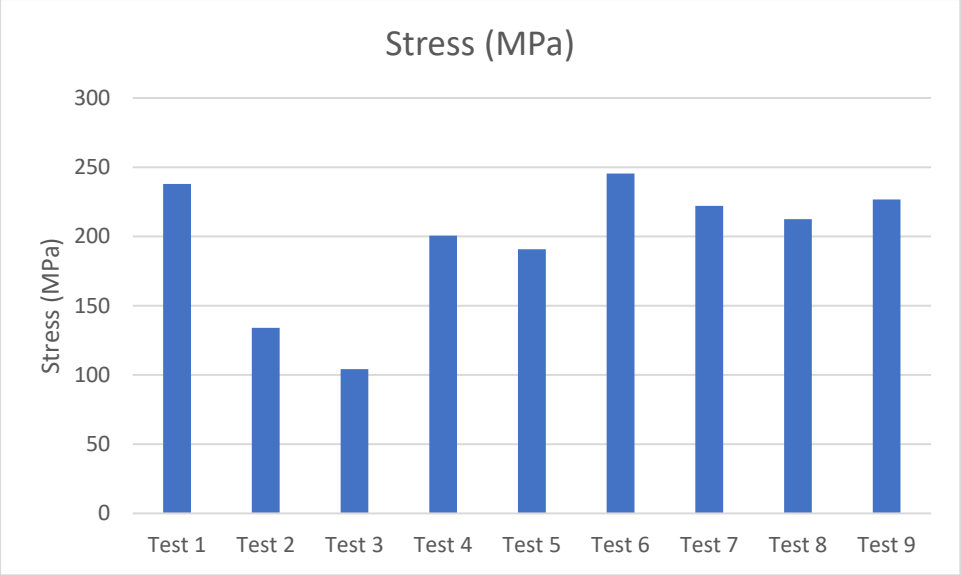

Figure 72 Harakeke Fibre -The mean value of tensile stress at maximum tensile strength

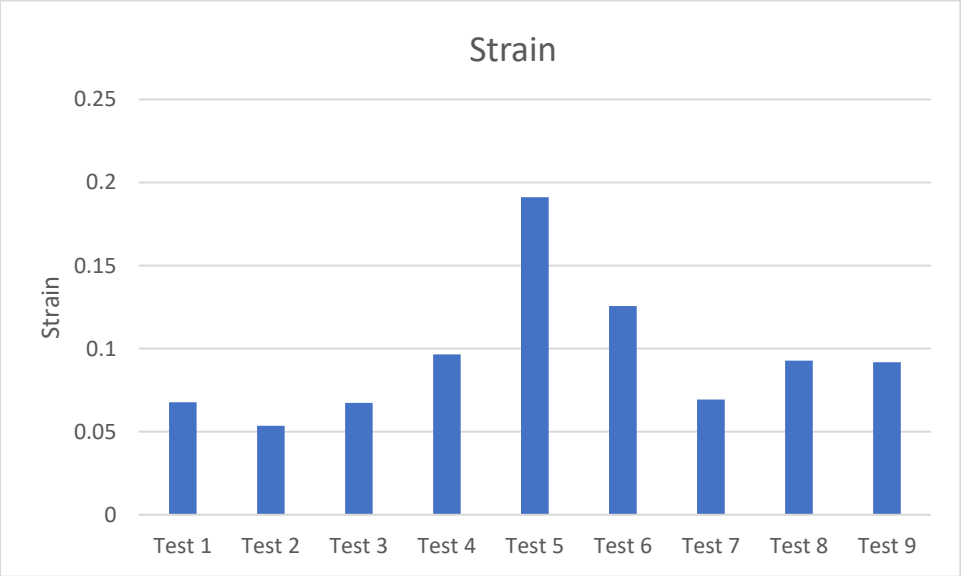

Figure 73 Harakeke Fibre -The mean value of tensile strain at maximum tensile strength

4.6.2.7.1 The influence of different effective lengths on tensile force

The distance between two clamps is also called the effective length or gauge length. In order to study the effect of gauge length on tensile properties, in this thesis, the tensile test speed for harakeke fibre was selected as 1 mm/min, and the fibre diameter was selected in the range of about 0.32 to 0.38 mm. There are five different distances between the two clamps which are 50 mm, 60 mm, 80 mm, 100 mm and 120 mm. Each gauge length was tested 10 times. Table 10 and Figure 75 shows the experimental results of the various gauge lengths or distance between the clamps.

Table 10: Effect of different clamp gauge lengths

Specimen Variable						
	Distance bwtween the clamp(mm)	Stretching speed(mm/min)	Average diameter of samples(mm)	Maximum Load Force(N)	Strain	Stress(Mpa)
Test 5	50	1	0.3770	21.3	1.912E-01	190.8
Test 6	60	1	0.3065	18.1	1.256E-01	245.4
Test 4	80	1	0.3607	20.5	9.650E-02	200.6
Test 2	100	1	0.3677	14.2	5.360E-01	134.0
Test 7	120	1	0.3503	21.4	6.940E-02	222.1

It can be seen in Table 10 that the gauge length has no significant influence on the mean value of the load force in tensile strength. The mean value of the load force in tensile strength of the samples tested using five different gauge lengths is similar, all of which are between 15 and 20N. Only the result of the second set of specimens are lower than the results of the other groups. From the tensile stress figures (Figure 75), if the test results are excluded at the minimum and maximum value of the gauge lengths (being 50 mm and 120 mm) it can be seen that the tensile strength and elongation at break decrease gradually with the increase of the spacing between the clamps. This is because the harakeke fibre's cross-sectional area along the length of the structure is non-uniform throughout. Therefore, the cross section strength of the same fibre is not entirely the same. When the fibre is subjected to a tensile test, the fracture is always at the weakest part of the fibre. When the length of the fibre is longer, the most vulnerable parts of the fibres are more likely to be detected. Therefore, the median value of tensile stress at tensile strength is lower. The reason why the maximum distance between the clamps was chosen as 120 mm, and not greater than 120 mm, is the specimen will break at the end of the sample. In other words, the clip securing the specimen to the jaws causes the specimen to break outside the gauge length. In the experiment at 120 mm gauge length, there was also a proportion of the fibres that didn't break in the middle of the sample. These results will not be as accurate as a consequence.

Thus, at the conclusion of the test, it can be said that the load and tensile stresses are relatively high when the spacing of the clamps is 60 mm to 80 mm. For future tests, the optimal test interval for the gauge length is from 60 mm to 80 mm.

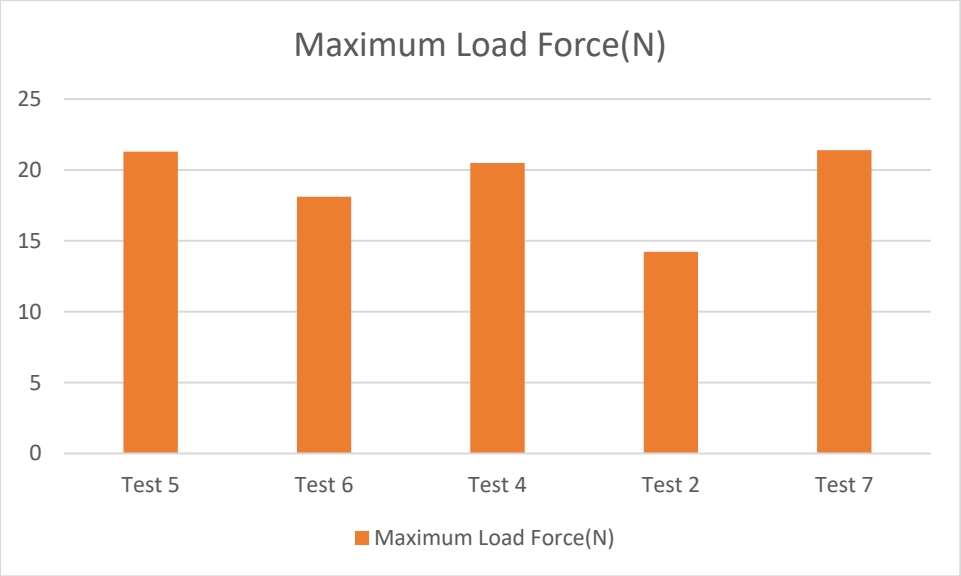

Figure 74 Load Force of harakeke fibres with different gauge lengths

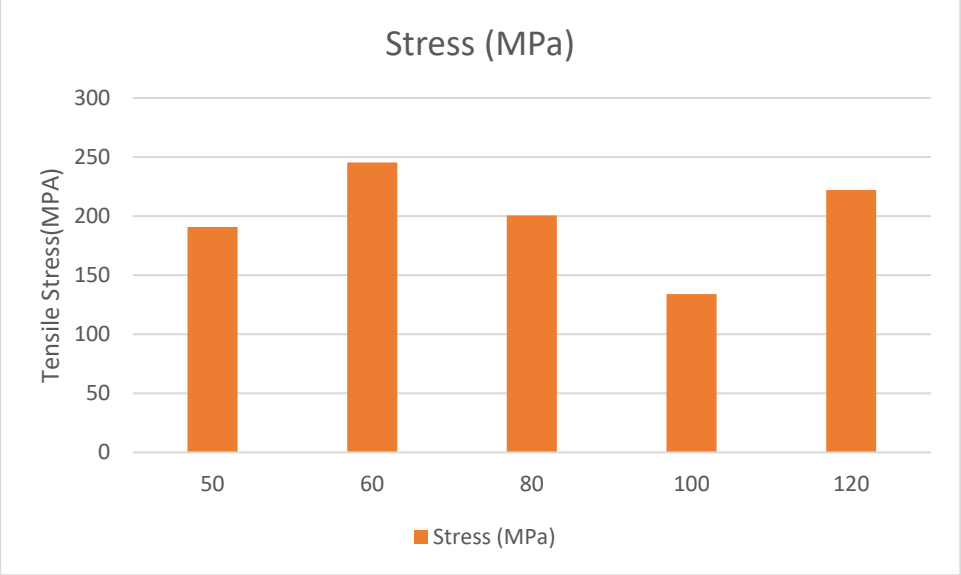

Figure 75 Tensile stress of harakeke fibres with different gauge lengths

4.6.2.7.2 Different influences on tensile test speed

In order to better examine the effect of speed on tensile properties, the harakeke fibre was stretched at a speed of 1 mm/min, 3 mm/min and 5 mm/min. Each set of specimens consisted of 10 tests. When the diameter of the specimen is about 0.3 mm and the spacing between clamps is 100 mm, the tensile test results of each set of fibres at different tensile test speed are shown in Table 11.

Table 11: The effect of different tensile test speed

Specimen Variable						
	Distance bwtween the clamp(mm)	Stretching speed(mm/min)	Average diameter of samples(mm)	Maximum Load Force(N)	Strain	Stress(Mpa)
Test 2	100	1	0.3677	14.2	5.360E-01	134.0
Test 8	100	3	0.3650	22.2	9.278E-02	212.5
Test 9	100	5	0.3250	18.8	9.181E-02	226.7

It can be seen from Figure 76 that the tensile speed has a great influence on the tensile strength and elongation at break. The tensile strength and elongation at break are gradually increasing as the velocity increases, i.e., the shortening of the break time. However, if the test speed is too fast, the sample can be fractured in the transition zone outside the gauge length or the marked area. If the tensile test speed is too fast, for example over 10 mm/min, the test sample is likely to break at both ends during the test, rather than in the middle of the sample. This will not accurately reflect the properties of the material, so the test speed should be reduced to a reasonable rate.

According to the following graphed test results, it can be seen that the tensile strength data of test set 2 are low which occurs at a tensile test speed of 1 mm/min. The mean value of load force is less than 15 N and the mean value of the tensile stress at tensile strength is less than 150 MPa. The mean value of tensile stress of set 8 and set 9 is higher than 200 MPa. But set 9's mean value for the load force at tensile strength is lower than the set 8. This is because the tiny differences in diameter greatly affects the stress values.

In conclusion, as can be seen from the tensile stress to tensile strength data, at speeds ranging from 3 mm/min to 5 mm/min, the tensile stress at the tensile strength and elongation at break data for harakeke fibres are better. In future experiments, the test speed should be selected in the range of 3 mm/min to 5 mm/min.

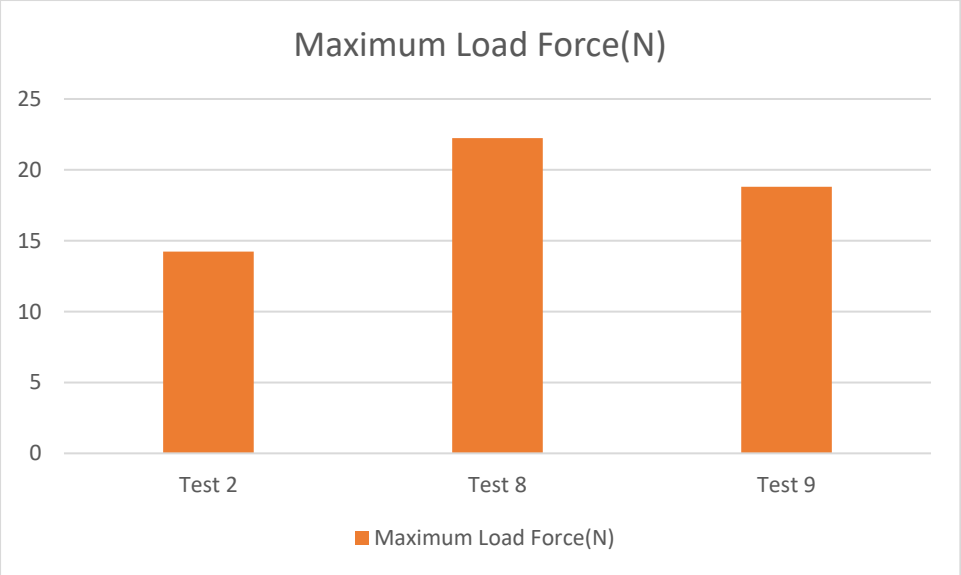

Figure 76 Load Force of harakeke fibres with different tensile test speed

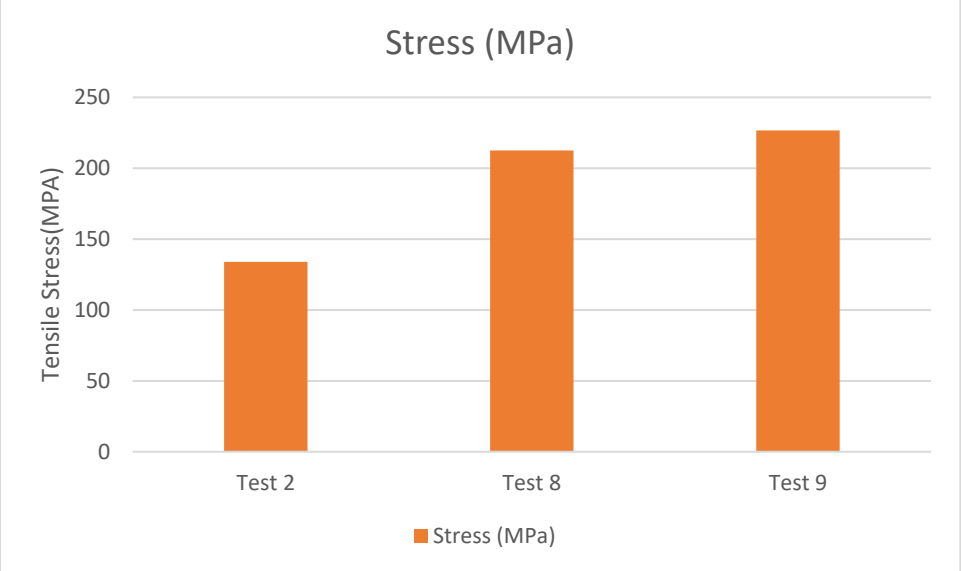

Figure 77 Tensile stress of harakeke fibres with different tensile test speed

4.6.2.7.3 Influences on different harakeke fibre diameters

In order to better study the effect of speed on tensile properties, different diameters of harakeke fibre were selected in the 0.2, 0.3 and 0.4 mm range. Each set of samples consisted of 10 specimens. With the tensile test speed set to 1 mm/min and the spacing between clamps at 100 mm, the tensile test results of each set of harakeke fibres are shown in Table 12.

Table 12: Tensile test results of samples sorted by fibre diameter

Specimen Variable						
	Distance bwtween the clamp(mm)	Stretching speed(mm/min)	Average diameter of samples(mm)	Maximum Load Force(N)	Strain	Stress(Mpa)
Test 1	100	1	0.2540	12.1	6.770E-02	237.9
Test 2	100	1	0.3677	14.2	5.360E-01	134.0
Test 3	100	1	0.4479	16.4	6.730E-02	104.2

As can be seen from the figure below, different harakeke fibre diameters have a significant impact on tensile strength and elongation at break. The tensile stress and elongation at break decreased with the larger diameter of the samples, but the mean value of the load force at tensile strength increased with the larger diameter of the samples. This is explained by the fact that the tensile stress is the force per unit area applied to the material. Even if set 2 and set 3 have a higher mean value for the load force than set 1, set 1 has a higher mean value of tensile stress. As can be seen from Figure 81 below, the loading force of the three samples are similar, ranging from 12 to 16 N. However, the tensile stress of set 1 was about 250 MPa, much higher than that of set 2 and 3 (Figure 79). However, it can be seen from the data that set 2 is a relatively consistent set among all the sample sets.

Therefore, the harakeke fibre with diameters in the range of 0.3 mm should be chosen as far as possible in future tests.

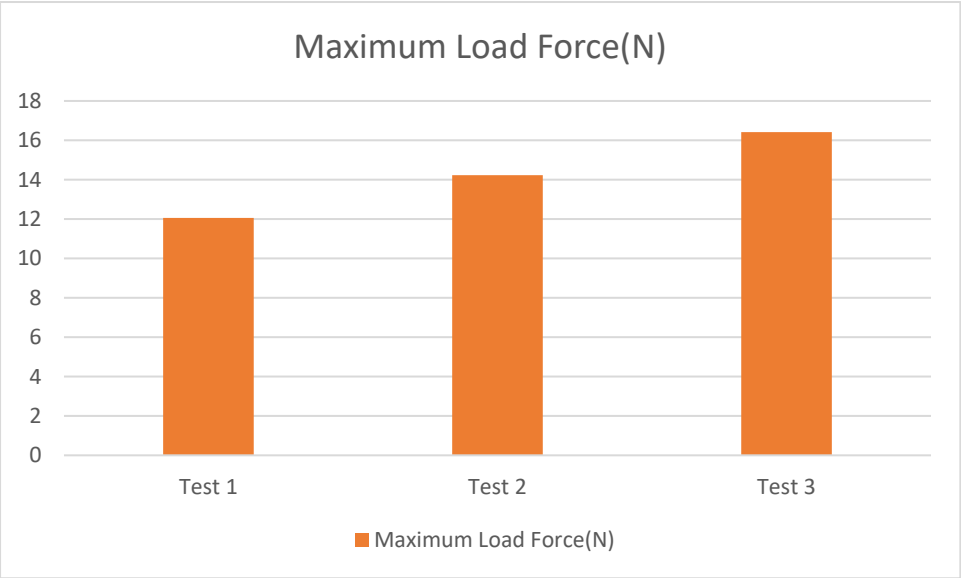

Figure 78 Load force of harakeke fibres with different sample diameters

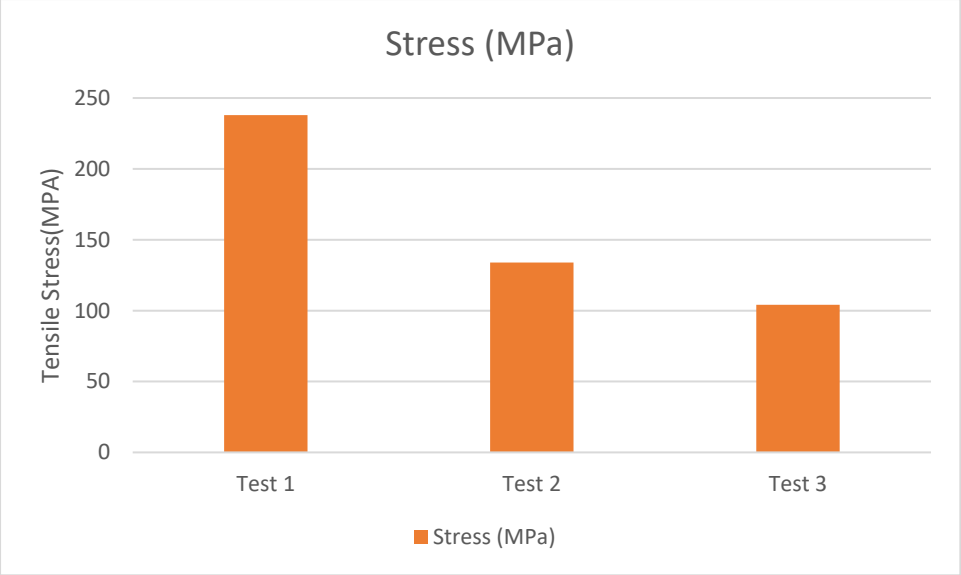

Figure 79 Tensile stress of harakeke fibres with different sample diameters

4.7 Analysis of experimental results and influencing factors

4.7.1 Influencing factors to strength measurement

4.7.1.1 Sample preparation damage

Although the tensile strength of harakeke fibre is relatively good, the maximum stress it can withstand under bending load is small. In sample preparation, it is very easy to cause a stress concentration in the fibre, which will cause premature failure, that is, the success rate of sample preparation is low. In the same way, other factors including variation of sample preparation, bond failure and damage, over clamping and other influences will lead to experimental errors and failure in the tensile test. Even if the whole test is very standardized, there are unavoidable errors in strength elongation. Eliminating the above issues are the key to measuring an accurate tensile strength of harakeke fibre.

4.7.1.2 Deviation from sample preparation

When sticking a single harakeke fibre on the jig, if it has a certain angle from the vertical direction, in the process of stretching, the fibre is not only stretched, but also subjected to bending and shear, especially at the root of the fibre. For drafting separation L_0, the real separation of tilted fibre with large slants, L_0 '= L_0 /cos θ (cosine theta). In view of the increase of L_0, the probability of weak joints within fibres increases, which will also affect the measured strength of harakeke fibre monofilament [27].

4.7.1.3 Bond damage

Adhesion is the combination of a mechanical bond, chemical bond and physical adsorption between the binder and the surface of harakeke fibre. The chemical action of the binder has little effect on the strength of the fibre body [27], which can be ignored.

4.7.1.4 Failure of bonding

When the sample is not well adhered, there may be part of the harakeke fibre pasted on the fixture that is pulled out under the action of the tensile force. At this time, measured monofilament strength may only be the bond strength of harakeke fibre and binder. Generally, this situation can be reflected by the large extension curve of harakeke fibre, as shown in Figure 80: Curve A is the σ-ε curve of fibre fracture in the bond zone. Curve B is the σ-ε curve for completely drawn out fibres resulting from bond failure. The curve does not accurately express the full strength and elongation of harakeke fibre when this occurs.

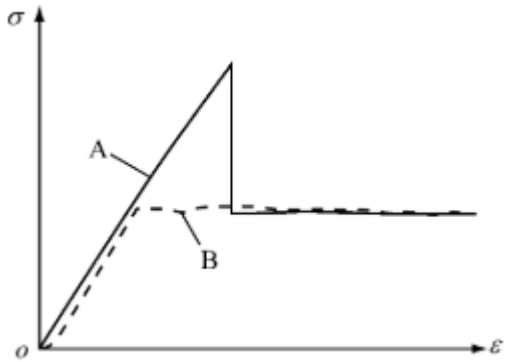

Figure 80 Stress strain curve showing insufficient adhesion

In the following figure (Figure 81) we can see that specimen 3 has a failure of bonding, as at about the 5 mm extension mark the curve dips and then partially recovers. At this time, measured monofilament strength may only be the bond strength between the harakeke fiber and binder. Therefore, this specimen could not fully express the strength and elongation of the harakeke fibre.

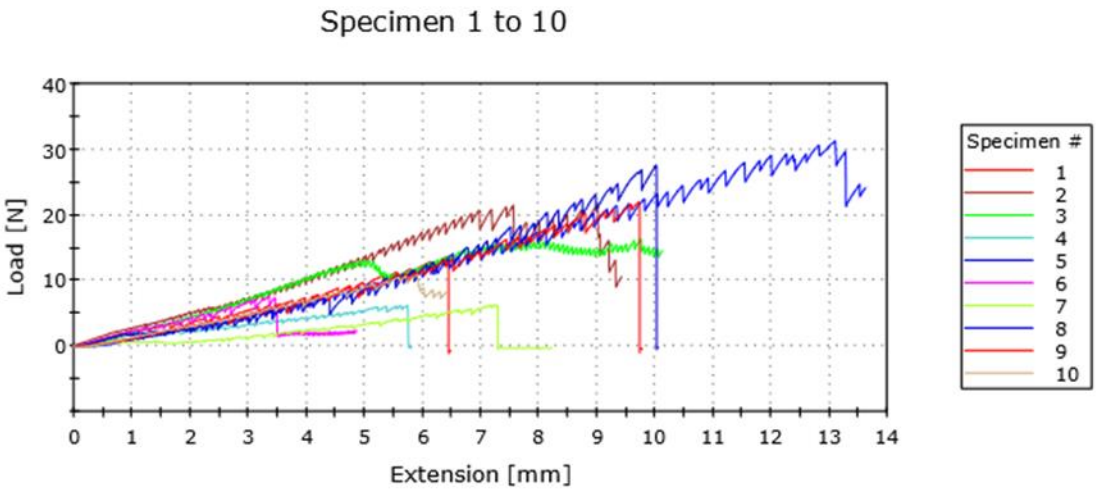

Figure 81 Failure curves of specimen 1-10.

4.7.1.5 The effect of clamping

If the length direction of the clamping fixture is not parallel to the tensile direction, the force is equivalent to the situation where the harakeke fibre is not perpendicular to the clamping fixture. This is exhibited by the fact that in the process of stretching, the fibre is not only subjected to tensile action, but also subjected to bending and shear forces. Standard tensile samples are not designed to be subjected to bending or shear.

4.7.1.6 Weak segments of the fibre itself

The measured strength of harakeke fibre is usually lower than the theoretical strength estimated by its uniform structure, which indicates that there are weak joints or defects in harakeke fibre. The fracture characteristics of the fibre, especially the strength, depend on the weakest part of the fibre [38], that is, the strength of the weakest joint of the harakeke fibre. Therefore, weak joints and their distribution are the prime reason for the dispersion of fibre strength.

4.7.1.7 Analysis of fibre fracture segment after stretching

If the fibre is pulled, and the fracture does not occur at the clamping end or binding end, then the damage of these can be ignored, and the mechanical properties of the fibre body can be well described by this measurement. However, during the tensile testing of harakeke fibre, although the fracture occurs between the two jaw spaces, the impact of the fracture process and the non-coaxial fibre shrinkage causes the fibre to vibrate and sway, and the fibre will bend and break. Most of these breaks occur at the bond holding end. On the one hand, the real fracture surface of the fibre cannot be retained; On the other hand, the fibres can be misjudged as to breaking at the root. This occurrence is a major impediment to the study of mechanical properties and structure of fibre.

Among the 100 fibres tested, 84 fibres retained the fracture tip, and the actual probability of fracture was 84%. The specimen fracture is ordered and is truncated from a complete monofilament into a number of slender fibrils. The result shows the retention rate at the bonding point was better when the harakeke fibre was broken [27].

4.8 Chapter conclusions

The influence on the mechanical properties of harakeke fibre monofilament using different tensile test speeds, gauge lengths and various cross-sectional areas of harakeke fibres was carefully investigated. The results show that the three different factors can influence the mechanical properties of the harakeke fibre to different degrees. Of the three, the extension speed has the greatest influence on the mechanical properties of the tensile test.
In order to reduce accidentally introduced stress damage and strain error and increase the retention rate of the fractured end of the fibre, it is necessary to keep the axial direction of the harakeke fibre in line with its tensile direction. At the same time, attention should be paid to avoid pretension of the harakeke fibre when making the sample card and the over tensioning of the fibre when clamping, to avoid fibre damage as much as possible. In addition, the analysis and modification of the harakeke fibre strength and extension curve should be carried out to eliminate the influence of the deviation in the bonding position, the tension and bending of the sample, the partial failure of the bonding effect, and the result of bond failure and stretching.

Factors affecting results:
The influence of tensile test speed on test results: To ensure the accuracy of test results, a relatively high tensile test speed can be selected from 3 to 5 mm/min to maintain test efficiency. It is recommended that high tensile test speed can be selected when the sample itself has a high elongation. The lower the elongation of the sample, the lower the tensile test speed should be selected.
There was only a slight difference between the tensile strength using tensile test speed of 3 and 5 mm/min. It has a significant effect on the tensile strength of harakeke fibre, when the tensile test speed is lower than 3 mm/min.

The influence of different gauge lengths on test results: According to the test results, the maximum and minimum outliers were excluded. The larger the gauge length, the lower the mean value of tensile stresses at tensile strength. The worse the consistency of the tested samples, the greater the influence of the longer gauge length on the measured strength. Because the longer the harakeke fibre, the greater the probability that its vulnerable parts will appear. Elongation at break also decreases with increasing gauge length.

From the conclusion of the tensile strength of different gauge lengths, it can be said that the load and tensile stresses are relatively high when the spacing of the clamps is 60 mm to 80 mm. In future testing, the optimal interval for the gauge length is about 60 mm.
The tensile stress and elongation at break decreased with the larger diameter samples, but the mean value of the load force in tensile strength increased with the larger diameter of the samples. This is explained by the fact that the tensile stress applied to a material is the force per unit area applied to the material.
The harakeke fibre with a diameter of about 0.3 mm should be chosen as much as possible in future tests.

In summary: From this research, sample set 6 showed the highest tensile stresses. Therefore, if the test results for the fibre samples are to achieve their maximum potential strength, the diameter of the harakeke fibre should be selected in the range of 0.3 mm, the gauge length should be 60 mm and the tensile test speed should be 3 mm/min.

5 Conclusions

Detailed analysis for the development of a continuous new 3D natural fibre weaving machine and an optimal test method for determining the tensile strength of New Zealand flax fibre monofilament are presented in this thesis. Important findings for this project are summarised below:

（1）The most exciting prospect of this intelligent 3D continuous natural fibre wire feeding system is that it can be used in the construction industry of the future. When robots are combined with materials, especially intelligent materials, they can "make" products directly by operating the movement of the mechanical arm. In this machine, continuous European flax fibre is used as material (a harakeke analogue), attached to a pre-designed steel screwed plate structure. In the computer, the track and sequence of the sliding table are arranged in advance and then converted into Arduino code. The end of the robot arm is equipped with weaving and feeding tools, and the movement of the robot arm is used to weave the skin texture, which is constructed similarly to "weaving cloth". With the ever-changing application of robots, different tools, different motion paths and different programming code, it will produce a variety of "products". Intelligence is also the general trend in future society, and a kind of indispensable part of an intelligent building robot. It widely involves artificial intelligence, computer vision, automatic control, precision instruments, sensing and information in a series of innovative research disciplines and these research results can be widely applied to the actual field of the construction industry. In our future work and life, there will be increasingly a need for robots to replace humans to work and complete some difficult or heavy tasks, and the demand for these practical robots will also be greater and greater. Therefore, the prospect for robot research and development is immeasurable.

（2）The 3D weaving machine designed in this paper is not very perceptive. It does not possess the ability to learn and control itself independently, and it can only weave using the wire feeding system by manual control or pre-programmed form. Construction site preparation and module assembly are operations that need to be completed in the field in the construction process, and it is also very difficult for robots to automate the whole process at present. The main reason is that the construction of the plant involves a wide variety of materials and tools, the robot adaptability requirements are very high. This may be applied in the developing construction industry. The next development is to design the weaving machine to have the ability to learn and control itself independently and adaptively, achieving full automation with the required properties and architecture. The main obstacle is the development of computer software to control the construction robots. Therefore, the design of this machine in the future can pay greater attention to the development and design of intelligent software.

（3）This thesis involved focused research on the mechanical properties of harakeke fibre monofilament with different tensile test speeds, different gauge lengths and varying cross-sectional areas of the harakeke fibres. The results show that the three different factors do influence the mechanical properties of the harakeke fibre. The tensile test speed has the greatest influence on the mechanical properties. From the conclusion of the tensile strength using different gauge lengths, it can be said that the load and tensile stresses are relatively high when the spacing of the clamps is 60 mm to 80 mm. According to the test results, the maximum and minimum outliers were excluded. The larger the gauge length, the lower the mean value of tensile stresses at tensile strength. The worse the consistency of the tested samples, the greater the influence of the longer gauge length on the measured strength. Because the longer the harakeke fibre, the greater the probability that its vulnerable parts will appear. Elongation at break also decreases with increasing gauge length.

Influence of tensile test speed on test results: To ensure the accuracy of test results, a relatively high tensile test speed can be selected from 3-5 mm/min to improve test efficiency. The tensile stress and elongation at break decreased with the larger diameter samples, but the mean value of the load force in tensile strength was increased with the larger diameter samples. Therefore, for the test results of the fibre samples to achieve their maximum strength, the diameter of the harakeke fibre should be selected in the region of 0.3 mm, the gauge length should be about 60 mm and the tensile test speed should be 3 mm/min.

In the 21st century, oil resources are becoming increasingly scarce, and the environment is increasingly protected. The cultivation of NZ plants, including harakeke and hemp plants, which are easy to grow, require little fertilizer, have a short harvest time, etc. can meet people's requirements for many natural, green products and maintain environmental protection. Natural fibre from harakeke, hemp and other plants have characteristics of high strength, small elongation, abrasion resistance and good hygroscopicity. Therefore, composite materials with such natural fibre as the reinforcement system has great development potential and has broad development prospects.

With the rapid advance of science and technology, the reform of industry has brought about innovation and development of other fields, and the construction industry has also been strongly impacted and affected. Digital design has been widely adopted by the industry, how to make digital construction meet the needs of design, can be effectively, efficiently and reasonably used in realistic projects. This is what we need to study and constantly explore. Fortunately, New Zealand has been very quick to introduce innovative technologies, and this area is now receiving a lot of attention. Many years ago, most of my friends in the industry did not know what a 3D printer was. In the last two years, they have been recognised and accepted by very many people. Similarly I believe that the application of robots in architecture will soon be known to all. More and more people are involved in development and research in this field, so that robots can better serve our industry.

6 Recommendations for Future Work

The research conducted in thesis has led to some valuable work for the future in this research area:

(1) In the process of measuring the harakeke fibre properties, the accuracy of the results could be improved in a future study in the following areas. Regarding the improvement of test equipment, design of a fixture that can better hold the fibre vertically would help rather than the winding fixture used in this test. At the same time, harakeke fibre material with better quality could be selected for consistent and equal material separation. The harakeke fibre material can also be chemically treated and/or subjected to tensile tests in different environments for research and analysis in the future.

(2) Corresponding to the adaptive computing design strategy, a prototype robot manufacturing process for continuous natural fibre reinforcement in the construction industry could be fully developed. In the process of fibre placement, stiffness changes of pneumatic form work and the resulting deformation fluctuations pose a special challenge to robot control. In the future, a pneumatic glue spraying device could be designed in the wire feeding system to make the single continuous fibre sent out sticky and automatically cover the construction surface.

(3) In the process of fibre placement, the fibre placement mode and position pose a unique challenge to robot control. In order to adapt to these parameters during the production process, the current position and contact force are recorded by an embedded sensor system and integrated into the robot control in real time. The development of this physics network system allows for continuous feedback between actual production conditions and the numerical generation of robot control codes. This represents not only an important development in the context of the project, but also a new opportunity for adaptive robot construction processes in general.

In our future work and life, there will be an increasing need for robots to replace humans to work and complete some difficult, heavy or complex tasks, and the demand for these practical robots will become greater and greater. Therefore, the prospects of robot research and their development are immeasurable. It demonstrates advanced computational design, simulation and manufacturing technologies, and the innovative potential of interdisciplinary research and teaching. The prototype expresses the anisotropy of fibre composites of an architectural quality and reflects the underlying process with a novel texture and structure. The result is not only a particularly convenient building technique, but also an innovative and expressive architectural demonstration.

7 References

[1] TechNewsDaily, "Robot cheetah sets new speed record, "*foxnews.com*, InnovationNewsDaily, Mar. 6, 2012. [Online]. Available: https://www.foxnews.com/tech/robot-cheetah-sets-new-speed-record. [Accessed: Apr. 19, 2018].

[2] ConRes, "Top 10 Tech Trends: Autonomous Agents and Things," *conres.com*, Conres, Mar. 22, 2016. [Online]. Available: https://www.conres.com/news/top-10-tech-trends-autonomous-agents-things/. [Accessed: Apr. 19, 2018].

[3] H. B. Cary and S. C. Helzer, *"Modern Welding Technology,"* New Jersey: Pearson Education, p. 316, 2015.

[4] F. D. Turek, "Machine Vision Fundamentals, How to Make Robots See," *NASA Tech Briefs magazine*, vol.35, pp. 60-62, Jun., 2011.

[5] T.S. Hong, M. Ghobakhloo, and W. Khaksar, "Robotic Welding Technology," *Comprehensive Materials Processing*, vol.6, pp. 77-99, Jun. 4, 2014.

[6] J. Villafuerte, "Advances in robotic welding technology," *Welding journal*, vol. 84, pp. 28-33, Jan., 2005.

[7] H. B. Cary SourceSecurity, "Robotics: Redefining crime prevention, public safety and security," *SourceSecurity.com*, SourceSecurity, Apr. 3, 2018. [Online]. Available: https://www.sourcesecurity.com/tags/counter-terror.html?ref=nav. [Accessed: Dec. 3, 2018].

[8] E. Pollock, "Construction Robotics Industry Set to Double by 2023," *engineering.com*, Emily Pollock, Jun. 7, 2018. [Online]. Available: https://www.engineering.com/BIM/ArticleID/17059/Construction-Robotics-Industry-Set-to-Double-by-2023.aspx. [Accessed: Dec. 3, 2018].

[9] TIMES, "Best Inventions of 2008 – TIME," *time.com*, TIMES, Oct. 29, 2008, [Online]. Available: https://www.time.com. [Accessed: Dec. 3, 2018].

[10] S. Ogden, "Kismet: Robot at MIT's AI Lab Interacts with Humans," Oct. 12, 2017, [Online].Available: https://www.engadget.com/2017/09/07/ibm-watson-ai-lab-mit/ [Accessed: Dec. 3, 2018].

[11] Arduino.cc, "Getting Started: FOUNDATION > Introduction," *arduino.cc*, Jun. 8, 2017. [Online]. Available: https://www.arduino.cc/en/Guide/HomePage. [Accessed: Dec. 3, 2018].

[12] D. Kushner, "The Making of Arduino," *IEEE Spectrum*, vol.84, pp. 30-35, Oct. 26, 2011.

[13] J. Lahart, "Taking an Open-Source Approach to Hardware," *mendeley.com*, Wall Street Journal, Nov. 27, 2009. [Online]. Available: https://www.mendeley.com/catalogue/taking-opensource-approach-hardware/. [Accessed: Dec. 3, 2018].

[14] H. Barragán, "The Untold History of Arduino," Mar. 6, 2016. [Online]. Available: http://arduinohistory.github.io/. [Accessed: Dec. 5, 2018].

[15] Massimo, "How many Arduinos are in the wild? About 300,000," May 2011. [Online]. Available: https://blog.adafruit.com/2011/05/15/how-many-arduinos-are-in-the-wild-about-300000/. [Accessed: Dec. 5, 2018].

[16] Malmö University,"Arduino FAQ – With David Cuartielles," Malmö University. Apr. 5, 2013. [Online]. Available: https://mau.se/en. [Accessed: Dec. 6, 2018].

[17] N. Stockton, "Arduino's New CEO, Federico Musto, May Have Fabricated His Academic Record," *wired.com*, WIRED, Dec. 22, 2017. [Online]. Available: https://www.wired.com/2017/04/arduinos-new-ceo-federico-musto-may-fabricated-academic-record/. [Accessed: Dec. 6, 2018].

[18] M. Doerstelmann, J. Knippers, V. Koslowski, A. Menges, M. Prado, G. Schieber, et al., "ICD/ITKE Research Pavilion 2014-15: Fibre Placement on a Pneumatic Body Based on a Water Spider Web," *Architectural Design*, vol. 85, pp. 60-65, Sept., 2015.

[19] S. Zhou, "The development direction and opportunity analysis of artificial intelligence and robot technology," *zhihu.com*, Zhihu, Mar. 10, 2018. [Online]. Available: https://zhuanlan.zhihu.com/p/34376187. [Accessed: Dec. 6, 2018].

[20] Mmsonline, "The successful application of industrial robots in the structural design of modern digital buildings," *mmsonline.com*, Mmsonline, Mar., 2010. [Online]. Available: https://www.mmsonline.com.cn/info/236624.shtml. [Accessed: Dec. 6, 2018].
[21] Metropole Architects, " From robot building to robot creation | school of architecture," *archcollege.com*, ArchitectureDaily, Feb. 2, 2018. [Online]. Available: http://www.archcollege.com/archcollege/2016/04/25273.html. [Accessed: Dec. 7, 2018].
[22] T. Kalil and L. Whitman, "The Materials Genome Initiative: The First Five Years," *obamawhitehouse.archives.gov*, obamawhitehouse, Aug. 2, 2016. [Online]. Available: https://obamawhitehouse.archives.gov/blog/2016/08/01/materials-genome-initiative-first-five-years. [Accessed: Dec. 7, 2018].
[23] S. Zhou, "Artificial intelligence and robotics technology development direction and opportunity," *zhihu.com*, Zhihu, Mar. 10, 2018. [Online]. Available: https://zhuanlan.zhihu.com/p/34376187. [Accessed: Dec. 6, 2018].
[24] R. Hu and J. K. Lim, "Fabrication and Mechanical Properties of Completely Biodegradable Hemp Fiber Reinforced Polylactic Acid Composites," *Journal of Composite Materials*, vol. 41, pp. 1655-1669, Jul., 2007.
[25] B. Duchemin and M. P. Staiger, "Treatment of Harakeke fiber for biocomposites," *Journal of Applied Polymer Science*, vol. 112, pp. 2710-2715, Jun. 5, 2009.
[26] R. H. Newman, E. C. Clauss, J. E. P. Carpenter, and A. Thumm, "Epoxy composites reinforced with deacetylated Phormium tenax leaf fibres," *Composites Part A: Applied Science and Manufacturing*, vol. 38, pp. 2164-2170, Oct. 2007.
[27] I. M. De Rosa, J. M. Kenny, D. Puglia, C. Santulli, and F. Sarasini, "Tensile behavior of New Zealand flax (Phormium tenax) fibers," *Journal of Reinforced Plastics and Composites*, vol. 29, pp. 3450-3454, Dec., 2010.
[28] Y. Li, Y. W. Mai, and L. Ye, "Sisal fibre and its composites: a review of recent developments," *Composites Science and Technology*, vol. 60, pp. 2037-2055, Aug., 2000.
[29] X. Ma, J. Yu, and J. F. Kennedy, "Studies on the properties of natural fibers-reinforced thermoplastic starch composites," *Carbohydrate Polymers*, vol. 62, pp. 19-24, Oct. 17, 2005.
[30] Landcareresearch, "Harakeke and Whahariki," *landcareresearch.co.nz*, Information sheets, Mar. 10, 2018. [Online]. Available: https://www.landcareresearch.co.nz/science/plants-animals-fungi/plants/ethnobotany/weaving-plants/information-sheets/harakeke-and-whahariki. [Accessed: Dec. 6, 2018].
[31] Y. Li, Y. W. Mai, and L. Ye, "Effects of fibre surface treatment on fracture-mechanical properties of sisal-fibre composites," *Composite Interfaces*, vol. 12, pp. 141-163, Jan. 1, 2005
[32] S. Sarısaman, "A Public Order Problem During the First World War: Şebinkarahisar Armenian Rebellion," *Journal of History Studies*, vol.10, pp.221-239, Oct. 7, 2018.
[33] Aishenghuoxuexi, "How much do you know about open source hardware?," *elecfans.com*, forum, Jul. 26, 2018. [Online]. Available: http://bbs.elecfans.com/forum.php?mod=viewthread&page=1&tid=1621606. [Accessed: Dec. 6, 2018]
[34] L. Chen, "*Arduino program design basics*," Beijing: Beijing aerospace publishing house, pp. 5-6, 2014.
[35] D. J. Stokes, "Principles and Practice of Variable Pressure/Environmental Scanning Electron Microscopy (VP-ESEM)," *Principles and Practice of Variable Pressure/Environmental Scanning Electron Microscopy (VP-ESEM)*, pp. 1-221, Nov. 27, 2008.
[36] H. U. Zaman, M. A. Khan, and R. A. Khan, "Comparative experimental studies on the mechanical and degradation properties of natural fibers reinforced polypropylene composites," *Composite Interfaces*, vol. 19, pp. 59-70, Feb., 2012.
[37] E. Bodros and C. Baley, "Study of the tensile properties of stinging nettle fibres (Urtica dioica)," *Materials Letters*, vol. 62, pp. 2143-2145, May. 15, 2008.

[38] D. R. Askeland and P. P. Phulé, *The science and engineering of materials (5th ed.)*, US: Cengage Learning, p.198, 2001.
[39] Z. P. Xia, J. Y. Yu, L. D. Cheng, L. F. Liu, and W. M. Wang, "Study on the breaking strength of jute fibres using modified Weibull distribution," *Composites Part A: Applied Science and Manufacturing*, vol. 40, pp. 54-59, Jan., 2009.
[40] J. Andersons, E. Sparnins, R. Joffe, and L. Wallstrom, "Strength distribution of elementary flax fibres," *Composites Science and Technology*, vol. 65, pp. 693-702, Mar., 2005.
[41] J. Andersons, E. Poriķe and E. Spārniņš, "The effect of mechanical defects on the strength distribution of elementary flax fibres," *Composites Science and Technology*, vol. 69, pp. 2152-2157, Oct. 1, 2009.
[42] N. E. Zafeiropoulos, G. G. Dijon, and C. A. Baillie, "A study of the effect of surface treatments on the tensile strength of flax fibres: Part I. Application of Gaussian statistics," *Composites Part A: Applied Science and Manufacturing*, vol. 38, pp. 621-628, Feb., 2007.
[43] S. Batchu, "Generic MMPDS Mechanical Properties Table," *stressebook.com*, Stress engineering, Dec. 6, 2014, [Online]. Available: http://www.stressebook.com/mmpds-mechanical-properties-table/. [Accessed: Dec. 6, 2018].
[44] J. T. Black, *DeGarmo's Materials and Processes in Manufacturing*, US: Wiley, p.31, 2003.
[45] W. F. Smith, *Foundations of Materials Science and engineering*, New York: McGraw-Hill, p.223, 2006.
[46] C. Luebkeman and D. Peting, "Stress–strain curves," *uoregon.edu*, Apr. 28, 2012. [Online]. Available: http://pages.uoregon.edu/struct/courseware/461/461_lectures/461_lecture24/461_lecture24.html. [Accessed: Dec. 6, 2018].
[47] F. Beer and R. Johnston, *Mechanics of materials*, New York: McGraw-Hill, p.51, 2009.
[48] R. Moreton, "The effect of gauge length on the tensile strength of R.A.E. carbon fibres," *Fibre Science and Technology*, vol. 1, pp. 273-284, Apr., 1969.
[49] H. Pan and S. Huang, "Effects of surface and interface and adhesion mechanism", *Adhesion*, vol.24, no.3, pp.41-46, 2003.

8 Appendix

8.1 Appendix 1 Harakeke Fibre Tensile Test Results

8.1.1 Set 1

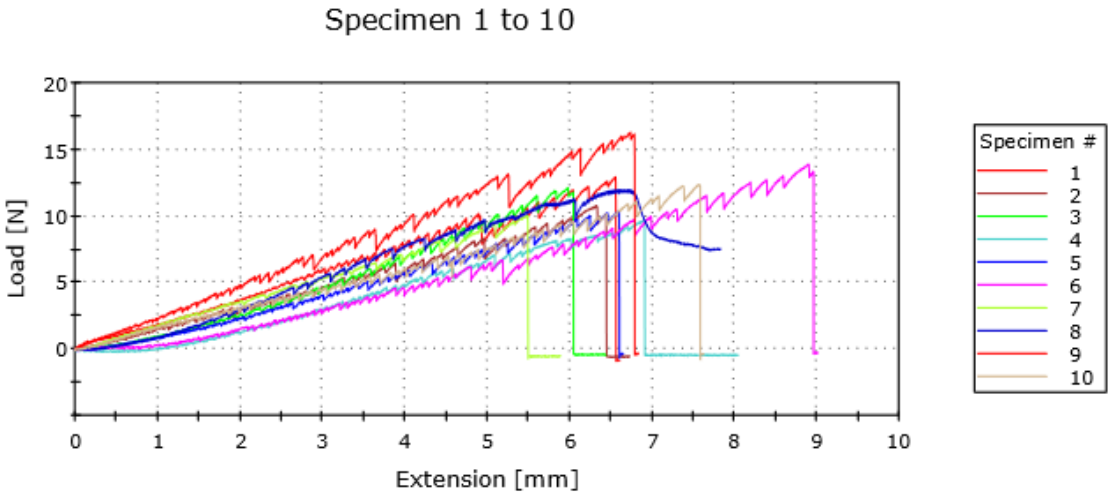

8.1.2 Set 2

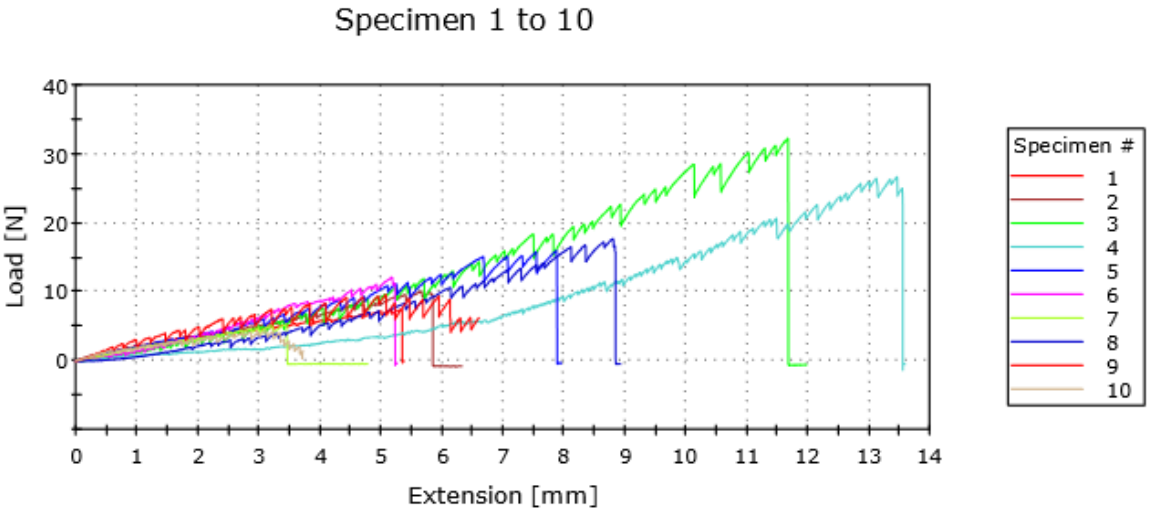

8.1.3 Set 3

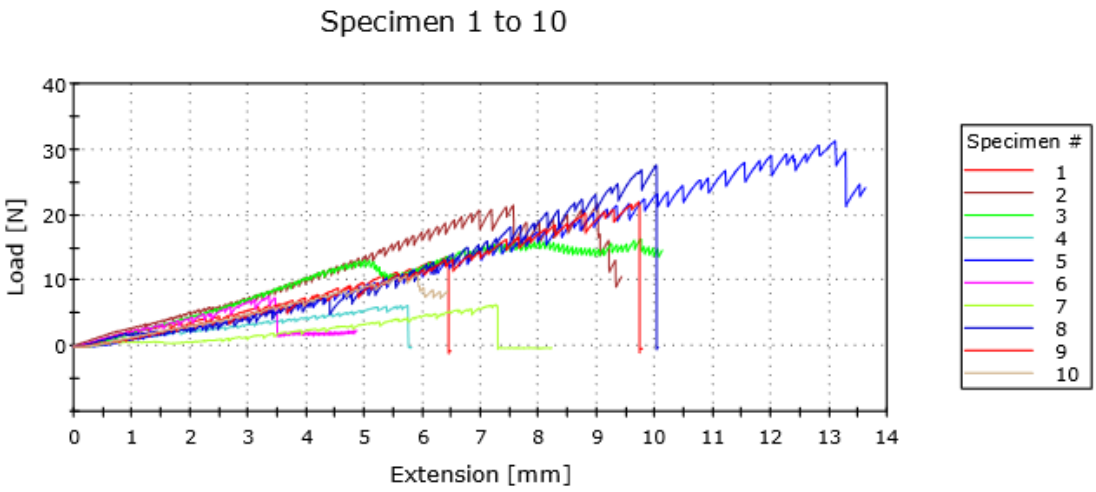

8.1.4 Set 4

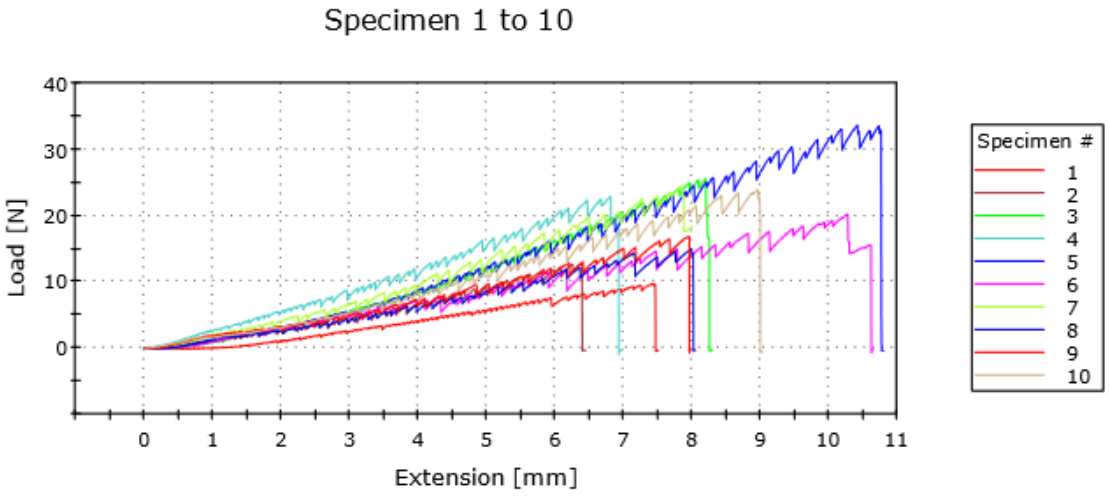

8.1.5 Set 5

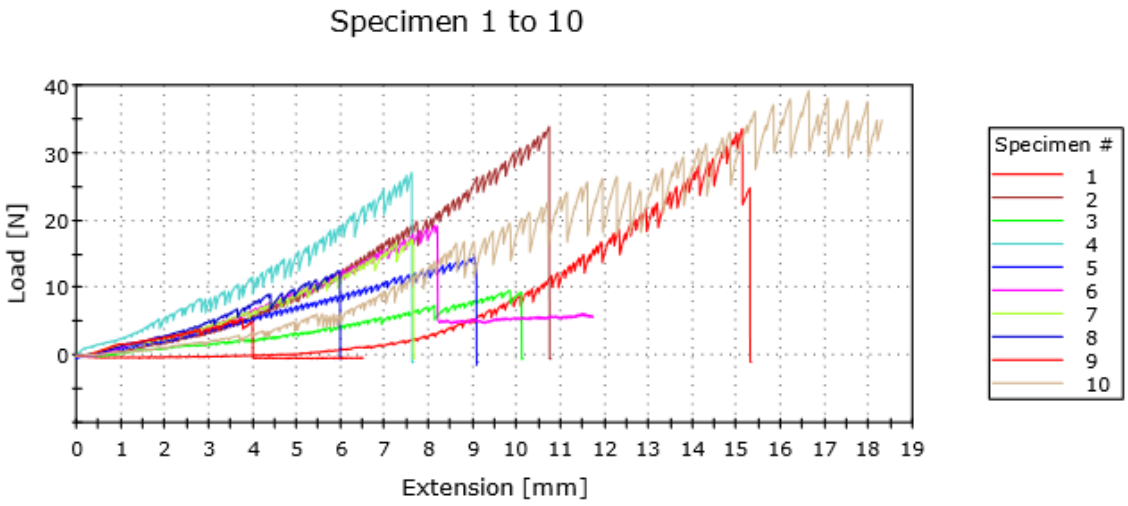

8.1.6 Set 6

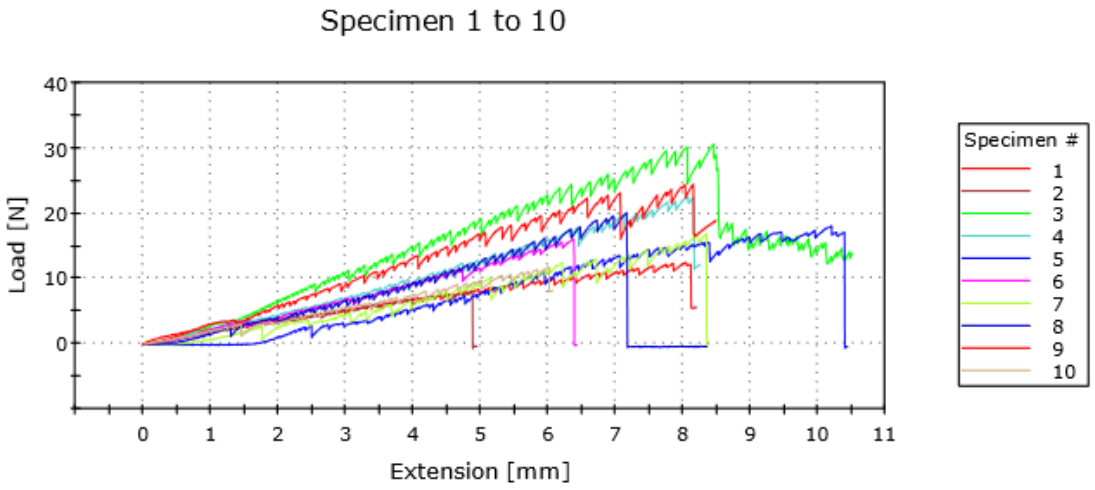

8.1.7 Set 7

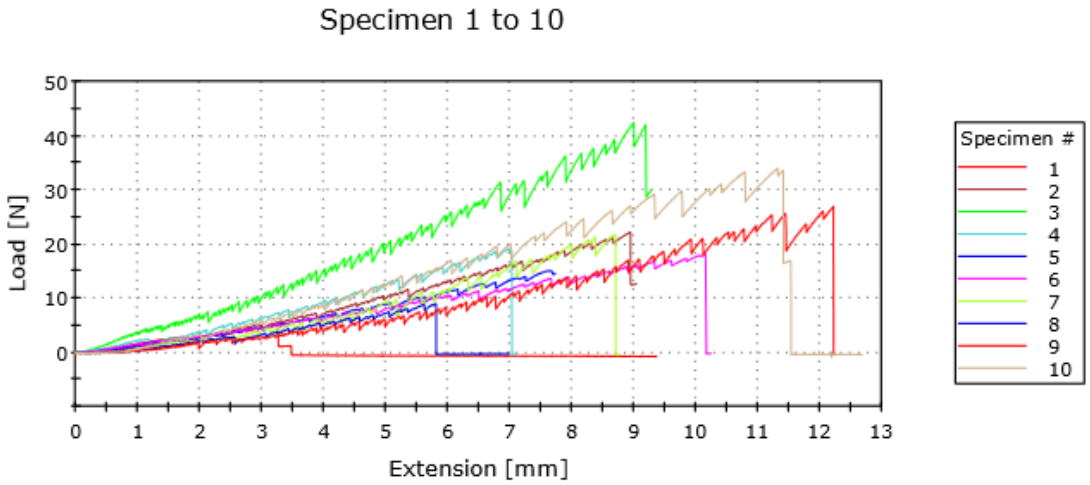

8.1.8 Set 8

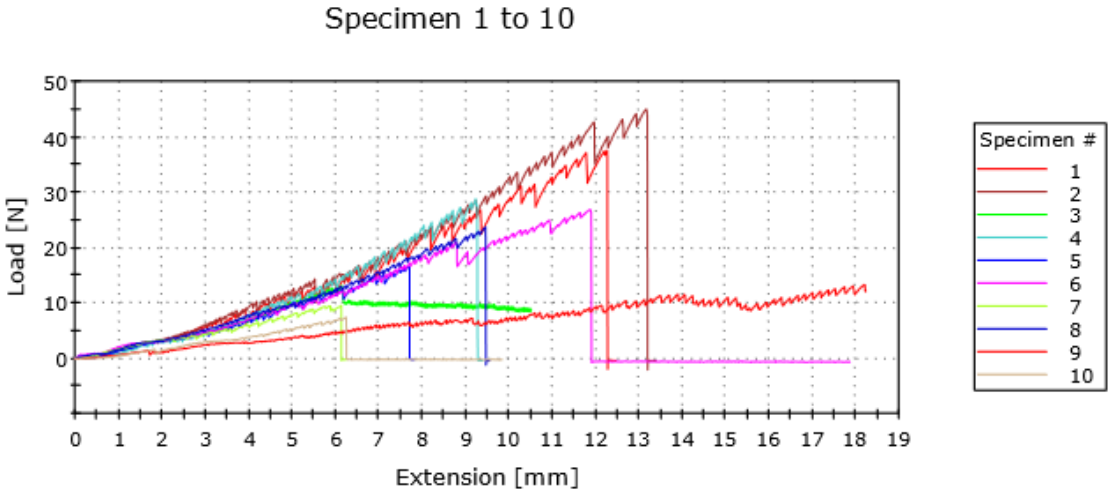

8.1.9 Set 9

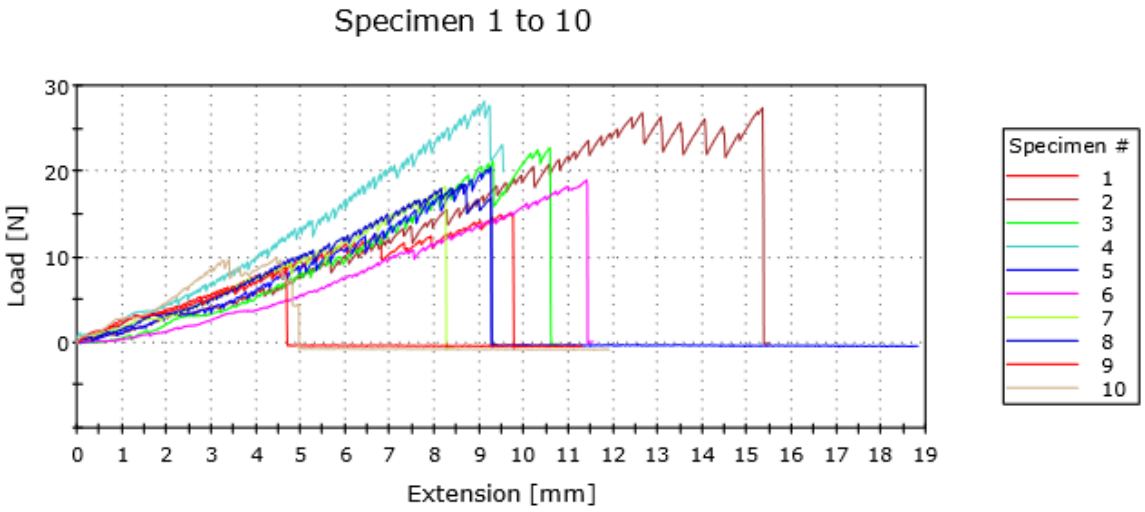

8.2 Appendix 2: Program Listing

```
//Automated Design Code - Junyi Lin

//Slide Table Stepper Motor Driver Pins
#define CLK 6
#define CW 5
#define EN 4
#define CLK2 9
#define CW2 8
#define EN2 7
#define CLK3 12
#define CW3 11
#define EN3 10

//Limit Switch Parameters
const int L1 = 1;  //Pin for x-axis slide table limit Switch
const int L2 = 2;  //Pin for y-axis slide table limit Switch
const int L3 = 3;  //Pin for z-axis slide table limit Switch


int user_input = 0;  // The user type in the input instruction



void setup() {
pinMode(CLK,OUTPUT);
pinMode(CW,OUTPUT);
pinMode(EN,OUTPUT);
pinMode(CLK2,OUTPUT);
pinMode(CW2,OUTPUT);
pinMode(EN2,OUTPUT);
pinMode(CLK3,OUTPUT);
pinMode(CW3,OUTPUT);
pinMode(EN3,OUTPUT);
Serial.begin(9600);

  pinMode(L1,INPUT);
  pinMode(L2,INPUT);
  pinMode(L3,INPUT);
 // Set Dir to switch
  digitalWrite(L1,LOW); // Enables the motor to move in a particular direction
  digitalWrite(L2,LOW); // Enables the motor to move in a particular direction
  digitalWrite(L3,LOW); // Enables the motor to move in a particular direction
}
```

```
void loop() {
 if(Serial.available()){
   // when it is turn on the power
    user_input = Serial.read();
    Serial.println(user_input);
 // if the user type a word flowing the user instuuction
 // which is manual mode
    if((user_input =='q')){//move the x-axis slide table forward
        eject();
    }if(user_input == 'w'){//move the x-axis slide table backward
      eject1();
    }if(user_input == 'a'){//move the y-axis slide table forward
      eject2();
    }if(user_input =='s'){//move the y-axis slide table backward
      eject3();
    }if(user_input == 'z'){//move the z-axis slide table forward
      eject4();
    }if(user_input == 'x'){//move the z-axis slide table backward
      eject5();

    // The flowing function is auto mode
    }if(user_input =='e'){
      //atuo to weaving with construction wall model
      eject6();
    }if(user_input == 'r'){
      //atuo to weaving with Winding model one
      eject7();
    }if(user_input == 't'){
      //atuo to weaving with Winding model two
      eject8();
    }
    if(user_input == 'y'){
     //auto mode to move to the origional point
     // move x-axis to origional point
    int xswitch = digitalRead(L1);
    if( xswitch == HIGH && (digitalRead(L1) == LOW) ){
        xmotorStep(1);
    }
    else if( xswitch == LOW && (digitalRead(L1) == LOW) ){
          digitalWrite(L1,HIGH);
          delay(2000);
    }
    if( (digitalRead(L1) == HIGH) ){
        xmotorStep(4000);
        digitalWrite(L1,LOW);
        delay(2000);
```

```
      // move y-axis to origional point
    int yswitch = digitalRead(L2);
    if( yswitch == HIGH && (digitalRead(L2) == LOW) ){

        ymotorStep(1);
    }
    else if( yswitch == LOW && (digitalRead(L2) == LOW) ){
          digitalWrite(L2,HIGH);
          delay(2000);
    }
    if( (digitalRead(L2) == HIGH) ){
        xmotorStep(4500);
        digitalWrite(L2,LOW);
        delay(2000);
    }

          // move z-axis to origional point
    int zswitch = digitalRead(L3);
    if( zswitch == HIGH && (digitalRead(L3) == LOW) ){

        zmotorStep(1);
    }
    else if( yswitch == LOW && (digitalRead(L3) == LOW) ){
          digitalWrite(L3,HIGH);
          delay(2000);
    }
    if( (digitalRead(L3) == HIGH) ){
        xmotorStep(2500);
        digitalWrite(L3,LOW);
        delay(2000);
    }
    }
 }
}


void xmotorStep( int MAX){
  digitalWrite(CW,HIGH);
   for(int x = 0; x < MAX; x++) {
        digitalWrite(L1,HIGH);
        delayMicroseconds(1000);
        digitalWrite(L1,LOW);
        delayMicroseconds(1000);
      }
}
```

```
void ymotorStep( int MAX){
  digitalWrite(CW2,LOW);
   for(int x = 0; x < MAX; x++) {
        digitalWrite(CLK2,HIGH);
        delayMicroseconds(1000);
        digitalWrite(CLK2,LOW);
        delayMicroseconds(1000);
      }
}
void zmotorStep( int MAX){
  digitalWrite(CW3,HIGH);
   for(int x = 0; x < MAX; x++) {
        digitalWrite(CLK3,HIGH);
        delayMicroseconds(1000);
        digitalWrite(CLK3,LOW);
        delayMicroseconds(1000);
      }
}
```

```
void  eject(void) {
while (digitalRead(L1) != HIGH);
digitalWrite(CW,HIGH);
for(int i=0;i<200;++i)
{
digitalWrite(CLK,HIGH);
delayMicroseconds(1000);
digitalWrite(CLK,LOW);
delayMicroseconds(1000);
}
}

void  eject1(void) {
while (digitalRead(L1) != LOW);
digitalWrite(CW,LOW);
for(int i=0;i<200;++i)
{
digitalWrite(CLK,HIGH);
delayMicroseconds(1000);
digitalWrite(CLK,LOW);
delayMicroseconds(1000);
}
}
```

```
void  eject2(void) {
while (digitalRead(L2) != HIGH);
digitalWrite(CW2,LOW);
for(int i=0;i<200;++i)
{
digitalWrite(CLK2,HIGH);
delayMicroseconds(1000);
digitalWrite(CLK2,LOW);
delayMicroseconds(1000);
}
}

void  eject3(void) {
while (digitalRead(L2) != LOW);
digitalWrite(CW2,HIGH);
for(int i=0;i<200;++i)
{
digitalWrite(CLK2,HIGH);
delayMicroseconds(1000);
digitalWrite(CLK2,LOW);
delayMicroseconds(1000);
}
}

void  eject4(void) {
while (digitalRead(L3) != HIGH);
digitalWrite(CW3,HIGH);
for(int i=0;i<200;++i)
{
digitalWrite(CLK3,HIGH);
delayMicroseconds(1000);
digitalWrite(CLK3,LOW);
delayMicroseconds(1000);
}
}

void  eject5(void) {
while (digitalRead(L3) != LOW);
digitalWrite(CW3,LOW);
for(int i=0;i<200;++i)
{
digitalWrite(CLK3,HIGH);
delayMicroseconds(1000);
digitalWrite(CLK3,LOW);
delayMicroseconds(1000);
}
```

```
//auto mode
//atuo to weaving with construction wall model
void  eject6(void) {
for ( int j=0;j<9;++j){
digitalWrite(CW,HIGH);
for(int i=0;i<2000;++i)
{
digitalWrite(CLK,HIGH);
delayMicroseconds(1000);
digitalWrite(CLK,LOW);
delayMicroseconds(1000);
}
delay(500);
digitalWrite(CW2,LOW);
for(int i=0;i<2800;++i)
{
digitalWrite(CLK2,HIGH);
delayMicroseconds(1000);
digitalWrite(CLK2,LOW);
delayMicroseconds(1000);
}
delay(500);
digitalWrite(CW,LOW);
for(int i=0;i<2000;++i)
{
digitalWrite(CLK,HIGH);
delayMicroseconds(1000);
digitalWrite(CLK,LOW);
delayMicroseconds(1000);
}
delay(500);
digitalWrite(CW2,HIGH);
for(int i=0;i<2800;++i)
{
digitalWrite(CLK2,HIGH);
delayMicroseconds(1000);
digitalWrite(CLK2,LOW);
delayMicroseconds(1000);
}
digitalWrite(CW3,HIGH);
for(int i=0;i<10;++i)
{
digitalWrite(CLK2,HIGH);
delayMicroseconds(1000);
digitalWrite(CLK2,LOW);
```

```
//atuo to weaving with Winding model one
void eject7(void){
digitalWrite(CW2,LOW);
for(int i=0;i<2200;++i)
{
digitalWrite(CLK2,HIGH);
delayMicroseconds(1000);
digitalWrite(CLK2,LOW);
delayMicroseconds(1000);
}
digitalWrite(CW,HIGH);
for(int i=0;i<200;++i)
{
digitalWrite(CLK,HIGH);
delayMicroseconds(1000);
digitalWrite(CLK,LOW);
delayMicroseconds(1000);
}
digitalWrite(CW2,HIGH);
for(int i=0;i<2200;++i)
{
digitalWrite(CLK2,HIGH);
delayMicroseconds(1000);
digitalWrite(CLK2,LOW);
delayMicroseconds(1000);
}
digitalWrite(CW,LOW);
for(int i=0;i<220;++i)
{
digitalWrite(CLK,HIGH);
delayMicroseconds(1000);
digitalWrite(CLK,LOW);
delayMicroseconds(1000);
}
digitalWrite(CW2,LOW);
for(int i=0;i<220;++i)
{
digitalWrite(CLK2,HIGH);
delayMicroseconds(1000);
digitalWrite(CLK2,LOW);
delayMicroseconds(1000);
}
digitalWrite(CW,HIGH);
for(int i=0;i<220;++i)
{
digitalWrite(CLK,HIGH);
delayMicroseconds(1000);
digitalWrite(CLK,LOW);
delayMicroseconds(1000);
}

digitalWrite(CW2,HIGH);
for(int i=0;i<220;++i)
{
digitalWrite(CLK2,HIGH);
delayMicroseconds(1000);
digitalWrite(CLK2,LOW);
delayMicroseconds(1000);
}

digitalWrite(CW,HIGH);
for(int i=0;i<200;++i)
{
digitalWrite(CLK,HIGH);
delayMicroseconds(1000);
digitalWrite(CLK,LOW);
delayMicroseconds(1000);
}

for ( int j=0;j<9;++j){
digitalWrite(CW2,LOW);
for(int i=0;i<2200;++i)
{
digitalWrite(CLK2,HIGH);
delayMicroseconds(1000);
digitalWrite(CLK2,LOW);
delayMicroseconds(1000);
}
digitalWrite(CW,LOW);
for(int i=0;i<200;++i)
{
digitalWrite(CLK,HIGH);
delayMicroseconds(1000);
digitalWrite(CLK,LOW);
delayMicroseconds(1000);
}

digitalWrite(CW2,HIGH);
```

```
digitalWrite(CW2,HIGH);
for(int i=0;i<2200;++i)
{
digitalWrite(CLK2,HIGH);
delayMicroseconds(1000);
digitalWrite(CLK2,LOW);
delayMicroseconds(1000);
}
digitalWrite(CW,HIGH);
for(int i=0;i<220;++i)
{
digitalWrite(CLK,HIGH);
delayMicroseconds(1000);
digitalWrite(CLK,LOW);
delayMicroseconds(1000);
}
digitalWrite(CW2,LOW);
for(int i=0;i<220;++i)
{
digitalWrite(CLK2,HIGH);
delayMicroseconds(1000);
digitalWrite(CLK2,LOW);
delayMicroseconds(1000);
}
digitalWrite(CW,LOW);
for(int i=0;i<220;++i)
{
digitalWrite(CLK,HIGH);
delayMicroseconds(1000);
digitalWrite(CLK,LOW);
delayMicroseconds(1000);
}
digitalWrite(CW2,HIGH);
for(int i=0;i<220;++i)
{
digitalWrite(CLK2,HIGH);
delayMicroseconds(1000);
digitalWrite(CLK2,LOW);
delayMicroseconds(1000);
}
```

```
}
digitalWrite(CW,HIGH);
for(int i=0;i<420;++i)
{
digitalWrite(CLK,HIGH);
delayMicroseconds(1000);
digitalWrite(CLK,LOW);
delayMicroseconds(1000);
}
digitalWrite(CW3,HIGH);
for(int i=0;i<10;++i)
{
digitalWrite(CLK3,HIGH);
delayMicroseconds(1000);
digitalWrite(CLK3,LOW);
delayMicroseconds(1000);
}
}
}
```

```
//atuo to weaving with Winding model two
void  eject8(void) {

digitalWrite(CW2,LOW);
for(int i=0;i<2200;++i)
{
digitalWrite(CLK2,HIGH);
delayMicroseconds(1000);
digitalWrite(CLK2,LOW);
delayMicroseconds(1000);
}
digitalWrite(CW,HIGH);
for(int i=0;i<200;++i)
{
digitalWrite(CLK,HIGH);
delayMicroseconds(1000);
digitalWrite(CLK,LOW);
delayMicroseconds(1000);
}
digitalWrite(CW2,HIGH);
for(int i=0;i<2200;++i)
{
digitalWrite(CLK2,HIGH);
delayMicroseconds(1000);
digitalWrite(CLK2,LOW);
delayMicroseconds(1000);
}


digitalWrite(CW,LOW);
for(int i=0;i<220;++i)
{
digitalWrite(CLK,HIGH);
delayMicroseconds(1000);
digitalWrite(CLK,LOW);
delayMicroseconds(1000);
}
digitalWrite(CW2,LOW);
for(int i=0;i<220;++i)
{
digitalWrite(CLK2,HIGH);
delayMicroseconds(1000);
digitalWrite(CLK2,LOW);
delayMicroseconds(1000);
}

digitalWrite(CW,HIGH);
for(int i=0;i<220;++i)
{
digitalWrite(CLK,HIGH);
delayMicroseconds(1000);
digitalWrite(CLK,LOW);
delayMicroseconds(1000);
}

digitalWrite(CW2,HIGH);
for(int i=0;i<220;++i)
{
digitalWrite(CLK2,HIGH);
delayMicroseconds(1000);
digitalWrite(CLK2,LOW);
delayMicroseconds(1000);
}
digitalWrite(CW,HIGH);
for(int i=0;i<200;++i)
{
digitalWrite(CLK,HIGH);
delayMicroseconds(1000);
digitalWrite(CLK,LOW);
delayMicroseconds(1000);
}
for ( int j=0;j<9;++j){
digitalWrite(CW2,LOW);
for(int i=0;i<2200;++i)
{
digitalWrite(CLK2,HIGH);
delayMicroseconds(1000);
digitalWrite(CLK2,LOW);
delayMicroseconds(1000);
}
digitalWrite(CW,LOW);
for(int i=0;i<200;++i)
{
digitalWrite(CLK,HIGH);
delayMicroseconds(1000);
digitalWrite(CLK,LOW);
delayMicroseconds(1000);
}
```

```
digitalWrite(CW2,HIGH);
for(int i=0;i<2200;++i)
{
digitalWrite(CLK2,HIGH);
delayMicroseconds(1000);
digitalWrite(CLK2,LOW);
delayMicroseconds(1000);
}
digitalWrite(CW,HIGH);
for(int i=0;i<220;++i)
{
digitalWrite(CLK,HIGH);
delayMicroseconds(1000);
digitalWrite(CLK,LOW);
delayMicroseconds(1000);
}
digitalWrite(CW2,LOW);
for(int i=0;i<220;++i)
{
digitalWrite(CLK2,HIGH);
delayMicroseconds(1000);
digitalWrite(CLK2,LOW);
delayMicroseconds(1000);
}
digitalWrite(CW,LOW);
for(int i=0;i<220;++i)
{
digitalWrite(CLK,HIGH);
delayMicroseconds(1000);
digitalWrite(CLK,LOW);
delayMicroseconds(1000);
}
digitalWrite(CW2,HIGH);
for(int i=0;i<220;++i)
{
digitalWrite(CLK2,HIGH);
delayMicroseconds(1000);
digitalWrite(CLK2,LOW);
delayMicroseconds(1000);
}
}
digitalWrite(CW,HIGH);
for(int i=0;i<420;++i)
{
digitalWrite(CLK,HIGH);
delayMicroseconds(1000);
digitalWrite(CLK,LOW);
delayMicroseconds(1000);
}
digitalWrite(CW3,HIGH);
for(int i=0;i<10;++i)
{
digitalWrite(CLK3,HIGH);
delayMicroseconds(1000);
digitalWrite(CLK3,LOW);
delayMicroseconds(1000);
}
}
}
```